ABSTRACT

Title of Document:	HIGHLY SIDEROPHILE ELEMENT AND TUNGSTEN SYSTEMATICS OF HAWAIIAN PICRITES
	Thomas J. Ireland, Ph.D., 2009
Directed By:	Professor Richard J. Walker, Department of Geology

A suite of Hawaiian picrites (MgO > 13 wt.%), and associated basalts, that represent some of the most primitive melts from the Hawaiian mantle source regions were analyzed for their W, highly siderophile element (HSE: Os, Ir, Ru, Pt, Pd and Re) and ^{186}Os-^{187}Os isotope systematics. These picritic samples are among the most primitive samples produced from the Hawaiian main-shield stage volcanoes. As such, they may preserve considerable information about the mantle source regions from which they were derived. Hawaii is of particular interest because there is geochemical and geophysical evidence that suggest that the Hawaiian plume may originate at the core-mantle boundary. If any outer core material is incorporated into plume lavas, it could carry important geochemical information. The primary goal of this study is to improve our understanding of the processes and materials that may affect the mantle source regions of the Hawaiian volcanoes.

Abundances of HSE and W, as well as Os isotopes, are useful tools for evaluating the mantle source regions of ocean island basalts because their absolute and relative abundances may be affected by various mantle processes, including the recycling of oceanic crust and sediment, mantle metasomatism, and other forms of crystal-liquid fractionation. In addition, these elements may be suitable for addressing the question of core-mantle interaction, because the core is highly concentrated in both the moderately siderophile and highly siderophile elements, and may have a distinct Os isotopic composition relative to the mantle.

The collected data imply that W abundances in the Hawaiian mantle sources are similar for all volcanic centers, and enriched relative to depleted MORB mantle. This suggests that W may be controlled by a primary source component that is less depleted in incompatible elements than the depleted mantle. HSE abundances in the picrites are controlled predominantly by crystal-liquid fractionation processes, and may reflect the presence of residual sulfides in the mantle sources. Lastly, the $^{187}Os/^{188}Os$ variations are consistent with some proportion of a recycled oceanic crust component; however, variations in $^{186}Os/^{188}Os$ require another process, such as the incorporation of variable Pt-enriched base-metal sulfides, or mixing with an ^{186}Os-^{187}Os enriched reservoir.

HIGHLY SIDEROPHILE ELEMENT AND TUNGSTEN SYSTEMATICS OF
HAWAIIAN PICRITES

By

Thomas J. Ireland

Dissertation submitted to the Faculty of the Graduate School of the
University of Maryland, College Park, in partial fulfillment
of the requirements for the degree of
Doctor of Philosophy
2009

Advisory Committee:
Professor Richard J. Walker, Chair
Professor William F. McDonough
Professor Roberta L. Rudnick
Associate Research Scientist Igor S. Puchtel
Associate Professor Derek C. Richardson

Dedication

This work is dedicated to my family, particularly my mom who passed away during the course of my studies. Thank you for all of your support and encouragement throughout my entire graduate career (not to mention my whole life). You guys are awesome!

Acknowledgements

A big thank you goes to my advisor, Dr. Richard Walker, who supported and mentored me throughout the course of this project. His door was always open to me and other students, and I benefited greatly from his guidance. I have learned a huge amount just by observing the way that Rich approaches science, which is with an open mind, a willingness to listen to new arguments and ideas, and always with a keen intellect. His ability to assess the strengths and weaknesses of his own ideas, along with those of others, continues to amaze me.

Dr. Bill McDonough also provided advice and support, but most importantly challenged me to critically evaluate scientific problems from multiple angles. This lesson was difficult for me at times, but it has made this dissertation stronger and allowed me to become a more rounded scientist.

I would also like to thank my other committee members. Dr. Roberta Rudnick presented thoughtful questions and comments that caused me to view my data and interpretations in different ways. Dr. Igor Puchtel, who also provided invaluable assistance in the lab, is one of the most careful and precise scientists I have met, and I benefited from discussions with him. Lastly, the Dean's Representative on my committee was Dr. Derek Richardson from the Astronomy department, whose time and comments were appreciated.

Dr. Phil Piccoli aided with electron microprobe analyses and with general humour. Dr. Richard Ash provided assistance on the ICP-mass spectrometers. Dr. Diane McDaniel, Dr. Alan Brandon and Dr. James Day were extremely helpful with regards to ^{186}Os procedures, both in terms of sample preparation and in using the

Triton mass spectrometer. I would like to acknowledge Dr. Mike Garcia and Dr. Don DePaolo, who were kind enough to provide the samples that were used in this study.

I would like to extend a personal thanks to the support staff of the Geology department, including Sandy Romeo, Dorothy Brown, Ginette Villeneuve, Jeanne Martin, Suzanne Martin and Todd Karwoski, for their help and for always contributing a kind word. Thank you to the other faculty members of the Geology department for your support and encouragement.

To my fellow graduate students, you guys rock! Thank you for your friendship and for making my time at the University of Maryland enjoyable. In particular, I would like to thank Ricardo Arevalo Jr., who not only is a great friend, but a collaborator on some of the science presented here. Thank you to Kate Scheiderich, Lin Qiu, Ruth Schulte and John Jamieson for being excellent officemates, and Dr. Barry Reno and Dr. Katya Klochko who were along for the long haul.

Most importantly, I would like to thank Rachel Potter, who stood by me in my moments of insanity and self-doubt. Your love and support are incredible, and I think you are amazing.

Table of Contents

List of Tables

List of Figures

Chapter 1: Introduction

1. Ocean Island Basalts

Ocean island basalt (OIB) volcanism provides a small, yet invaluable, window into the interior of the Earth. In the classic plate tectonic paradigm, OIB are commonly thought to be the surface manifestation of hot, upwelling plumes of mantle material (Morgan, 1971), an interpretation that was originally based on the distinct age progression of volcanoes observed in the Hawaiian Island-Emperor Seamount Chain (Wilson, 1963). Wilson (1963) envisaged a "hot spot" scenario, whereby the Pacific lithospheric plate moved over a stationary "hot" temperature anomaly in the sub-lithospheric mantle. This hypothesis was later modified by Morgan (1971) who pictured this "hot spot" as a plume of hot mantle material rising from deep within the Earth to produce the OIB volcanism. Presently, a mantle plume can be broadly defined as the focused, upward flow of mantle material, originating at a boundary layer within the Earth (Campbell and Griffiths, 1990). Generally, it is assumed that this focused flow results in areas of high igneous activity occurring both in intraplate settings (e.g., Hawaii, Deccan Traps), and occasionally on ridges (e.g., Iceland; Figure 1.1).

Based on fluid dynamic models, mantle plume theory predicts that plumes originate at chemical or thermal boundary layers within the Earth, with the core-mantle boundary (CMB) and the 670 km seismic discontinuity being the most probable locations of origin (Morgan, 1971; Griffiths and Campbell, 1990).
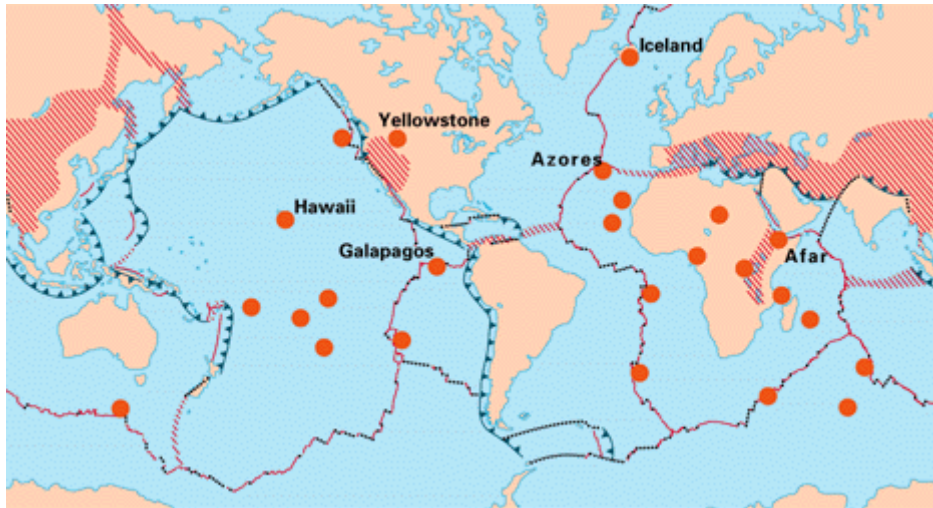
Figure 1.1: Putative mantle plumes around the world, including ocean island basalts and inter-continental localities (orange dots). Lined regions denote areas of diffuse plate boundaries. Figure from USGS.

The origin of plumes at the CMB has been supported by current mantle tomographic studies of some plumes (Figure 1.2; van der Hilst et al., 1997; Montelli et al., 2004). Some authors, however, have questioned the need to invoke deep mantle sources for intraplate volcanism, and instead have suggested that upper mantle processes can account for most aspects attributed to a plume origin (Anderson, 1998; Smith and Lewis, 1999; Meibom and Anderson, 2003; Nui and O'Hara, 2003). Regardless of the exact nature of the initiation depth of OIB, it is clear that important information about the Earth's mantle, particularly with respect to its chemical composition, can be gleaned from OIB-derived samples. The implications of these geochemical data may significantly impact our understanding of several Earth processes, including crustal recycling, mantle metasomatism, mantle convection, core-mantle interaction, and the mixing and preservation of mantle reservoirs.

This study explores a suite of elements, comprised of tungsten (W) and the highly siderophile elements (HSE: Os, Ir, Ru, Pt, Pd and Re), in picritic samples from the Hawaiian Islands. These elements are of interest because they may be particularly suitable to evaluate models that involve core-mantle interaction, while also being affected by various other important mantle processes. The following sections outline the general geochemical traits of OIB, with a focus on the importance of Hawaii, before further discussing the chosen elemental suite and the motivation behind the research.

1.1 General Geochemistry of OIB

Chemical analysis of global OIB localities and mid-ocean ridge basalt (MORB) volcanism provides strong evidence that the mantle is chemically heterogeneous.
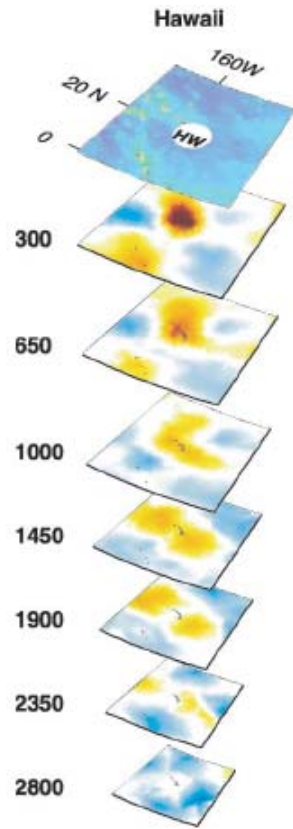
Figure 1.2: Mantle tomographic image showing that the Hawaiian OIB may reach

the core-mantle boundary (modified from Montelli et al., 2004).

Ratios of long-lived radiogenic isotope systems, such as $^{87}Sr/^{86}Sr$, $^{143}Nd/^{144}Nd$, $^3He/^4He$ and Pb, require that at least some of these heterogeneities are ancient (Figure 1.3; Zindler and Hart, 1986; Hart et al., 1992; Hofmann, 2003). Well-correlated trends between these isotopic systems have been used to broadly define five mantle end-member components (Figure 1.4), although the exact nature of these components (i.e. physically distinct reservoirs versus extremes in a spectrum of isotopic compositions) is still a matter of considerable debate (Hofmann, 2003). Despite the complexities, it is possible to relate the geochemical characteristics of these components to various reservoirs and processes that contribute to the source regions of OIB.

Conceptually, the most straightforward mantle end-member that may contribute to OIB is the Depleted MORB Mantle (DMM), although this reservoir may be highly variable when examined in detail (e.g., White and Schilling, 1978; Hofmann, 1988; Hofmann, 2003; Workman and Hart, 2008). The DMM represents the source reservoir from which MORB are derived. The DMM tends to be depleted in incompatible major and trace elements as a result of the melting processes that produce MORB. Therefore, it is characterized by the least radiogenic $^{87}Sr/^{86}Sr$ and Pb isotopic ratios of the five end-members, which reflects long-term depletions in Rb/Sr, U/Pb and Th/Pb ratios.

HIMU-type OIB, such as manifested in lavas from Mangaia and Tubuai in the Cook-Austral Chain, are characterized by highly radiogenic lead isotopes, which require long-term elevated U/Pb and Th/Pb ratios in their mantle sources (e.g.,
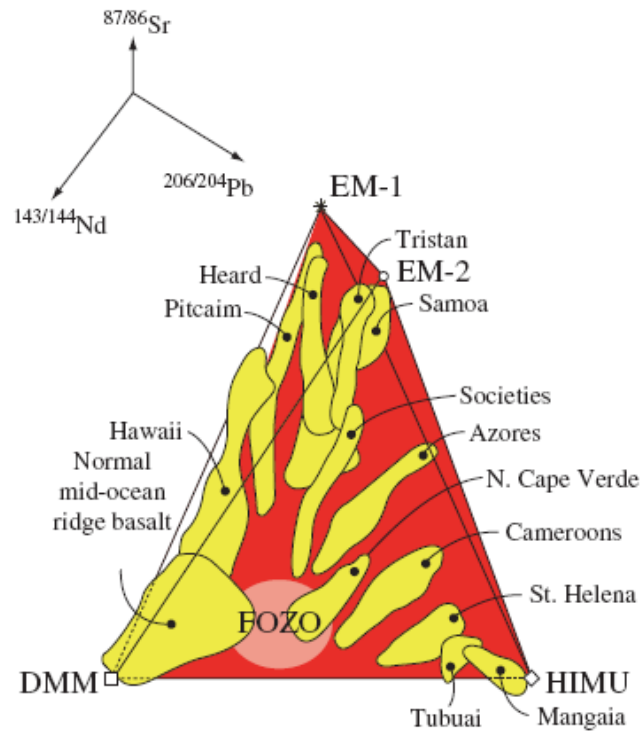
Figure 1.3: Mantle end-member tetrahedron as defined by OIB samples and the $^{87}Sr/^{86}Sr$, $^{143}Nd/^{144}Nd$ and $^{206}Pb/^{204}Pb$ isotopic systems. Note the Hawaii OIB extends from a DMM/FOZO component towards the EM-1 component. Figure from Hofmann (2003), after Hart et al. (1992).
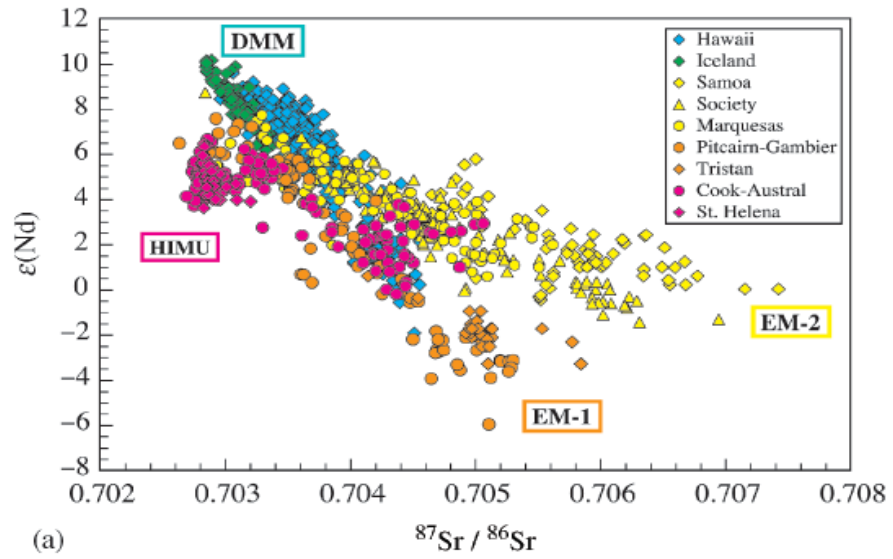
Figure 1.4 A global OIB compilation of ε_{Nd} versus $^{87}Sr/^{86}Sr$ that shows the well-correlated trends between the mantle end-members (from Hofmann, 2003).

Chauvel et al., 1992). This feature, coupled with $^{87}Sr/^{86}Sr$ ratios that are similar to those of DMM, has often been attributed to the presence of recycled ancient oceanic crust, including sediment, which has experienced alteration during subduction, resulting in the removal of both Rb and Pb (Hofmann and White, 1982; Chauvel et al., 1992; 1995). An alternative theory involves the metasomatism of oceanic lithosphere by low degree partial melts that would have elevated U/Pb and Th/U ratios due to magmatic enrichment (Sun and McDonough, 1989; Hofmann, 2003).

EM1-type (enriched-mantle 1) OIB are distinguished by relatively radiogenic $^{87}Sr/^{86}Sr$ ratios, as well as high $^{208}Pb*/^{206}Pb*$, a ratio which reflects the time-integrated Th/U ratio over Earth's history and is defined by:

$$\frac{^{208}Pb*}{^{206}Pb*} = \frac{(^{208}Pb/^{204}Pb)_{sam} - (^{208}Pb/^{204}Pb)_{init}}{(^{206}Pb/^{204}Pb)_{sam} - (^{206}Pb/^{204}Pb)_{init}},$$

where $(^{208}Pb/^{204}Pb)_{init}$=29.475 and $(^{206}Pb/^{204}Pb)_{init}$=9.307 (Galers and O'Nions, 1985).

The Pitcairn Islands are a prominent locality of EM1-type volcanism. The EM1 mantle end-member has been postulated to originate from the incorporation of delaminated subcontinental lithospheric mantle into the OIB source (Hawkesworth et al., 1986), or by the recycling of ancient pelagic sediment (Plank and Langmuir, 1998), since both of these reservoirs may have the requisite high Rb/Sr and Th/U ratios necessary to produce EM1-type OIB. Additional evidence in favour of the pelagic sediment hypothesis includes the high $^{176}Hf/^{177}Hf$ ratios and low $^{143}Nd/^{144}Nd$ ratios observed in some EM1-type OIB. Some pelagic sediments have high Lu/Hf and low Sm/Nd ratios, which would satisfy the observed isotopic constraints of EM1-type OIB (Plank and Langmuir, 1998; Blichert-Toft et al., 1999).

Samoa and the Society Islands best represent the EM2-type mantle end-member, which is characterized by the most radiogenic $^{87}Sr/^{86}Sr$ ratios. This end-member has been suggested to result from the recycling of oceanic crust and terrigenous sediment (White and Hofmann, 1982), although Workman et al. (2003) hypothesized that the Samoan mantle source may be affected by the recycling of metasomatically enriched oceanic lithosphere.

A fifth mantle end-member has been termed FOZO, meaning "focused zone", and has been postulated to represent a deep mantle reservoir (Hart et al., 1992). The most distinguishing feature of the FOZO component is a high $^{3}He/^{4}He$ ratio, which may be indicative of a relatively undegassed reservoir. In terms of the isotopic projection, the FOZO component is isotopically similar to DMM, albeit slightly more radiogenic in terms of $^{87}Sr/^{86}Sr$ and Pb isotopes.

Within this framework of five mantle end-members, a wide spectrum of compositions can occur within individual volcanic chains. This suggests that several mantle processes, such as those discussed above, may affect the mantle source regions of a single OIB locality. A classic OIB example, and the focus of this study, is the Hawaiian Islands.

1.2 Source Components in the Hawaiian plume

1.2.1 Hawaii Overview

The Hawaiian OIB is an important, archetypical example of intra-plate volcanism. Hawaiian shield volcanism represents the hottest mantle temperatures (Putirka, 2008) and the greatest mass buoyancy flux (Sleep, 1990) of any modern OIB. As a result, large volumes of picritic (high MgO) and tholeiitic basalts have been erupted from

the various shield volcanoes along the chain. Some of these rocks, particularly

picritic samples, may represent relatively primitive melts of their mantle sources

(Norman and Garcia, 1999); therefore, these samples can be used to constrain the

processes that may be affecting the OIB source regions of Hawaii. Additionally,

some geophysical studies have suggested that the Hawaiian mantle source may

originate at the CMB (Russell et al., 1998; Zhao, 2001; Montelli et al., 2004). Within

the five mantle end-member tetrahedron discussed above, Hawaii spans a

compositional space ranging from a DMM-like component to EM-1, with a FOZO

component also present (Figure 1.3). When viewed in detail, however, the Hawaiian

OIB can be broken down into several discrete source components to explain the

isotopic variations observed amongst the Hawaiian shield volcanoes.

1.2.2 Source Components from Lithophile Isotopic Systems

Previous isotopic studies of Hawaiian samples, using the same traditional isotopes

as discussed in the previous section ($^{87}Sr/^{86}Sr$, $^{143}Nd/^{144}Nd$, $^{3}He/^{4}He$ and Pb isotopes),

have generally identified three main source components in the Hawaiian plume,

which are best expressed in lavas from Mauna Kea, Loihi and Koolau (Makapuu-

stage lavas) (Figure 1.5; Staudigel et al., 1984; West et al., 1987; Kurz et al., 1996;

Eiler et al., 1996; Huang et al., 2005). The Kea component is characterized by low

$^{87}Sr/^{86}Sr$, chondritic to slightly suprachondritic $^{187}Os/^{188}Os$, as well as high

$^{143}Nd/^{144}Nd$, $^{176}Hf/^{177}Hf$ and Pb isotopic ratios (Lassiter et al., 1996; Blichert-Toft and

Albarede, 1999). In general, the Kea component spans an isotopic range from the

DMM to slightly more evolved compositions (Hoffman, 2003). The second source

constituent, termed the Loihi component, is distinguished mainly by elevated $^{3}He/^{4}He$
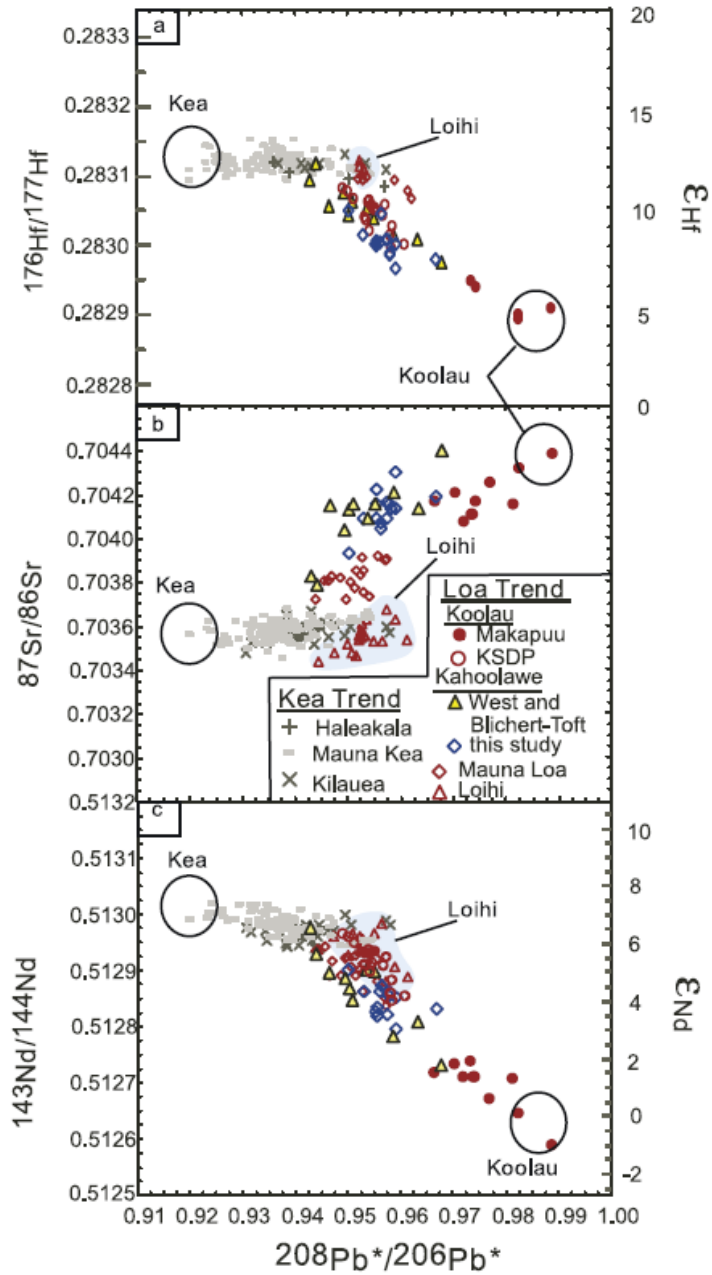
Figure 1.5: Isotopic plots for Hawaii showing the three end-member components (Kea, Loihi, Koolau) in the Hawaiian OIB (from Huang et al., 2005).

ratios, which may represent a relatively undegassed deep mantle reservoir that is related to the FOZO component (e.g., Kurz et al., 1983; Mukhopadhyay et al., 2003). This component is also defined by slightly more radiogenic $^{87}Sr/^{86}Sr$ and $^{187}Os/^{188}Os$ ratios relative to the Kea component, as well as less radiogenic $^{143}Nd/^{144}Nd$ (Huang et al., 2005). The Koolau (Makapuu) component is identified by the most radiogenic $^{87}Sr/^{86}Sr$ and $^{187}Os/^{188}Os$, accompanied by the lowest $^{143}Nd/^{144}Nd$, $^{176}Hf/^{177}Hf$ and Pb isotopic ratios in the Hawaiian lavas. This component has been linked to recycled oceanic crust and sediment to explain the isotopic extremes observed (West et al., 1987; Roden et al., 1994; Hauri, 1996; Lassiter and Hauri, 1998; Blichert-Toft et al., 1999; Huang and Frey, 2005). Additionally, a fourth component, which is similar to DMM, may be required to explain the Pb isotopic characteristics of some post-shield Hawaiian lavas. This component is not thought to have had an effect on the main shield-stage lavas that are examined in this study (Abouchami et al., 2000; Mukhopadhyay et al., 2003).

The three major end-member components are manifested at the surface as two geographically parallel, but geochemically diverse trends (Frey and Rhodes, 1993; Hauri, 1996; Lassiter et al., 1996; Ren et al., 2005; Huang et al., 2005). The Kea-trend volcanoes (Mauna Kea, Kilauea, Kohala) are dominated by the Kea and Loihi source components, while the Loa-trend volcanoes (Mauna Loa, Loihi, Hualalai, Koolau) are controlled by the Loihi and Koolau source components (Huang et al., 2005).

1.2.3 Core signature in Hawaii?

In addition to the source components outlined above, a role for a core contribution to the Hawaiian source regions has been postulated (Brandon et al., 1998, 1999; Humayun et al., 2004), based on observed coupled enrichments between ^{186}Os-^{187}Os isotopes in Hawaiian picrites (^{187}Re $\rightarrow$ ^{187}Os + $^-\beta$ λ=1.67x10^{-11} yr^{-1}; ^{190}Pt $\rightarrow$ ^{186}Os + α λ=1.48x10^{-12} yr^{-1}), as well as elevated Fe/Mn ratios in Hawaiian basalts (Humayun et al., 2004). Brandon et al. (1998, 1999) argued that the crystallization of the inner core may have led to the fractionation of Pt and Re from Os, potentially creating an outer core with distinctly enriched Pt/Os and Re/Os ratios relative to chondrites, which over time would lead to enrichments in ^{186}Os and ^{187}Os. Thus, these authors interpreted the coupled enrichments to be the result of the incorporation of small amounts ($\leq$0.5 wt.%) of outer core material. The implications of a possible core component in the mantle sources of OIB are significant, and include consequences for the rate and timing of inner core crystallization, the nature of the CMB (composition and dynamics), the thermal evolution of the Earth, and the style of mantle convection (e.g., Buffett et al., 1996; Labrosse et al., 2001; Brandon et al., 2003; Brandon and Walker, 2005).

However, this interpretation has been heavily debated based on recent thermal models for the late inception of inner core crystallization (Buffett et al., 1996; Labrosse et al., 2001), and alternate hypotheses for the mechanisms responsible for producing the coupled ^{186}Os-^{187}Os enrichments have been generated (Smith, 2003; Baker and Jensen, 2004; Luguet et al., 2008). These alternate mechanisms generally involve the recycling of different types of materials during the subduction process,

such as Mn-crusts and nodules, that may be incorporated into the OIB source (Smith, 2003; Baker and Jensen, 2004; Scherstén et al., 2004), or to the presence of a pyroxenite component, with associated base-metal sulfides (BMS) that may be present in a hybrid peridotite-pyroxenite source (Smith, 2003; Meibom et al., 2004; Sobolev et al., 2005, 2007; Ballhaus et al., 2006; Luguet et al., 2008). These materials may have the requisite high Pt/Os and Re/Os ratios to produce enrichments in ^{186}Os and ^{187}Os.

1.3 Scope of the Study

This dissertation focuses on a suite of elements, comprised of W and the HSE elements, along with the two Os isotopic systems, in a set of Hawaiian picrites. This elemental suite may be beneficial in evaluating various mantle processes, including the recycling of oceanic crust and sediment, mantle metasomatism and other forms of crystal-liquid fractionation. Furthermore, these elements and isotopic systems may be particularly suitable for addressing the question of core-mantle interaction and the role it may play in the source regions of the Hawaiian shield volcanoes because the core is highly concentrated in the siderophile and highly siderophile elements relative to the mantle (McDonough, 2003), and the outer core may have a distinct Os isotopic composition. This study assesses these elements in a group of well-characterized Hawaiian picrites, as well as several related basalts, which represent the most primitive samples produced from the Hawaiian main-shield stage volcanoes (Garcia et al., 1995) and may preserve information about the mantle source regions of Hawaii.

1.3.1 W in Hawaiian Picrites

Tungsten is a trace element that has had distinctly different geochemical behaviours during the evolution of the Earth. Under the reducing conditions of core segregation, W likely behaved as a moderately siderophile element and was preferentially sequestered into the core, with metal/silicate partitioning values suggesting that ≥90% of the terrestrial W budget is in the core (Jagoutz et al., 1979; Sun, 1982; Newsom and Palme, 1984; Newsom et al., 1996; McDonough, 2003). In contrast, during more oxidized mantle melting events, W behaves as a highly incompatible element and strongly partitions into liquid phases, becoming more concentrated in oceanic and continental crust (Rudnick and Gao, 2003; Hu and Gao, 2008). Therefore, the mantle is depleted in W relative to both the core and crust due to these two processes, and W abundances in mantle-derived melts may be effective in evaluating the physical mixing between these reservoirs (Figure 1.6; Arevalo and McDonough, 2008).

The W and U systematics of the Hawaiian picrites are documented in Chapter 2. In this chapter, the concentrations of both W and U in Hawaiian samples, as determined by LA-ICP-MS (laser ablation inductively coupled plasma mass spectrometry) are related to that of an estimated parental melt for each volcanic center in order to constrain the abundances of these elements in the mantle sources of the Hawaiian shield volcanoes. These mantle source abundances are used to evaluate the possible roles of several processes that may contribute to the sources of the Hawaiian shield volcanoes, including oceanic crust and sediment recycling, as well as core-mantle interaction.

15

Geochemical Behaviour of W

Highly Incompatible:
- during most oxidized mantle melting events
- enriched in both oceanic and continental crust

Stage 1: Core Segregation

Stage 2: Oceanic and Continental Crust Formation

Moderately Siderophile:
- under reducing conditions
- ≥90% sequestered into core
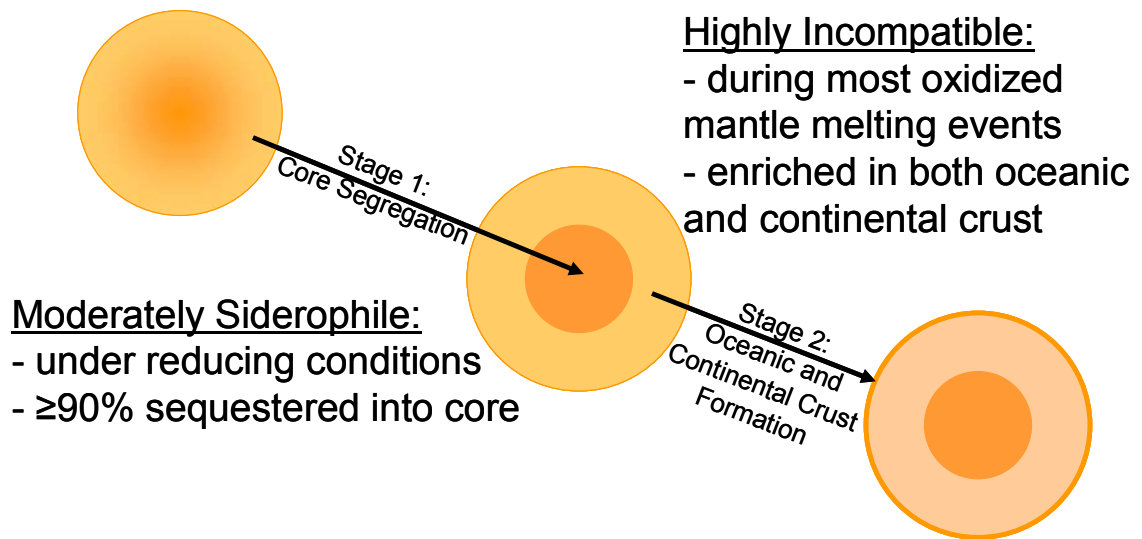
Figure 1.6: Schematic diagram showing the different geochemical behaviour of W during core segregation and formation of the crust.

1.3.2 HSE and ^{187}Os Systematics of the Hawaiian Picrites

The absolute and relative abundances of the HSE, coupled with the associated Os isotopic systems, can be modified by several diverse mantle processes and can potentially be used to evaluate the processes of partial melting, melt refertilization, crustal recycling and crystal-liquid fractionation processes. In addition to mantle processes, the HSE may also be a useful tool to investigate models of core-mantle interaction. The HSE, by definition, have a high affinity for metallic Fe, with low pressure-temperature partitioning data suggesting metal/silicate partition coefficients of greater than 10,000 (Fleet et al., 1999). Based on comparisons to primitive meteorites, mass balance calculations indicate that the Earth's core contains ~98% of the terrestrial HSE budget (McDonough, 2003). If minor chemical exchange occurred between the mantle source regions of the Hawaiian plume and the core, it would likely have resulted in a mantle source with distinctive HSE and Os isotopic characteristics (Walker et al., 1995; Snow and Schmidt, 1998; Brandon and Walker, 2005).

Chapter 3 documents the absolute and relative abundances of the HSE in 52 Hawaiian picrites and associated tholeiitic basalts from nine Hawaiian shield volcanoes. Based on the estimated MgO contents of parental melts, the HSE abundances in the parental melts for each volcanic center are calculated. These estimations are used to evaluate the causes of HSE variations observed between volcanic centers. Chapter 3 also presents ^{187}Os/^{188}Os data for the sample suite and explores how variations in this ratio, which must reflect ancient source heterogeneities in Re/Os ratios, correlate with HSE abundances.

1.3.3 ^{186}Os in Hawaiian Picrites

In a similar fashion to ^{187}Os/^{188}Os ratios, variations in ^{186}Os/^{188}Os ratios reflect long term source heterogeneities in Pt/Os ratios. Coupled enrichments between ^{186}Os and ^{187}Os have been reported by earlier studies of Hawaiian picrites (Brandon et al., 1998, 1999) and were attributed to a core component being incorporated into the mantle source regions of Hawaii. However, several alternative theories have been postulated that may also explain the coupled enrichments, including the recycling Fe-Mn rich materials, hybrid pyroxenite-peridotite sources and the involvement of base-metal sulfides (Smith, 2003; Baker and Jensen, 2004; Scherstén et al., 2004; Luguet et al., 2008; Dale, 2009).

Chapter 4 examines ^{186}Os/^{188}Os ratios in a large picritic sample set that includes several samples from the previous study (Kil 1-18, ML 1868-9, Lo-02-02, Lo-02-04 and H-11). Using improved mass spectrometric techniques, this chapter investigates the relationships between ^{186}Os/^{188}Os with Pt/Os and ^{187}Os/^{188}Os ratios and attempts to resolve these associations with the processes that may be affecting the mantle source regions of the Hawaiian shield volcanoes.

1.3.4 Summary and Conclusions

In the final chapter, the results of the new geochemical and isotopic data are summarized, and a comprehensive discussion for the HSE and Os isotopic characteristics of the Hawaiian picrites is presented.

Chapter 2: Tungsten in Hawaiian picrites: A compositional model for the sources of Hawaiian lavas

Abstract

Concentrations of tungsten (W) and uranium (U), which represent two of the most highly incompatible elements during mantle melting, have been measured in a suite of Hawaiian picrites and primitive tholeiites from nine main-stage shield volcanoes. Tungsten abundances in the parental melts are estimated from correlations between sample W abundances and MgO contents, and/or by olivine correction calculations. From these parental melt determinations, along with independent estimates for the degree of partial melting at each volcanic center, we extrapolate the W content of the mantle sources for each shield volcano. The mantle sources of Hualalai, Mauna Loa, Kohala, Kilauea, Mauna Kea, Koolau and Loihi contain 9 ± 2 (2σ) ng/g, 11 ± 5 ng/g, 10 ± 4 ng/g, 12 ± 4 ng/g, 10 ± 5 ng/g, 8 ± 7 ng/g and 11 ± 5 ng/g respectively. When combined, the mean Hawaiian source has an average of 10 ± 3 ng/g W, which is three-times as enriched as the Depleted MORB Mantle (DMM; 3.0 ± 2.3 ng/g).

The relatively high abundances of W in the mantle sources that contribute to Hawaiian lavas may be explained as a consequence of the recycling of W-rich

oceanic crust and sediment into a depleted mantle source, such as the depleted MORB mantle (DMM). However, this scenario requires varying proportions of recycled materials with different mean ages to account for the diversity of radiogenic isotope compositions observed between Kea- and Loa-trend volcanoes. Alternatively, the modeled W enrichments may also reflect a primary source component that is less depleted in incompatible trace elements than the DMM. Such a source would not necessarily require the addition of recycled materials, although the presence of some recycled crust is permitted within our model parameters and likely accounts for some of the isotopic variations between volcanic centers.

The physical admixture of ≤ 0.5 wt.% outer core material with the Hawaiian source region would not be resolvable via W source abundances or W/U ratios; however, W isotopes may provide a more sensitive tracer of this mixing process. Recent W isotopic studies show no indication of core-mantle interaction, indicating that either such a process does not occur, or that mechanisms other than physical mixing may operate at the core-mantle boundary.

Keywords: Tungsten; Hawaii; parental melt composition; mantle source; crustal recycling; core-mantle interaction

2.1 Introduction

The distinct geochemical behaviour of tungsten (W) makes this element particularly suitable for addressing a range of geologic phenomena, including constraining the proportion of recycled crustal materials in mantle source regions and

identifying potential core-mantle interactions in ocean island basalts (OIB). Tungsten behaves as a moderately siderophile (iron-loving) element under reducing conditions, which has resulted in the sequestration of ≥90% of the terrestrial W budget into the core (Jagoutz et al., 1979; Sun, 1982; Newsom and Palme, 1984; McDonough, 2003). Under the more oxidized conditions prevalent in the silicate portion of the Earth, however, W behaves as a highly incompatible element and strongly partitions into liquid phases during mantle melting. Consequently, core-mantle segregation and the production of oceanic and continental crust has depleted the mantle in W. Due to the large contrast in W abundances between the mantle and both the crust and core, W concentrations and elemental ratios may provide useful geochemical tracers of physical mixing between these reservoirs (Arevalo and McDonough, 2008).

The Hawaiian source, which represents the greatest mantle buoyancy flux (Sleep, 1990) and hottest potential temperature (e.g., Putirka, 2008) of any modern intraplate ocean island, serves as an archetype of OIB volcanism. Consequently, primitive Hawaiian lavas may provide new insight to the utility of W as a geochemical tracer for both crustal recycling and core-mantle interactions. There is abundant geochemical support for the incorporation of recycled oceanic crustal materials into the mantle sources of the Hawaiian main-shield stage volcanoes (e.g., Bennett et al., 1996; Eiler et al., 1996; Hauri, 1996; Hofmann and Jochum, 1996; Lassiter and Hauri, 1998; Blichert-Toft et al., 1999; Sobolev et al., 2000, 2005). The source region of the Hawaiian shield volcanoes has also been suggested to extend as deep as the core-mantle boundary, based on geophysical evidence (e.g., Russell et al., 1998; Zhao, 2001; Courtillot et al., 2003; Montelli et al., 2004), as well as geochemical evidence

based on Os isotopes and Fe/Mn ratios (e.g., Brandon et al., 1999; Humayun et al., 2004). Tungsten isotopes have been implicated as a useful proxy to assess a potential core contribution to the Hawaiian source (Scherstén et al., 2004; Hawkesworth and Scherstén, 2007). Although W studies have not identified a core signature in Hawaiian lavas, an important aspect of W isotopic modeling is the accurate estimation of W abundances in the mantle sources.

Traditionally, the budget of W in mantle reservoirs (e.g., Newsom and Palme, 1984; Newsom et al., 1986; Sims et al., 1990; Arevalo and McDonough, 2008) and the continental crust (e.g., Rudnick and Gao, 2003; Hu and Gao, 2008) has hinged on relating well-established lithophile element abundances (e.g., Ba, Th and U) to W via relatively constant concentration ratios in mid-ocean ridge basalts (MORB), mantle peridotites and crustal samples. Here, we report W and U concentrations for a suite of Hawaiian picritic lavas that represent primitive melts from the Hawaiian source region. As both W and U are highly incompatible elements, the relative abundances of these elements in a partial melt of the mantle reflect the composition of the source. The main objective of this study is to constrain the abundance of W in the mantle sources that feed the Hawaiian main-stage shield volcanoes by relating sample W concentrations to that of an estimated parental melt for each volcanic center. By establishing the mantle source abundances of W, we seek to evaluate the processes that may have contributed to these sources.

2.2 Samples and Methods

The suite of picrites (≥13 wt% MgO; n = 22) and associated tholeiitic basalts (9-12 wt% MgO; n = 4) examined here include some of the most primitive melts from the Hawaiian source region and spans a wide range in MgO, indicative of both olivine removal (low-MgO) and accumulation (high-MgO; Norman and Garcia, 1999). The picrites were derived from high density melts that erupted on the flanks of the main-stage shield volcanoes and bypassed the summit reservoirs (Garcia et al., 1995). Hence, these lavas are less likely to have been affected by fractionation and/or assimilation processes that may operate in high-level magma chambers (Norman and Garcia, 1999), and thus are the best samples available to constrain the abundances of highly incompatible elements (e.g., W and U) in the mantle sources of Hawaiian lavas. Samples were obtained from submersible dives and submarine dredge hauls that sampled the flanks of the Hawaiian volcanoes, as well as from subaerial collection (Table 1). Nine volcanic centers are represented here, including Mauna Kea, Mauna Loa, Hualalai, Loihi, Kilauea, Koolau, Kohala, Lanai and Molokai. Two high-MgO alkalic basalts (186-5 and 187-1) and a basanitoid (186-11) from Loihi were also analyzed in this study for comparison.

In order to obtain precise concentrations of W and U, glassy and/or microcrystalline sample sections were analyzed via laser ablation inductively-coupled plasma mass spectrometry (LA-ICP-MS) following the analytical procedures of Arevalo and McDonough (2008). The utility and reliability of in-situ laser ablation methods for measuring trace elements in geologic materials have been previously validated through numerous analytical studies (e.g., Pearce et al., 1997; Eggins et al.,

1998; Norman et al., 1998; Jochum et al., 2005, 2006, 2007). Additionally, LA-ICP-MS methods allow for: i) the identification and analysis of unaltered sample surfaces; ii) low analytical blanks; iii) minimal sample destruction; and, iv) spatially resolved concentration measurements with typical lower limits of detection in the sub-ng/g range. The rocks examined in this study were analyzed using a New Wave frequency-quintupled Nd-YAG laser (213 nm light) coupled to a Thermo Finnigan Element2 single-collector ICP-MS at the University of Maryland.

Spectral matrix effects, particularly isobaric interferences from potential diatomic oxides, were limited by implementing a standard tuning procedure that maximized the elemental signal (based on ^{43}Ca and ^{232}Th spectra) and minimized oxide production (^{232}Th^{16}O/^{232}Th < 0.15%). Our method monitored four W isotope mass stations (^{182}W, ^{183}W, ^{184}W, and ^{186}W) and the ratios of these isotopes in order to ensure that no isobaric interferences hindered our concentration measurements. Non-spectral matrix effects resulting from differences in chemical compositions between the analyte and a standard reference material were accounted for by externally calibrating our W measurements to multiple tholeiitic basalts and our U analyses to a suite of silicate reference glasses spanning a range in concentration. The basaltic standards were measured via solution ICP-MS, including both isotope dilution and high-precision standard addition analyses. Details on the calibration of our trace element analyses and the specific laser and mass spectrometer parameters utilized for the measurements of this study are reported in Arevalo and McDonough (2008).

Following determination of trace element abundances in the glassy and/or microcrystalline matrices, data were corrected to whole rock values by accounting for

the dilutional effect of olivine, the only major phenocryst phase present. Olivine

phenocrysts analyzed in this study had W and U concentrations at or below our

analytical limits of detection (<1.0 ng/g). The modal fraction of olivine in each

sample was independently determined by point counting of thin sections (between

500 and 1000 points each) and/or mass balance of MgO abundances in the matrix,

olivine and whole rock. To test the robustness of these methods, both techniques were

applied to several samples with consistent results (see Supplemental Table 2.S1).

The precision of the matrix W and U concentrations were not limited by counting

statistics and are typically reported with ≤5% uncertainty ($2\sigma_m$; external

reproducibility), which translates to uncertainties of ≤6% and ≤10% in the whole rock

calculations via mass balance and point counting respectively. Major element

abundances, as well as average olivine compositions, were previously reported by

Ireland et al. (2009). The current study includes samples previously examined by

Brandon et al. (1999; ML 2-50, ML 1868-9, Lo-02-02, Lo-02-04, H-11, Kil 1-18,

KOH 1-28) for which a core contribution was inferred based on coupled enrichments

of ^{186}Os and ^{187}Os, as well as three samples analyzed by Scherstén et al. (2004) for

their W isotopic compositions.

2.3 Tungsten in Hawaiian Picrites

Tungsten and U concentration data and W/U ratios for samples from nine

Hawaiian shield volcanoes are presented in Table 2.1. The calculated whole-rock

abundances of W in the Hawaiian picrites range from as low as 25 ng/g (Koolau

sample K98-08) up to 458 ng/g (Loihi sample 186-11). The highest W (and U)

Table 2.1: W and U abundance data for Hawaiian picrites

Volcano	Sample Name	MgO_{wr} (wt%)[e]	W_{glass} (ng/g)	$2\sigma_m$	U_{glass} (ng/g)	$2\sigma_m$	W/U	%ol calc[g]	%ol point count	# points	W_{wr} (ng/g)[h]	$2\sigma_m$	U_{wr} (ng/g)	$2\sigma_m$
Mauna Kea														
	MK-1-6[a]	17.24	170	2	307	1	0.55	27	23	500	124	3	225	4
Mauna Loa														
	ML-2-50[a]	19.92	121	3	182	5	0.66	33			81	2	122	4
	ML KAH-1	21.66	171	10	297	26	0.57		34	500	113	10	196	21
	ML 1868-9	21.48	162	3	248	7	0.65		36	1000	103	5	159	8
Hualalai[a]														
	H-2	13.63	114	4	178	5	0.64	20	19	500	91	4	142	5
	H-7[b]	11.23	107	3	177	7	0.60	13	13	500	93	4	155	7
	H-9[b]	11.30	125	5	194	7	0.65	12	14	500	110	5	170	8
	H-11	13.67	113	2	161	4	0.70	18	18	500	92	3	132	4
	H-27	14.91	108	3	165	4	0.65	21			85	3	130	4
	H-P	23.19	102	3	161	5	0.63	40	44	1000	61	2	97	3
	average olivine[f]	47.73												
Loihi[a]														
	LO-02-02	24.21	265	4	337	11	0.79	40			158	4	202	7
	LO-02-04	26.58	313	6	365	7	0.86	56			139	3	162	4
	158-9	16.57	414	8	763	31	0.54	23			320	9	589	27
	186-5[c]	19.52	352	4	480	10	0.73		30	1000	247	12	336	18
	186-11[d]	13.76	572	11	739	13	0.77		21	1000	452	32	584	37
	187-1[c]	25.16	223	3	308	7	0.72	46			121	3	167	5
	average olivine[f]	46.80												
Kilauea														
	KIL-1-18[a]	13.80	165	5	361	9	0.46		15	1000	140	11	307	24
	KIL-2-3[a]	22.36	184	2	317	4	0.58		40	500	110	6	190	11
	KIL-2-4[a]	22.55	213	3	373	7	0.57	40			127	3	373	8
	KIL-3-1[a]	19.24	230	6	429	8	0.54	33			155	5	288	7
	KIL 1840-2	14.27	230	6	406	16	0.57		21	500	182	17	321	30
	average olivine[f]	48.15												
Koolau														
	K98-08	17.78	36	4	164	16	0.22		29	500	25	3	116	14
	S497-6[a]	21.55	198	24	306	22	0.65		42	500	115	15	177	16
	S500-5B[a]	21.22	109	2	170	1	0.64	39			67	2	104	2
Kohala[a]														
	KO-1-10	13.54	164	4	262	3	0.62		20	500	131	12	210	19
	KO-1-20[b]	9.60	199	10	316	16	0.63	10	10	500	180	11	286	17
	KOH-1-28	20.52	157	5	254	12	0.62	35			102	4	165	8
	average olivine[f]	47.53												
Lanai														
	LWAW-4	14.48	62	5	121	6	0.51		15	1000	53	6	103	9
	LWAW-7[b]	11.69	79	4	174	7	0.45		9	1000	72	8	158	17
Molokai[a]														
	S501-2	28.96	98	3	212	12	0.46	52	51	500	47	2	102	6

[a] submarine sample

[b] tholeiitic basalt (MgO < 13 wt%)

[c] alkali basalt

[d] basanitoid

[e] MgO contents from Ireland et al. (2009) and references therein

[f] average olivine MgO content from Ireland et al. (2009)

[g] see table S1 for correction procedure

[h] example correction calculation: The matrix for MK-1-6 contains 170 ng/g W and olivine comprises 27% of this sample. The matrix concentration was converted to a whole rock concentration by accounting for the olivine present using the following formula: W(wr) = W(matrix)*(1-ol%). Following this calculation, the whole rock W concentration for MK-1-6 is 124 ng/g.

concentrations were observed in the alkalic basalt (186-5 and 187-1), pre-shield

picrite (158-9) and basanitoid (186-11) samples from Loihi, which are representative

of the pre-shield stage of volcanism and likely represent different sources and lower

degrees of melting than the later shield stage volcanism (Garcia et al., 1995). Koolau

sample S500-5B was reported to have been affected by Mn-crust alteration by Ireland

et al. (2009); however, the rock section analyzed in this present study was carefully

selected to avoid the obvious alteration and no apparent effect was noticed. A

duplicate measurement of the matrix of sample H-11, which was previously analyzed

by Arevalo and McDonough (2008), was found to be statistically indistinguishable

from the previously reported value.

Although the calculated whole-rock W concentrations of the entire Hawaiian

picrite suite appear to show no correlation with MgO (a proxy for crystal-liquid

fractionation processes), data for several individual volcanic centers show linear

trends (Figure 2.1a; 2.2). In general, W abundances decrease with increasing MgO

content at each main-stage shield volcano, reflecting the highly incompatible nature

of W; Mauna Loa and Koolau appear to serve as exceptions, although each of these

volcanoes are represented by only 3 samples that span a narrow range in MgO.

The W/U ratio of the silicate Earth (0.65 ± 0.45, 2σ) has been demonstrated to be

invariant between mantle and crustal sources and is independent of bulk rock MgO,

indicating analogous behaviour of these elements during mantle melting and crystal-

liquid fractionation (Arevalo and McDonough, 2008). The average W/U ratio of our

suite of primitive Hawaiian lavas is 0.62 ± 0.19 (2σ; Figure 1b), consistent with the

terrestrial average. However, Koolau sample K98-08, which has the lowest W

27
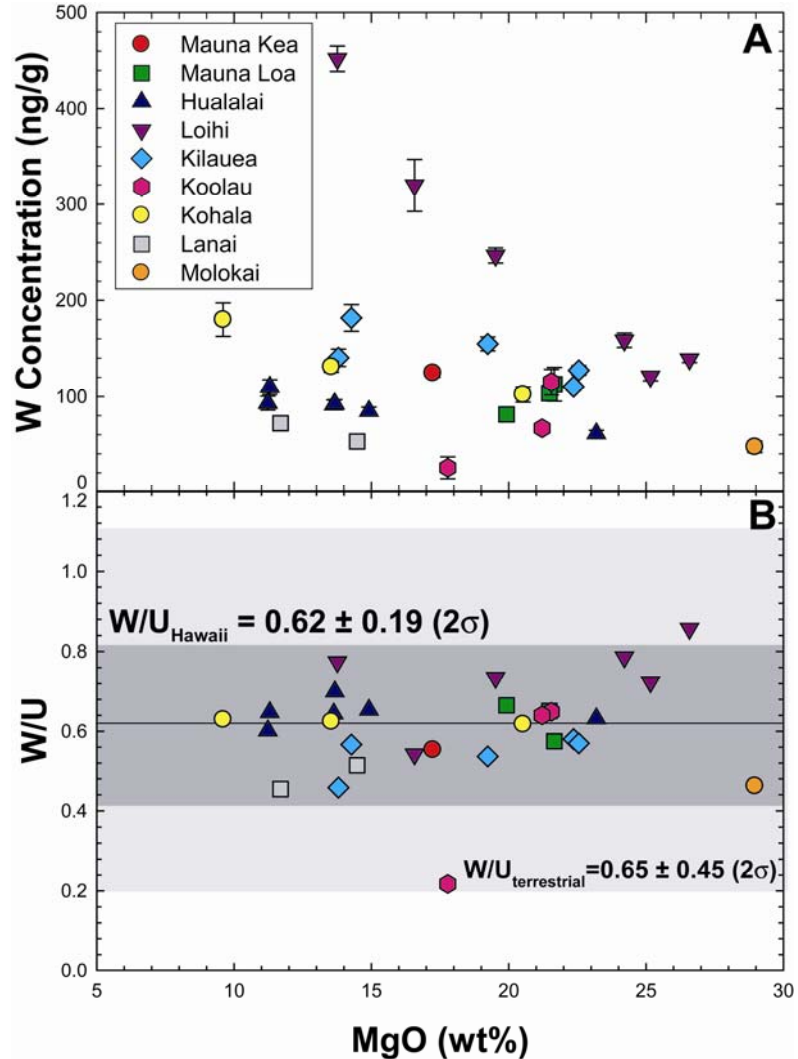
Figure 2.1: A) Tungsten versus MgO content for the primitive Hawaiian lavas analyzed in this study. Tungsten concentrations were determined by high-precision laser ablation ICP-MS following the analytical protocol of Arevalo and McDonough (2008). In general, W abundances decrease with increasing MgO content at each individual volcanic center with ≥3 samples (with the exception of Koolau). B) The average W/U ratio of primitive Hawaiian melts (0.62 ± 0.19; dark shaded area) does not vary as a function of MgO and is identical to the terrestrial value established by Arevalo and McDonough (2008; 0.65 ± 0.45; lightly shaded area).
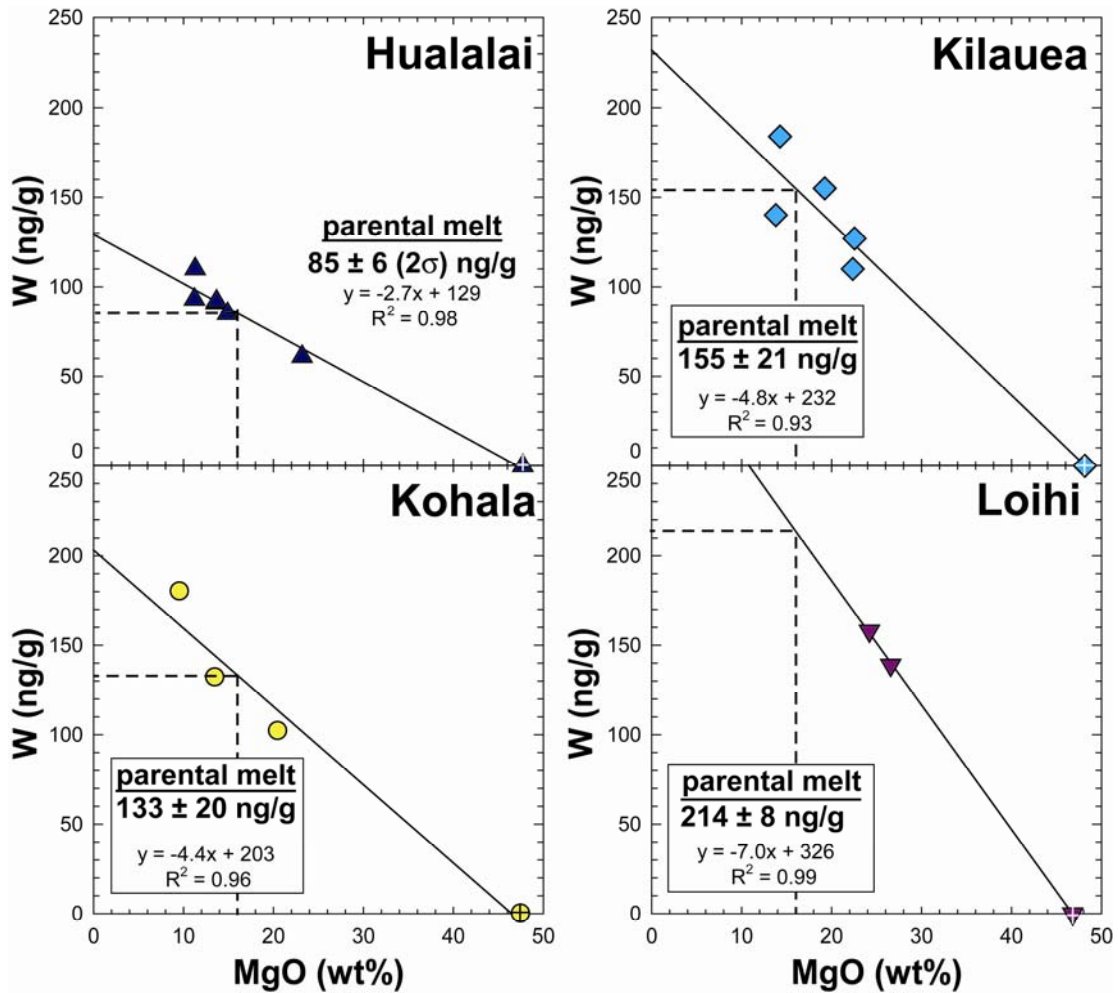
Figure 2.2: Estimated concentrations of W (in ng/g) in parental melts from the Hualalai, Kilauea, Kohala and Loihi main-stage shield volcanoes. Tungsten abundances were determined from the intersection of the linear regressions of the data with 16 ± 1 wt% MgO, the parental melt MgO content as determined by Norman and Garcia (1999) and Ireland et al. (2009). Co-existing olivine, which contains negligible W, is also included as part of the linear regression trends and is denoted by the crossed symbols.

concentration (25 ng/g) of the samples analyzed here but a typical U content (115 ng/g), has an anomalously low W/U ratio (W/U = 0.22). This value is outside of the range of our picritic dataset, and is suggestive of a preferential loss of W, perhaps due to alteration effects. Hualalai lavas, in general, have the lowest W abundances (average of 90 ng/g; n=6), but possess normal W/U ratios (0.65 ± 0.06). Conversely, Loihi lavas are characterized by the highest W concentrations (up to 458 ng/g; n=6) and W/U ratios (0.74 ± 0.21), although they reside within the range of variance defined by mantle-derived rocks.

Although visibly fresh rock chips were selected for analysis, several samples show evidence for alteration. Lanai samples LWAW-4 and LWAW-7, and Molokai sample S501-2 have high LOI values, as well as low alkali abundances (Ireland et al., 2009), which are indicative of fluid-rock reactions involving the breakdown of igneous minerals (Crocket, 2000). These three samples also have low W concentrations and W/U ratios, suggesting that W may be affected by this alteration process to a slightly greater extent than U. Koolau sample K98-08 may have been affected by a similar alteration process, although it is not reflected in the LOI or alkali abundances for this sample. Norman and Garcia (1999) noted high LOI contents for Lo-02-02 and Lo-02-04, but concluded that this feature was not due to alteration because Pb isotope, trace element and alkali characteristics were similar to other lavas from Loihi.

2.4 The W content of Hawaiian mantle source regions

To model the mantle source W composition for each volcanic center considered here, various critical parameters must be estimated, including a suitable bulk crystal/melt partition coefficient (D) for W during mantle melting, the W content of the parental melts from each volcanic center and the degree of partial melting (F). As mentioned previously, W partitions in a similar manner to U during mantle melting, so a bulk crystal/melt partition coefficient of 0.001 is used. This estimate is similar to that determined for U in basaltic melts and partitioning experiments (0.001 to 0.0001; e.g., www.earthref.org/GERM). Sections 2.4.1 and 2.4.2 document our procedures for estimating the parental melt compositions for the Hawaiian shield volcanoes, and the degree of partial melting.

2.4.1 W content of Hawaiian parental melts

Parental melts are primary magmas produced from a mantle source region with minimal fractionation or contamination, and thus, can be used to place constraints on the composition of the source. Based on whole rock MgO and Al_2O_3 relationships of the samples analyzed in this study, in addition to olivine-melt equilibria, the parental melts for all of the Hawaiian shield volcanoes have been established to contain 16 ± 1 (2σ) wt% MgO (Norman and Garcia, 1999; Ireland et al., 2009). Two different techniques were used to constrain the W content of the Hawaiian parental melts. The first method utilizes a linear regression of the MgO-W trends, as well as the average olivine composition for each volcanic center, to interpolate the W content at the primary MgO content of 16 ± 1 wt.%. The second approach is to individually correct

each sample for olivine accumulation or removal to a MgO content of 16 wt.% and

take an average of the samples at each volcanic center. The second technique is

independent of the shape of the MgO-W trends and is more appropriate for those

volcanic centers that do not show a linear correlation or are represented by few

samples. For these estimations, it is essential that only those picritic and tholeiitic

samples that are most likely to represent a parental melt of similar initial composition

are used; therefore, the alkali basalts (186-5 and 187-1), pre-shield picrite (158-9) and

the basanitoid (186-11) from Loihi that likely represent a different source from the

Loihi shield picrites, as well as samples that may have experienced alteration (i.e.

LWAW-4, LWAW-7 and S501-2) are not considered in the following exercise.

2.4.1.1 Linear regression of MgO-W trends

Although the MgO content of Hawaiian picrites vary, primarily as a result of

olivine accumulation and/or removal, the W content of the parental melts can be

estimated by the intersection between the linear regressions of the MgO-W data and

the determined parental melt MgO content of 16 ± 1 wt.% (Figure 2.2). Since olivine

is the only major phenocryst phase present, these regressions represent olivine control

lines and the average composition of co-existing olivine for each volcanic center is

also plotted as part of the trend (Figure 2.2 and Table 2.1). As mentioned previously,

olivine contains negligible concentrations of W (and U), so the linear regressions

should intersect the MgO axis at an equivalent MgO content as the average olivine.

This method was employed for four of the Hawaiian shield volcanoes, with the

parental melts from Hualalai, Kohala, Kilauea and Loihi estimated to contain 85 ± 6

(2σ) ng/g, 133 ± 20 ng/g, 155 ± 21 ng/g and 214 ± 10 ng/g W, respectively (Table 2.2).

2.4.1.2 Olivine correction to 16 wt.% MgO

A second way to determine the W abundance of a Hawaiian parental melt is to individually correct each sample for olivine accumulation or removal to 16 wt.% MgO (e.g., Garcia et al., 1995; Hauri, 1996; Danyushevsky et al., 2000; Huang and Frey, 2003). For samples that have lost olivine (MgO<16 wt.%), equilibrium olivine was mathematically added in 0.1% increments until the calculated whole rock MgO content reached 16 wt.% MgO following the procedure of Danyushevsky et al. (2000). Likewise, for samples with accumulated olivine, Fo_{90} olivine (corresponding to the most magnesian olivine present in the sample suite) was subtracted from the sample until the whole rock MgO content reached 16 wt.% MgO. In this manner, an average W content for each volcanic center is calculated at an MgO content of 16 wt.%, which is presumed to be representative of the parental melt (Table 2).

The main advantage of this calculation is that it is independent of the shape of the MgO-W trends, so it can be used for those volcanic centers with poor correlations between W and MgO (Mauna Loa, Koolau) and for those volcanic centers with small datasets (Mauna Kea). Following the olivine correction, the parental melts for Hualalai, Mauna Loa, Kohala, Kilauea, Mauna Kea, Koolau and Loihi are determined to contain 83 ± 18 (2σ) ng/g, 111 ± 40 ng/g, 129 ± 39 ng/g, 149 ± 42 ng/g, 127 ± 46 ng/g, 104 ± 84 ng/g and 185 ± 20 ng/g W, respectively. The parental melt for Mauna

Kea, based upon one data point, is estimated to contain 127 ± 46, using the same relative error from Mauna Loa (40%).

Both parental melt estimation techniques were utilized for Hualalai, Kohala, Kilauea and Loihi, with the results of each method producing statistically indistinguishable estimates. Due to the smaller uncertainties on the W content from the MgO-W linear regression method, we use these values for the calculation of source composition.

2.4.2 Degree of partial melting

The degree of partial melting of the mantle source regions of the Hawaiian shield volcanoes is a key parameter for calculating the W contents of these sources; however, such estimations are far from straightforward and often require making significant assumptions about the initial source composition and/or mineralogy (Feigenson et al., 2003). The assumptions inherent to melting models introduce a potentially large source of error into our calculations of source W contents, so an appropriate model must be carefully chosen. Several melting models have been suggested for Hawaii, based on different geochemical arguments, including incompatible element abundances (Norman and Garcia, 1999), rare earth element (REE) systematics (Feigenson et al., 1996; 2003) and U-series disequilibria (Sims et al. 1995, 1999; Pietruszka et al., 2006).

Norman and Garcia (1999) used relationships between incompatible trace element ratios that are sensitive to the partial melting process, such as La/Yb, Sm/Nd and Lu/Hf, to infer that the degree of partial melting for the Hawaiian picrites was

between 4 to 10%. These authors also indicated that the average degree of partial melting increases in the sequence: Loihi < Koolau < Kilauea < Mauna Kea < Kohala ≤ Hualalai ≤ Mauna Loa. However, a significant assumption of their melting model involves a common source composition for all the picrites, which they modeled as a mixed spinel and garnet lherzolite source.

In a similar fashion, Feigenson et al. (1996; 2003) used REE inverse modeling to estimate the degree of partial melting necessary to produce Mauna Kea basalts, ranging from alkalic to tholeiitic in composition, in the HSDP drill cores. The primary magmas at Mauna Kea were determined to result from 8 to 15% partial melting of the mantle source for alkalic and tholeiitic basalts respectively, based on equilibrium and accumulated fractional melting models of calculated primary magmas. Their primary magma for Mauna Kea was estimated to contain 19 to 21% wt.% MgO, which is higher than other estimates for Hawaiian primary magmas which suggest that Hawaiian primary magmas contain ~16 wt.% MgO (e.g. Hauri, 1996; Norman and Garcia, 1999).

Sims et al. (1995; 1999) examined U-series disequilibria in Hawaiian basalts, ranging from basanitic to tholeiitic in composition, to determine melting zone porosity and mantle upwelling rates in the Hawaiian system. Their modeling indicates that total melt fractions range from 3% for alkali basalts up to 15% for tholeiitic basalts. In a similar study of U-series disequilibria, Pietruszka et al. (2006) modeled Kilauean basalts as a result of an average of 10% partial melting. These melting models assume a constant melt productivity rate, and are reliant on the thickness of the melting zone. U-series disequilibria studies also require an accurate

knowledge of eruption age and suitable partition coefficients for U, Th, Ra and Pa in an presumed source mineralogy.

Despite different analytical and theoretical methods, the three melting models outlined above all provide similar estimates of the maximum degrees of partial melting (10 to 15%). For the purposes of our study, we use the relative degrees of partial melting outlined by Norman and Garcia (1999), coupled with conservative melting ranges (a 5% melting window) for each volcanic center (Table 2.2). The Norman and Garcia (1999) melting model best describes our picritic sample suite for several reasons: i) several samples from Norman and Garcia (1999) are included in our current work; ii) we estimate a similar parental melt MgO content of 16 wt.% (Ireland et al., 2009); and, iii) La/Yb, Lu/Hf and Sm/Nd ratios for each volcanic center (our data; Norman and Garcia, 1999; Gurriet, 1998; see Supplemental Table 2.S2) mirror the trends observed by Norman and Garcia (1999). Accordingly, we model Hualalai and Mauna Loa from 7.5 to 12.5% partial melting, Kohala, Kilauea, Mauna Kea and Koolau from 5 to 10% partial melting and Loihi from 2.5 to 7.5% partial melting.

2.4.3 W abundances of Hawaiian mantle source regions

To infer the W content for the mantle source regions of the Hawaiian shield volcanoes, an equilibrium batch melting model is employed (e.g., Shaw, 1970):

$$\left(\frac{C_l}{C_o} = \frac{1}{D + (1-D)F} \right)$$

with the parameters for the bulk partition coefficient (D), parental melt concentration and degree of partial melting (F) outlined above, where C_l and C_o are

the parental melt composition and mantle source composition respectively. Since W

behaves incompatibly during mantle melting, aggregated fractional melting and

equilibrium melting models yield essentially identical results. Following the

equilibrium melting model described above, we generate estimates for the W content

of the Hawaiian mantle source regions of 9 ± 2 (2σ) ng/g, 11 ± 5 ng/g, 10 ± 4 ng/g, 12

± 4 ng/g, 10 ± 5 ng/g, 8 ± 7 ng/g and 11 ± 5 ng/g for Hualalai, Mauna Loa, Kohala,

Kilauea, Mauna Kea, Koolau and Loihi respectively (Figure 2.3; Table 2.2).

Overall, the mean W contents of the mantle sources for the Hawaiian shield

volcanoes show a limited range of 8 to 12 ng/g with all calculated source

compositions within statistical uncertainty of each other. The similar W

concentrations in the mantle sources of each individual Hawaiian shield volcano

suggest that the mantle components that contribute to each shield volcano have

comparable absolute abundances of W, as well as analogous W/U ratios.

Accordingly, the mean Hawaiian source region is determined to have 10 ± 3 (2σ)

ng/g W, which is three-times more enriched than the Depleted MORB Mantle

(DMM; 3.0 ± 2.3 ng/g W), but comparable to the Primitive Mantle (PM: 13 ± 10 ng/g

W; Arevalo and McDonough, 2008). The mean W abundance of the Hawaiian

source, as determined in this study, is also consistent with the approximation by

Hawkesworth and Scherstén (2007), who estimated the Hawaiian source to contain

between 8 to 12 ng/g W based on Th/W ratios of similar picritic samples.

Similarly, the U abundances for the mantle sources of each volcanic center were

calculated following the same modeling parameters as outlined above. This

calculation not only provides an estimate for mantle source U abundance, but is also

Table 2.2: Estimates of the source composition of Hawaii from various shield volcano parental melts

Hawaiian Shield Volcano	Hualalai	Mauna Loa	Kohala	Kilauea	Mauna Kea	Koolau	Loihi
Method 1							
Parental Melt W (ng/g)	85 ± 6	-	133 ± 20	155 ± 21	-	-	214 ± 10
Degree of Partial Melting (F)	7.5-12.5	-	5-10	5-10	-	-	2.5-7.5
Mantle Source W (ng/g)	9 ± 2	-	10 ± 4	12 ± 4	-	-	11 ± 5
Linear Regression Results							
Slope	-2.7 ± 0.2	-	-4.4 ± 0.6	-4.8 ± 0.7	-	-	-7.0 ± 0.1
y-intercept	129 ± 4	-	203 ± 16	232 ± 18	-	-	326 ± 4
Parental Melt U (ng/g)	132 ± 10	-	212 ± 30	290 ± 30	-	-	263 ± 31
Degree of Partial Melting (F)	7.5-12.5	-	5-10	5-10	-	-	2.5-7.5
Mantle Source U (ng/g)	13 ± 3	-	16 ± 6	22 ± 8	-	-	13 ± 7
Linear Regression Results							
Slope	-4.3 ± 0.3	-	-6.9 ± 0.9	-9.2 ± 0.9	-	-	-8.6 ± 0.8
y-intercept	200 ± 7	-	324 ± 25	437 ± 24	-	-	400 ± 26
Method 2							
Parental Melt W (ng/g)	83 ± 18	111 ± 40	129 ± 39	149 ± 42	127 ± 46	104 ± 84	185 ± 20
Degree of Partial Melting (F)	7.5-12.5	7.5-12.5	5-10	5-10	5-10	5-10	2.5-7.5
Mantle Source W (ng/g)[a]	8 ± 3	11 ± 5	10 ± 4	11 ± 5	10 ± 5	8 ± 7	9 ± 5
Parental Melt U (ng/g)	129 ± 27	178 ± 40	206 ± 60	276 ± 77	231 ± 83	161 ± 127	225 ± 51
Degree of Partial Melting (F)	7.5-12.5	7.5-12.5	5-10	5-10	5-10	5-10	2.5-7.5
Mantle Source U (ng/g)[a]	13 ± 4	13 ± 4	15 ± 7	21 ± 9	17 ± 9	12 ± 10	13 ± 7
Averages							
Mantle Source W (ng/g)[b]	10 ± 3						
Mantle Source U (ng/g)[b]	15 ± 7						

[a] a bulk crystal/melt partition coefficient (D) of 0.001 was assumed for both W and U mantle source calculations
[b] averages calculated using *Method 1* for Hualalai, Kohala, Kilauea and Loihi, and *Method 2* for Mauna Loa, Mauna Kea and Koolau
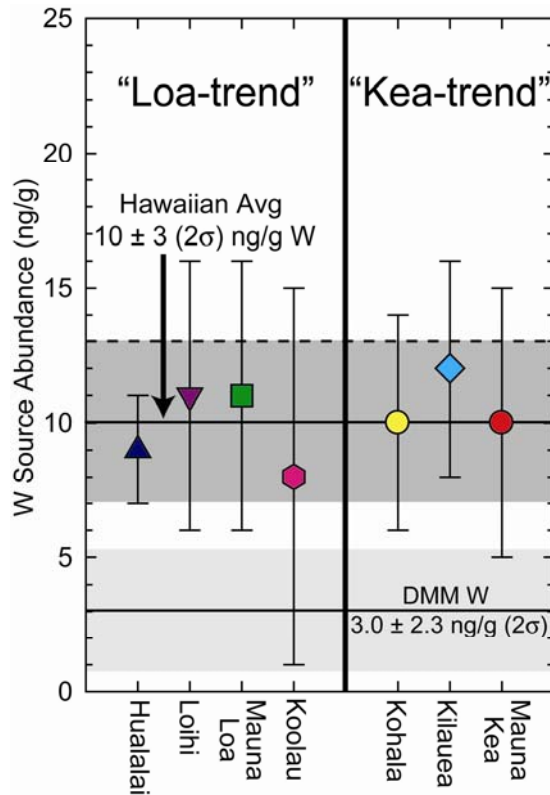
Figure 2.3: The estimated W abundances for the mantle source regions of Hualalai, Mauna Loa, Kohala, Kilauea, Mauna Kea, Koolau and Loihi are estimated to be 9 ± 2 (2σ) ng/g, 11 ± 5 ng/g, 10 ± 4 ng/g, 12 ± 4 ng/g, 10 ± 5 ng/g, 8 ± 7 ng/g and 11 ± 5 ng/g W, respectively. The average W source abundance is 10 ± 3 ng/g (dark shaded area), which is similar to that of PM (13 ± 10 ng/g W, dashed line), but three-times greater than DMM (3.0 ± 2.3 ng/g W; lightly shaded area).

an independent test of the consistency of our W modeling. The estimated U

abundances for the mantle source regions of Hualalai, Mauna Loa, Kohala, Kilauea,

Mauna Kea, Koolau and Loihi are 13 ± 3 (2σ) ng/g, 13 ± 4 ng/g, 16 ± 6 ng/g, 22 ± 8

ng/g, 17 ± 9 ng/g, 12 ± 10 ng/g and 13 ± 7 ng/g U respectively, with a mean value of

15 ± 7 ng/g U. These results demonstrate excellent agreement with those derived

from W abundances, with the mean Hawaiian mantle source having a W/U ratio of

≈ 0.65 and an U abundance three-times greater than DMM (4.7 ± 1.4 ng/g U; Salters

and Stracke, 2004), but similar to PM (20 ± 8 ng/g U; McDonough and Sun, 1995).

2.5 Origin of W in the Hawaiian source regions

2.5.1 Source components in the Hawaiian plume

Typically, three source components are invoked to explain the range of isotopic

variations amongst the Hawaiian shield volcanoes (Staudigel et al., 1984; West et al.,

1987; Kurz et al., 1996; Eiler et al., 1996). These three end-members are best

expressed by lavas from Mauna Kea, Loihi and Koolau (Makapuu-stage lavas). The

Kea component is characterized by relatively low $^{87}Sr/^{86}Sr$ and $^{187}Os/^{188}Os$, as well as

high $^{143}Nd/^{144}Nd$, $^{176}Hf/^{177}Hf$ and Pb isotopic ratios (Lassiter et al., 1996; Blichert-

Toft et al., 1999). Conversely, the Loihi component, which may represent a relatively

undepleted deep mantle reservoir, is defined by more radiogenic Sr and Os, and less-

radiogenic Nd, Hf and Pb isotopes relative to the Kea component. This end-member

is also distinguished by high $^{3}He/^{4}He$ ratios (Kurz et al., 1983; Mukhopadhyay et al.,

2003). The Koolau (Makapuu) component, which is not characterized by any of the

samples analyzed here, occupies the isotopic extreme with the highest ^{87}Sr/^{86}Sr and ^{187}Os/^{188}Os, coupled with lowest ^{143}Nd/^{144}Nd, ^{176}Hf/^{177}Hf and Pb isotopic ratios seen in Hawaiian lavas (West et al., 1987; Roden et al., 1994; Hauri, 1996; Lassiter and Hauri, 1998; Blichert-Toft et al., 1999; Huang and Frey, 2005). A fourth component, which may not significantly contribute to the shield stage volcanoes analyzed here, may be required to explain Pb characteristics of some post-shield stage Hawaiian lavas (Abouchami et al., 2000; Mukhopadhyay et al., 2003).

The surface manifestation of the three dominant components of the Hawaiian source region is expressed as two geographically parallel, but geochemically distinct trends, commonly referred to as the Kea- and Loa-trends (e.g., Frey and Rhodes, 1993; Hauri, 1996; Lassiter et al., 1996; Ren et al., 2005). Huang et al. (2005) suggested that the Kea-trend volcanoes (Mauna Kea, Kilauea, Kohala) are dominated by the Kea and Loihi source components with negligible contribution from the Koolau component. The Loa-trend volcanoes (Mauna Loa, Loihi, Hualalai, Lanai, Koolau), on the other hand, are controlled by the Loihi and Koolau components with insignificant contribution from the Kea component. In the following sections, we model the origin of the apparent W enrichment observed in the composite Hawaiian source region.

2.5.2 Recycled oceanic crust and sediment in Hawaiian mantle sources

2.5.2.1 Tungsten mobility during subduction

To consider if recycled oceanic crust and sediment may influence the W content of the Hawaiian mantle source regions, the mobility of W during subduction must be

addressed. Although Kishida et al. (2004) and Arnórrson and Óskarsson (2007) illustrate that W abundances are positively correlated with highly fluid-mobile elements (e.g., B) and are enriched in hydrothermal fluids relative to ambient seawater, Noll et al. (1996) found that W/Th ratios in a suite of subduction-related magmas: i) overlap with those of typical OIB and MORB; ii) do not decrease systematically with distance from the back-arc; and, iii) are independent of B/La ratios (a tracer of fluid flux), suggesting limited (if any) mobilization of W by hydrothermal fluids during subduction. Further, data from Noll (1994) indicate that W/Ba ratios in some arc lavas are actually depleted due to the preferential fluid-mobility of Ba compared to W in hydrothermal systems, and the continental crust is not enriched in W relative to Ba, Th or U, as would be expected if W was significantly more fluid-mobile (such as B, Pb, As and Sb).

König et al. (2008) have recently asserted that W behaves as a fluid-mobile species in hydrothermal systems based on the significant scatter seen in W/Th ratios in a representative sample suite of subduction-related volcanic rocks from the Solomon Islands and Cyprus, but the average W/U ratio of these samples is statistically indistinguishable from typical MORB samples. Additionally, the Cyprus samples show a similar magnitude of scatter in Nb/U and Ba/Th ratios but constant Th/U ratios that are within the realm of typical MORB rocks, indicating variable fluid mobility between all high field strength elements, which are generally considered immobile in fluid systems. Thus, W/U may be selectively fractionated to some degree by fluid systems, but systematic variations have yet to be documented and, thus, the fluid mobility of W, particularly when compared to U, has yet to be

resolved. For the purposes of our modeling, it is assumed that W is conserved during the subduction process.

2.5.2.2 Addition of recycled crust to the Hawaiian mantle source regions

The recycling of oceanic crust, including associated pelagic sediment, into the deep mantle is one of the dominant paradigms for the introduction of chemical heterogeneities into the source region of OIB (e.g., Hofmann and White, 1982; Hofmann, 1997, 2003 and references therein). For Hawaii, there is abundant geochemical support for the incorporation of recycled oceanic crustal materials in the Koolau component, as well as in the mantle sources of Loa-trend volcanoes (e.g., Bennett et al., 1996; Eiler et al., 1996; Hauri, 1996; Hofmann and Jochum, 1996; Lassiter and Hauri, 1998; Blichert-Toft et al., 1999; Sobolev et al., 2000, 2005). The presence of variable proportions and types of recycled materials may explain the trace element and isotopic characteristics of the Hawaiian shields and the variations between individual volcanic centers. Crustal recycling is also consistent, to a first order, with the W (and U) enrichment of the Hawaiian sources relative to the DMM.

Typical oceanic crust contains on the order of ~30 ng/g W, consistent with 8 to 12% partial melting of a DMM source (3 ng/g W; Arevalo and McDonough, 2008). Sediment is generally more enriched in W than oceanic crust, reaching concentrations in excess of ~1400 ng/g W for upper crustal-derived sediments (Rudnick and Gao, 2003; Hu and Gao, 2008). Pelagic sediments contain even higher concentrations of W than upper continental crust, with an average of ~2700 ng/g W (Strekopytov, 1998). The recycled component in the Hawaiian source region may contain as much

43

as 3% sediment derived from the upper crust without resulting in anomalous Nb/U ratios outside the variance seen in the Hawaiian lavas analyzed in this study. Here we model a hypothetical recycled package containing 97% oceanic crust and 3% upper crustal sediment resulting in a subducted package with ~70 ng/g W, consistent with the crust-to-sediment proportions estimated in the Koolau mantle end-member based on O and Os isotopes (Bennett et al., 1996; Lassiter and Hauri, 1998), presuming W is conserved during subduction (Figure 2.4).

If the Hawaiian source region ultimately originates from a depleted end-member, modeled here to be DMM, that is variably contaminated by a recycled component similar to our model recycled package, two-component mixing calculations require the addition of between 3 and 20% recycled materials to the DMM to satisfy the estimated W concentration in the sources of the individual shield volcanoes, and between 5 to 20% recycled material to satisfy the mean W budget of the composite Hawaiian source region. The distinct isotopic signatures displayed by Kea-trend and Loa-trend volcanic rocks, however, require either different proportions of recycled components, or incorporation of recycled components of different ages. Given the comparable W concentrations among the Hawaiian shield sources, the isotopic differences between volcanic centers may best be interpreted as the result of recycled materials with different mean ages. For example, the compositions of the Kea-trend volcanic centers can be satisfied by recycling 10 to 15% of young oceanic crust and sediment, whereas the Loa-trend trend volcanic rocks would require similar proportions of an ancient (>1.8 Ga) crust + sediment package in order to account for
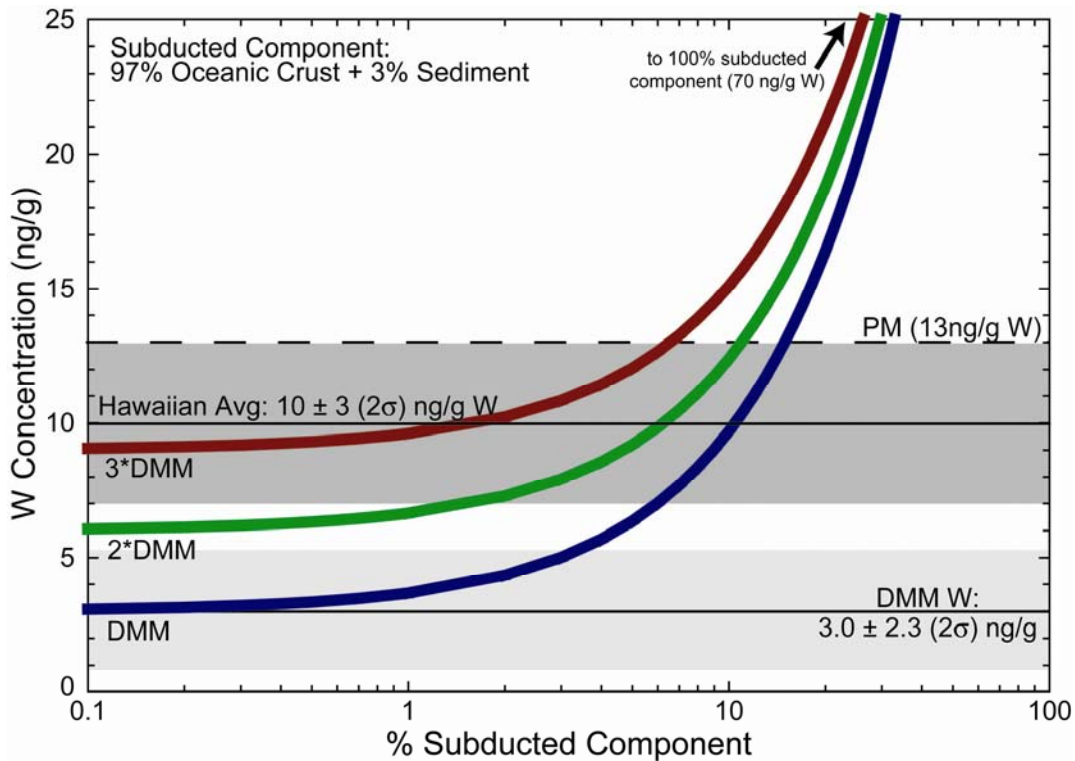
Figure 2.4: Addition of a model subducted component to various mantle reservoirs.

The subducted package consists of 97% oceanic crust (30 ng/g W) and 3%

continental sediment (1400 ng/g W), resulting in a recycled package containing ~70

ng/g W. Adding such a recycled package to DMM (3 ng/g W) requires 5 to 20% of a

subducted component to produce the average Hawaiian source W abundance.

However, if a more enriched reservoir (e.g., 3*DMM) is involved, no recycled

material may be required to explain the estimated W source characteristics. With this

second scenario, the addition of some recycled material is still permissible within the

uncertainties of the model, which may explain the isotopic differences between Loa-

and Kea-trend volcanoes. The dark shaded area represents the average W source

abundance (10 ± 3 ng/g W), while the lightly shaded area shows the composition of

DMM (3.0 ± 2.3 ng/g W).

the relatively high Sr and Os isotopic compositions, and the relatively low Nd, Hf and Pb isotopic ratios (Bennett et al., 1996; Lassiter and Hauri, 1998).

An alternative explanation for the apparent W enrichment of the Hawaiian source region is that the Hawaiian source does not originate from a depleted end-member like DMM, but rather from an end-member that is less depleted in incompatible elements prior to crustal recycling. This scenario is consistent with some isotopic studies which have suggested that the DMM is not directly involved in producing Hawaiian magmas (Bennett et al., 1996; Lassiter and Hauri, 1998; Blichert-Toft et al., 1999). If the Hawaiian source samples a primary component that is less depleted in incompatible trace elements relative to DMM, then the incorporation of recycled material in the Hawaiian source is not necessary to account for the observed enrichment of W (Figure 2.4). However, for this scenario, the addition of variable proportions of recycled crust (up to 10 to 12%) to account for the isotope characteristics associated with each volcanic center is permitted because this addition would not be resolvable within the W abundance uncertainties reported for the volcanic centers. For example, although the abundance of W in the sources of Mauna Loa and Loihi lavas (11 ± 5 ng/g) is within uncertainty of the rest of the shield volcanoes, the addition of as much as 11% recycled material to an undepleted source with ~9 ng/g W could be accommodated within the uncertainty of the estimated source composition. This scenario is consistent with the suggestion that Loa-trend volcanoes may involve some recycled material (i.e., the Koolau component), while the Kea-trend volcanoes may have incorporated little to none (Huang et al., 2005).

46

The ultimate origin of this hypothetical, less-depleted reservoir is uncertain. It would most likely represent a reservoir that has experienced little prior melt depletion, thereby preserving high incompatible element concentrations (McKenzie and O'Nions, 1995). If such a reservoir exists, it would likely be located in the deep mantle in order to avoid mixing and/or processing in the upper mantle over geologic time and may be related to the FOZO mantle component (FOcused ZOne; Hart et al., 1992; Hofmann, 2003). To account for the isotopic characteristics of Kea-trend volcanoes, this reservoir would have to be isotopically similar to the Kea end-member. Huang et al. (2005) showed that the Loihi end-member component is similar to the Kea end-member in terms of $^{87}Sr/^{86}Sr$, $^{143}Nd/^{144}Nd$ and $^{176}Hf/^{177}Hf$, albeit slightly more enriched. If this hypothetical reservoir is related to the Loihi end-member, the isotopic constraints of both Kea- and Loa-trend volcanoes can be satisfied.

2.5.3 Core-mantle interaction?

A role for core-mantle interaction in the Hawaiian plume has been suggested based on observed coupled enrichments in ^{186}Os-^{187}Os isotopes in Hawaiian picrites (Brandon et al., 1999), as well as elevated Fe/Mn ratios in Hawaiian basalts (Humayun et al., 2004). These authors proposed that the enrichments may result from the incorporation of small amounts (≤ 0.5 wt.%) of outer core material to the sources of some Hawaiian volcanoes. However, a lack of corresponding enrichments in the highly siderophile element abundances of the Hawaiian sources (Bennett et al., 2000; Ireland et al., 2009), recent thermal models for the core suggesting the

relatively late inception of inner core crystallization (Buffett et al., 1996; Labrosse et al., 2001), and the discovery of other possible mechanisms to create coupled ^{186}Os-^{187}Os enrichments (Smith, 2003; Hawkesworth and Scherstén, 2007; Luguet et al., 2008), have cast doubt on this hypothesis. Tungsten isotopes have been suggested as a more robust tracer of core-mantle interactions (Scherstén et al., 2004; Brandon and Walker, 2005; Hawkesworth and Scherstén, 2007; Takamasa et al., 2009) because the silicate portion of the Earth is isotopically enriched in ^{182}W (the decay product of ^{182}Hf) relative to chondrites. Consequently, mass balance arguments suggest that Earth's core has approximately 2 parts in 10,000 (ε_w units) less ^{182}W than the silicate Earth (Kleine et al., 2002).

The addition of core material to the Hawaiian source could, therefore, lead to a modest depletion in ^{182}W in lavas relative to the ambient upper mantle. Towards this end, Scherstén et al. (2004) observed no difference in W isotopic compositions between a terrestrial standard and three Hawaiian samples (H-11, Lo-02-02 and Lo-02-04) that had previously been suggested to record a core component (Brandon et al., 1999), leading these authors to conclude that no core material is involved in the Hawaiian source regions. The Scherstén et al. (2004) model, however, was strongly dependent on the assumed concentration of W in the mantle source that would have been contaminated with W from the outer core.

Our current study suggests that the W content of the mean Hawaiian source region (10 ± 3 ng/g) is most consistent with the "preferred" model of Scherstén et al. (2004) that assumed an initial W concentration of 8 ng/g. The addition of 0.5 wt.% of outer core material to the average Hawaiian source would raise the source W

concentration by only ~2 ng/g, which is unresolvable within the uncertainty on the mantle source W estimates. Arevalo and McDonough (2008) also showed that the incorporation of 0.5 wt.% core material would not have a resolvable effect on the W/U ratios.

However, the physical addition of this amount of outer core material would result in a ε_w of -0.45, which should be resolvable by W isotopes. The lack of an outer core W signature in the Hawaiian rocks suggests that either core-mantle interaction does not occur, or that mechanisms other than physical mixing may operate at the core-mantle boundary (Puchtel and Humayun, 2000; 2005; Humayun et al., 2004).

2.6 Conclusions

1) The concentration of W in Hawaiian picrites is highly variable, but within most individual shield volcanoes, linear trends are observed between W and MgO. The W/U ratios for Hawaiian picrites have an average of 0.62 ± 0.19 (2σ), which is indistinguishable from the W/U ratio for the sampled silicate Earth.

2) Estimates of the W content of the parental melts for the Hawaiian shield volcanoes were obtained by two different techniques, which yield statistically indistinguishable results. The parental melts for Hualalai, Mauna Loa, Kohala, Kilauea, Mauna Kea, Koolau and Loihi are determined to contain 85 ± 6 (2σ) ng/g, 111 ± 40 ng/g, 133 ± 20 ng/g, 155 ± 21 ng/g, 127 ± 46 ng/g, 104 ± 84 ng/g and 214 ± 8 ng/g W, respectively.

3) Correspondingly, the W abundances for the Hawaiian mantle sources are estimated to contain 9 ± 2 (2σ) ng/g, 11 ± 5 ng/g, 10 ± 4 ng/g, 12 ± 4 ng/g, 10 ± 5 ng/g, 8 ± 7 ng/g and 11 ± 5 ng/g for Hualalai, Mauna Loa, Kohala, Kilauea, Mauna Kea, Koolau

and Loihi respectively. As a result, the mean Hawaiian source region contains 10 ± 3 (2σ) ng/g W, about three-times more than the DMM (3.0 ± 2.3 ng/g W), but comparable to the PM (13 ± 10 ng/g W). The estimated U abundances for the mantle sources of the Hawaiian volcanic centers are consistent with those derived from W abundances.

4) Bulk addition of recycled oceanic material to the DMM alone can explain the enriched W composition of each individual Hawaiian shield volcano, but the mean age of the recycled material in Kea- and Loa-trend volcanoes would have to be fundamentally different to satisfy isotopic constraints. However, if the Hawaiian source regions originate from a less depleted mantle reservoir, crustal recycling is not necessary to produce the estimated source W abundances, although the addition of some recycled oceanic crust can be accommodated within the uncertainties of our model source compositions.

5) The incorporation of minor amounts (≤ 0.5 wt.%) of outer core material is unresolvable within the uncertainty of our W source modeling and W/U ratios, however, this addition should be detectable via W isotopes. The lack of a core W isotopic signature suggests that either core-mantle interaction does not occur, or that mechanisms other than physical mixing may operate at the core-mantle boundary.

Supplemental Material

Table 2.S1: Olivine correction of matrix W concentrations to whole rock W concentrations

Volcano	Sample Name	MgO$_{wr}$ (wt%)[e]	MgO$_{ol}$[b]	MgO$_{gl}$[b]	%ol calc[c]	2σ calc[d]	%ol point count	#points	2σ point count[e]
Mauna Kea									
	MK-1-6[d]	17.24	46.63	6.47	26.8	0.5	23	500	2
Mauna Loa									
	ML-2-50	19.92	49.27	5.49	33.0	0.5			
	ML KAH-1	21.66	49.34				34	500	2
	ML 1868-9	21.48	48.31				36	1000	2
Hualalai									
	H-2	13.63	47.97	4.96	20.2	0.4	19	500	2
	H-7	11.23	47.76	5.91	12.7	0.4	13	500	2
	H-9	11.30	47.88	6.12	12.4	0.4	14	500	2
	H-11	13.67	47.29	6.35	17.9	0.4	18	500	2
	H-27	14.91	48.29	5.97	21.1	0.4			
	H-P	23.19	47.17	7.26	39.9	0.6	44	1000	2
Loihi									
	LO-02-02	24.21	47.31	8.69	40.2	0.7			
	LO-02-04	26.58	46.29	1.89	55.6	0.6			
	158-9	16.57	48.53	7.17	22.7	0.5			
	186-5	19.52	46.67				30	1000	1
	186-11	13.76	45.59				21	1000	1
	187-1	25.16	47.36	6.49	45.7	0.7			
Kilauea									
	KIL-1-18	13.80	48.35				15	1000	1
	KIL-2-3	22.36	48.11				40	500	2
	KIL-2-4	22.55	48.89	4.87	40.2	0.6			
	KIL-3-1	19.24	47.60	5.33	32.9	0.5			
	KIL 1840-2	14.27	47.80				21	500	2
Koolau									
	K98-08	17.78	45.74				29	500	2
	S497-6	21.55	47.78				42	500	2
	S500-5B	21.22	47.98	4.37	38.6	0.5			
Kohala									
	KO-1-10	13.54	46.95				20	500	2
	KO-1-20	9.60	47.26	5.56	9.7	0.3	10	500	1
	KOH-1-28	20.52	48.37	5.52	35.0	0.5			
Lanai									
	LWAW-4	14.48	44.87				15	1000	1
	LWAW-7	11.69	47.92				9	1000	1
Molokai									
	S501-2	28.96	48.05	8.39	51.9	0.8	51	500	2

[a] MgO contents from Ireland et al. (2009) and references therein

[b] average olivine (n=8) and glass (n=5) MgO data collected on a JEOL JXA-8900 electron microprobe at the University of Maryland

[c] % ol calc=(MgO$_{WR}$-MgO$_{gl}$)/(MgO$_{ol}$-MgO$_{gl}$)*100

[d] 2σ calc was calculated assuming an external precision of 1% for MgO$_{WR}$ and 0.2% for MgO$_{gl}$ and MgO$_{ol}$

[e] 2σ point count was calculated using the method from: van der Plas, L. and Tobi, A.C. (1965) A chart for judging the reliability of point counting results. American Journal of Science 263, 37-90.

Table 2.S2: La, Yb, Lu, Hf, Sm and Nd data for Hawaiian picrites

Volcano	Sample Name	La (μg/g)	Yb	Lu	Hf	Sm	Nd
Mauna Kea							
	MK 1-6[a]	10.32	1.99	0.28	3.91	4.92	18.10
Mauna Loa							
	ML 2-50[a]	5.45	1.41	0.20	2.34	3.01	10.40
	ML KAH-1[a]	6.42	1.46	0.21	2.59	3.30	11.70
	ML 1868-9[a]	6.02	1.26	0.18	2.28	3.05	11.00
Hualalai							
	H-2[c]	6.80	1.51	0.20	2.15	3.68	12.92
	H-7[b]	7.41	1.76	0.22	2.74	3.84	14.30
	H-9[c]	9.24	2.10	0.29	3.09	4.91	17.33
	H-11[a]	7.19	1.65	0.23	2.61	3.52	12.60
	H-27[c]	7.08	1.76	0.25	2.56	3.81	13.11
	H-P[c]	5.01	1.36	0.18	1.99	3.00	10.00
Loihi							
	Lo-02-02[a]	7.73	1.03	0.14	2.16	2.69	11.10
	Lo-02-04[a]	8.43	1.08	0.15	2.26	2.94	11.90
Kilauea							
	KIL 1-18[a]	9.94	1.71	0.23	3.37	4.43	17.20
	KIL 2-3[c]	8.82	1.49	0.20	2.55	4.07	15.02
	KIL 2-4[c]	10.19	1.85	0.24	3.25	4.63	16.97
	KIL 3-1[c]	13.77	2.13	0.30	4.33	5.92	22.61
	KIL 1840-2[a]	9.68	1.71	0.24	3.37	4.52	17.00
Koolau							
	K 497-6[c]	8.70	1.57	0.23	2.95	4.35	15.77
	K 500-5B[c]	6.61	1.28	0.17	2.00	3.28	12.20
Kohala							
	Ko 1-10[c]	9.98	1.88	0.25	3.04	4.86	18.05
	Ko 1-20[c]	13.58	2.45	0.31	4.30	6.66	24.90
	Ko 1-28[a]	6.26	1.35	0.19	2.27	3.00	11.00

[a]Norman and Garcia, 1999

[b]Gurriet, 1988

[c]this study

Chapter 3: Highly siderophile element and [187]Os isotope systematics of Hawaiian picrites: Implications for parental melt composition and source heterogeneity

Abstract

Absolute and relative abundances of the highly siderophile elements (HSE) are reported for 52 Hawaiian picrites (MgO >13 wt%) and 7 related tholeiitic basalts (~7-12 wt% MgO) from nine volcanic centers (Mauna Kea, Mauna Loa, Hualalai, Loihi, Koolau, Kilauea, Kohala, Lanai and Molokai). The parental melts for all the volcanic centers are estimated to contain ~16 wt% MgO. Samples with higher MgO contents contain accumulated olivine. Samples with lower MgO contents have lost olivine.

Osmium, Ir and Ru abundances correlate positively with MgO. These elements are evidently sited in olivine and associated phases (i.e. chromite and PGE-rich trace phases) and behaved compatibly during crystal-liquid fractionation of picritic magmas. Platinum, Pd and Re show poor negative correlations with MgO. These elements behaved modestly incompatibly to modestly compatibly during crystal-liquid fractionation. Effects of crustal contamination and volatile losses on parental melt compositions were likely minor for most HSE, with the exception of Re for subaerially erupted lavas. The HSE abundances for the parental melts of each volcanic center are estimated by consideration of the intersections of HSE-MgO

trends with 16 wt% MgO. The abundances in the parental melts are generally similar for most volcanic centers: 0.5 ± 0.2 ppb Os, 0.45 ± 0.05 ppb Ir, 1.2 ± 0.2 ppb Ru, 2.3 ± 0.2 ppb Pt, and 0.35 ± 0.05 ppb Re. Samples from Loihi contain higher abundances of Pt, Pd and Re which may be a result of slightly lower degrees of partial melting. Hualalai parental melts have double the Os concentration of the other centers, the only discernable HSE concentration heterogeneity among these widely distributed volcanic centers.

Two types of HSE patterns are observed among the various picrites. Type-2 patterns are characterized by greater fractionation between IPGE (Os, Ir, Ru) and PPGE (Pt, Pd), with higher Pt/Ir and Pd/Ir ratios than Type-1 patterns. Both pattern types are present in most of the volcanic centers and do not correlate with MgO content. The differences between the two patterns are attributed to the inter-relationship between partial melting and crystal-liquid fractionation processes, and likely reflect both differences in residual sulfides and the loss of chromite-associated IPGE alloys or Mss during magma ascent.

The ranges in $^{187}Os/^{188}Os$ ratios obtained for rocks from each of these volcanic centers are in good agreement with previously published data. Variations in $^{187}Os/^{188}Os$ isotope ratios between volcanic centers must reflect ancient source heterogeneities. The variations in Os isotopic compositions, however, do not correlate with absolute or relative abundances of the HSE in the picrites. Minor source heterogeneities have evidently been masked by partial melting and crystal-liquid fractionation processes. There is no evidence of derivation of any picritic lavas

from sources with highly heterogeneous HSE, as has been implied by recent studies purporting to explain ^{186}Os isotopic heterogeneities.

Keywords: platinum-group elements; highly siderophile elements; fractionation; D values; parental melt composition; Hawaii; Os isotopes

3.1 Introduction

The highly siderophile elements (HSE; Os, Ir, Ru, Pt, Pd, Rh, Re and Au) have a high affinity for metallic Fe and, to a lesser degree, a high affinity for sulfides (Barnes et al., 1985; Walker et al., 2000). Abundances of HSE, coupled with Os isotopes (^{187}Re→^{187}Os + $^{-}$β; λ = 1.67x10^{-11} yr^{-1}), are important tools for characterizing the geochemical history of mantle reservoirs (Barnes et al., 1985; Brügmann et al., 1987; Barnes and Picard, 1993; Rehkämper et al., 1997; 1999; Brandon and Walker, 2005). The absolute and relative abundances of HSE in mantle rocks can be modified by, and therefore potentially be used to detect, diverse mantle processes including partial melting, melt refertilization, other forms of metasomatism, and crustal recycling (e.g., Rehkämper et al., 1997; Lassiter and Hauri, 1998; Rehkämper et al., 1999; Momme et al., 2003; Bockrath et al., 2004). Further, the core contains about 98% of the Earth's inventory of HSE with some models suggesting that the outer core may contain ~300 times greater HSE abundances relative to the mantle (McDonough, 2003). Minor chemical exchange between the core and mantle could result in mantle with distinctive HSE and Os isotopic characteristics (Walker et al., 1995; Snow and Schmidt, 1998; Brandon and Walker, 2005).

Mantle plumes are typically defined as the focused, upward flow of mantle material originating at a boundary layer within the Earth (Morgan, 1971; Campbell and Griffiths, 1990). Generally, mantle plumes occur in intraplate settings (e.g. Hawaii, Deccan Traps), but are also present on mid-ocean ridges (e.g. Iceland). The sources of materials present in plumes, among other plume-related issues, remain highly controversial (Campbell and Griffiths, 1990; Allègre and Moreira, 2004; Anderson, 1998; Smith, 2003; Baker and Jensen, 2004; Schersten et al., 2004; Brandon and Walker, 2005). The abundances of the HSE in plumes could provide new insights to the origin and mechanics of plumes, given the numerous prior studies of plumes that have invoked the presence of materials as diverse as recycled crust and contributions from the outer core (Brandon et al., 1999; Lassiter and Hauri, 1998; Smith, 2003; Baker and Jensen, 2004, Schersten et al., 2004).

Here we consider HSE abundances and $^{187}Os/^{188}Os$ ratios in Hawaiian lavas. The Hawaiian mantle plume is an important example of intra-plate volcanism. It is the largest and hottest currently active plume (Sleep, 1990; 1992). Both geophysical and geochemical studies have suggested that the Hawaiian mantle plume may originate at the core-mantle boundary (Brandon et al., 1999; Montelli et al., 2004). Thus, the Hawaiian mantle plume has been the focus of numerous geochemical studies that have attempted to assess the chemical characteristics of the plume source (Eiler et al., 1996; Hauri et al., 1996; Lassiter and Hauri, 1998; Brandon et al., 1999; Norman and Garcia, 1999; Bennett et al., 2000; Humayun et al., 2004; Bryce et al., 2005; Sobolev et al., 2005; Nielsen et al., 2006; Bizimis et al., 2007). For example, some previous studies of $^{187}Os/^{188}Os$ ratios in Hawaiian basalts have concluded that recycled oceanic

crust is an important component in the source region of the Hawaiian plume (Hauri et al., 1996; Lassiter and Hauri, 1998).

The absolute and relative HSE abundances in Hawaiian lavas have been considered in several studies. For example, Tatsumi et al. (1999) examined Mauna Loa and Kilauea tholeiites and hypothesized that the observed fractionations of the HSE resulted from the crystallization of phases such as chromite, olivine and clinopyroxene. They also suggested an important role for the separation of sulfides from the parental magmas. Bennett et al. (2000) studied the concentrations of several HSE along with $^{187}Os/^{188}Os$ ratios in a suite of picritic rocks from six Hawaiian shield volcanoes, several of which are included in the present study. They concluded that the variable HSE abundances in these picrites directly reflect plume source compositions, and suggested that residual sulfides in the plume source may be responsible for the absolute HSE abundance variations between the different Hawaiian volcanoes. They noted that the effects of the residual sulfides may obscure the contributions of various mantle HSE reservoirs to the plume.

To further efforts to better understand the HSE and ^{187}Os systematics of Hawaiian picrites, 52 picrites (MgO >13 wt%) were collected from nine volcanic centers (Mauna Kea, Mauna Loa, Hualalai, Loihi, Kilauea, Kohala, Koolau, Lanai and Molokai), including samples from both Hawaiian Scientific Drilling Project holes (HSDP-1 and -2). This sample suite represents some of the most primitive Hawaiian shield volcano melts. They may, thus, be particularly useful in preserving information about the concentrations of HSE in the mantle sources of the Hawaiian plume (Norman and Garcia, 1999). Seven related tholeiitic basalts (MgO ~7 to 12

wt%), which are more evolved than the associated picrites, were also included in the study as a comparison for crystal-liquid fractionation processes. The objectives of this study are: (1) to better define the relative and absolute abundances of HSE in primitive plume-derived lavas, (2) to compare the concentrations of HSE in the parental melts for the different Hawaiian volcanic centers, (3) if differences are resolved, to identify the causes of HSE variations among these lavas, and (4) to identify whether there are resolvable differences in the HSE characteristics of the mantle sources, and if so evaluate their causes.

3.2 Samples

The samples analyzed in this study are predominantly primitive tholeiitic picrites, which are representative of the shield building stage of Hawaiian volcanism (Norman and Garcia, 1999). The picritic lavas were derived from high density melts that erupted on the flanks of the Hawaiian volcanoes, and may have bypassed the summit reservoirs of the volcanoes (e.g., Garcia et al., 1995). These rocks are, therefore, less likely to have been affected by fractionation processes that may operate in high level magma chambers. The degree of partial melting to produce the picrites has been estimated to range from 4 to 10% (Norman and Garcia, 1999).

Samples were obtained from submersible dives and submarine dredge hauls from the submerged flanks of the Hawaiian volcanoes, subaerial flows and from both Hawaiian Scientific Drilling Project holes (Table 3.1). Our samples are from nine Hawaiian volcanoes that span approximately 3 Myr of eruption history. All five of the Big Island volcanoes are represented (Kohala, Hualalai, Mauna Kea, Mauna Loa

and Kilauea), along with samples from Loihi, Koolau (Oahu), Lanai and East Molokai. These samples were selected to provide a representative sampling of the HSE systematics for the Hawaiian picrites on both an intra- and inter-volcanic scale. Samples were collected as 100-400 g hand-sized masses, with the exception of the HSDP core samples (~100 to 200 g of rock chips and powders). For several HSDP samples, considerably smaller amounts of material were available (2-10 g for samples SR0683-5.75, SR0714-11.55, SR0750-12.45, SR0756-13.25, SR00762-4.60 and SR0846-2.80). These samples were only analyzed for abundances of Os and Re, as well as $^{187}Os/^{188}Os$ ratios. The majority of samples contain abundant phenocrysts of olivine (0.5 to 1.0 mm) in a fine grained matrix. Three more evolved samples (Lo 186-11, K98-08 and LWAW-7) also contain small amounts of plagioclase and clinopyroxene phenocrysts. Samples KOH-1-28, H-5, ML-2-50, Kil 1840, LO-02-02, LO-02-04, MK 1-6, H-11, H-23 and ML1868 were also studied by Bennett et al. (1996; 2000).

3.3 Analytical procedures

Visibly weathered surfaces on large hand samples were removed using a diamond rock saw. The samples were polished using SiC sandpaper to remove saw marks and were then broken into cm-sized chips using a high-tensile strength alloy mortar and pestle or with a ceramic-faced jaw crusher. These chips were screened again for weathered pieces and metal contamination. Finally, the samples were ground into a fine powder and homogenized using an agate shatterbox.

Major and trace element data for unpublished samples were obtained from the X-ray Laboratory at Franklin and Marshall College, which utilizes a Phillips 2404 XRF vacuum spectrometer. The accuracy and reproducibility of the analyses are estimated to be ~1% and ~5% for major and minor elements, respectively (Boyd and Mertzman, 1987).

Olivine compositions in polished thin sections were obtained using a JEOL JXA-8900 electron microprobe at the University of Maryland, using a 15 keV accelerating voltage, 20 nA beam current and a 10 μm spot size. A San Carlos olivine standard was analyzed concurrently with samples to monitor the external precision (n=30). External precision (2σ) for SiO_2, FeO, MgO, CaO, NiO and MnO are 0.3%, 0.7%, 0.2%, 4.7%, 3.0% and 7.0% respectively. External precision (2σ) for other trace elements in olivine was 30% for Cr_2O_3, 13% for Al_2O_3 and 19% for CoO.

Methods used in this study for the separation of the HSE are based upon procedures outlined by Shirey and Walker (1995) and Cohen and Waters (1996). Samples were dissolved and equilibrated with spike solutions by acid digestion in Pyrex Carius tubes. Approximately 2.5 g of the finely powdered sample, 3 g of Teflon-distilled concentrated HCl and 6 g of Teflon-distilled concentrated HNO_3 were used in the digestion. Spike solutions enriched in ^{190}Os, ^{185}Re and a mixed ^{191}Ir-^{99}Ru-^{194}Pt-^{105}Pd spike were used. The Carius tubes were sealed with an oxygen-propane torch, agitated and placed in an oven at 240°C for at least 48 hours to digest the sample.

Osmium was separated from the aqueous phase using a carbon tetrachloride (CCl_4) solvent extraction technique. Osmium was then back-extracted from the CCl_4

into concentrated HBr (Cohen and Waters, 1996), prior to a final microdistillation step to further purify the sample (Birck et al., 1997). The other HSE were separated from the aqueous phase by anion exchange chromatography using 2mL of Eichrom AG1X8 anion exchange resin. After several cleaning steps, Re and Ru were collected in 10 mL of 6N HNO_3. Iridium and Pt were collected in 15 mL of concentrated HNO_3. The final cut, containing Pd, was collected in 15 mL of concentrated HCl.

Isotopic measurements of the HSE were completed using two types of mass spectrometers. Osmium concentrations and isotopic compositions were measured by negative thermal ionization mass spectrometry using either a single collector NBS-style mass spectrometer, or a VG Sector-54 mass spectrometer, both at the University of Maryland's Isotope Geochemistry Laboratory. Following microdistillation, sample Os was loaded onto a Pt filament along with $Ba(OH)_2$, and then heated to ~830°C. External precision for $^{187}Os/^{188}Os$ ratios on repeat analyses of an Os standard solution was ±0.2% (2σ). Internal precision on individual samples was generally less than 0.2% ($2\sigma_m$). Osmium blanks averaged 3±1 pg and an $^{187}Os/^{188}Os$ of 0.18± 0.06 (n=8). Because of the high Os concentrations of the samples, blank corrections for Os were minimal. Age corrections do not modify the $^{187}Os/^{188}Os$ obtained.

The other HSE were analyzed by inductively coupled plasma mass spectrometry (ICP-MS) using a Nu Plasma mass spectrometer, at the Plasma Mass Spectrometry Lab at the University of Maryland. Following purification of the HSE via anion exchange chromatography, each of the HSE was analyzed in a static mode using 2 or 3 electron multipliers. Sample and standard solutions were interspersed throughout the analytical sessions to monitor and correct for instrumental fractionation. Samples

were diluted so that signals for the spike isotopes were between 1 and 5 mV. Well-characterized solutions of HSE separated from spiked iron meteorites that were diluted to give signals similar to the samples were occasionally measured to monitor accuracy. External precision (2σ) of these meteoritic standard solutions ranged between 1 and 5% for all elements (n=3). The total procedural blanks for the analyzed elements averaged: 5 ± 3 pg Ir, 14 ± 6 pg Ru, 540 ± 230 pg Pt, 140 ± 60 pg Pd and 4 ± 2 pg Re (n=5). Platinum and Pd blanks improved throughout the analytical session, as an internal cleaning step of the Carius tubes was implemented. All analyses were blank corrected. Duplicates performed on separate aliquots of the same sample powder demonstrated reproducibility ranging from ±1 up to 20% for Re, Ir, and Ru, and up to 30% for Pt and Pd. The larger discrepancy between duplicate runs likely indicates small-scale heterogeneities in the distribution of the HSE within aliquots of sample powder, commonly termed the "nugget effect"; however, the chondrite-normalized HSE patterns are similar between poorly reproduced samples, indicating that this had only a minor effect on the conclusions reached.

Several samples in this study were previously analyzed for some of the HSE by Bennett et al. (1996; 2000). In general, most of the HSE were within 30% of the prior results, however, larger discrepancies as great as 100% were observed. The largest discrepancies were observed between Re abundances, and to a lesser extent, Pt and Pd abundances. The explanation for these discrepancies is not immediately clear, since both studies yielded reproducible results. There are at least three possible causes for the differences. First, different powders were analyzed in each study, prepared from different pieces of the same rock. Therefore, the differences may be a

result of heterogeneities in the distribution of HSE carrier phases in these picritic rocks. This scenario is more likely to account for discrepancies in the platinum-group elements (PGE), rather than Re. Second, the largest inconsistencies for Re occur in subaerially-erupted samples. Rhenium can be lost as a volatile phase via igneous processes (Lassiter, 2003; Sun et al., 2003; Norman et al., 2004). Volatile loss is likely to be greater in subaerially-erupted samples. Third, Bennett et al. (2000) indicated that Carius tube digestion may result in incomplete dissolution of silicate phases, which may also retain a Re component. They implemented an added HF-digestion step to dissolve these phases, which resulted in variations of up to 100% with the Bennett et al. (1996) study. Despite differences in the absolute abundances of HSE, the chondrite normalized HSE patterns reported from the Bennett et al. (2000) study are generally similar to the HSE patterns observed in the present study. These minor differences do not impact our conclusions.

3.4 Results

Major element data for the 52 picrites and 7 tholeiitic basalts are presented in Table 3.1. Whole rock Mg#s ($Mg\# = \dfrac{Mg^{2+}}{Mg^{2+} + Fe^{2+}} * 100$) for the entire sample suite range from 53.7 to 85.4. The Mg#s have been shown to directly correlate with the abundance of olivine phenocrysts in analogous picritic samples (Norman and Garcia, 1999). Average olivine core compositions for each rock are reported in Table 3.2. Typical olivines tend to be normally zoned and have core forsterite (Fo) contents

Table 3.1: Major Element Data for Hawaiian Picrites

Volcano	Sample Name	SiO_2 (wt%)	TiO_2	Al_2O_3	$FeO^\dagger$	$Fe_2O_3^\dagger$	MnO	MgO	CaO	Na_2O	K_2O	P_2O_5	LOI	SUM	Mg#$_{wr}$	Ref
Mauna Kea																
	MK-1-6[M]	49.21	2.04	9.83	11.46		0.18	17.24	7.29	1.76	0.39	0.22		99.62	74.9	1
HSDP-1	R189-8.5B	43.89	1.16	5.99		13.17	0.17	28.25	5.86	0.08	1.15	0.12		99.84	82.5	2
	R197-0.8B	45.63	1.54	7.27		13.19	0.18	23.77	6.66	0.26	1.47	0.16		100.13	79.9	2
	R215-7.2B	45.39	1.49	7.40		12.86	0.17	23.99	6.86	0.19	1.33	0.15		99.83	80.4	2
HSDP-2	SR0129-5.20[+]	46.57	2.88	15.64		13.17	0.18	6.93	11.76	2.19	0.25	0.28	0.26	99.85	53.7	3
	SR0328-3.10	44.66	1.25	6.22		12.81	0.17	27.19	5.81	1.09	0.20	0.13	-0.35	99.53	82.4	3
	SR0346-5.60	46.97	1.86	9.80		12.83	0.18	17.97	8.27	1.60	0.23	0.18	0.00	99.89	75.5	3
	SR0401-2.85	45.03	1.21	6.46		12.96	0.18	26.70	5.75	1.09	0.19	0.12	-0.21	99.69	81.9	3
	SR0450-3.55	45.41	1.33	6.99		12.74	0.18	25.08	6.83	0.98	0.08	0.14	1.06	99.76	81.3	3
	SR0502-4.85	45.26	1.15	6.47		12.75	0.18	26.46	6.30	0.80	0.05	0.11	1.85	99.53	82.0	3
	SR0683-5.75	47.22	1.63	9.10		12.4	0.17	19.55	7.85	1.36	0.15	0.16	0.57	99.59	77.6	3
	SR0714-11.55[+]	49.69	2.33	12.73		12.26	0.18	9.36	10.80	2.00	0.26	0.23	0.18	99.84	62.7	3
	SR0720-18.25	46.96	1.63	8.82		12.53	0.17	20.40	7.42	1.47	0.21	0.17	-0.08	99.78	78.2	3
	SR0741-7.90	46.45	2.00	10.66		12.97	0.18	16.21	9.03	1.75	0.22	0.19	0.17	99.66	73.3	3
	SR0750-12.45	46.63	1.89	10.31		12.77	0.18	17.23	8.71	1.69	0.18	0.18	0.75	99.77	74.8	3
	SR0756-13.25	46.38	1.77	9.70		12.69	0.17	18.91	8.16	1.54	0.21	0.17	0.77	99.70	76.6	3
	SR0762-4.60	46.69	1.82	9.98		12.68	0.18	17.93	8.40	1.63	0.25	0.17	-0.10	99.73	75.7	3
	SR0846-2.80[+]	49.73	2.55	12.33		12.26	0.18	10.00	10.21	2.01	0.31	0.26	0.47	99.84	64.2	3
	SR0891-15.10[M]	46.45	1.52	8.19		12.63	0.18	22.04	7.20	1.24	0.09	0.15	1.30	99.69	79.3	3
	SR0940-18.35[M]	46.99	2.22	11.61		13.18	0.18	13.59	9.71	1.79	0.28	0.20	2.16	99.75	69.4	3
	SR0954-8.00[M]	47.67	1.97	9.64		12.3	0.17	18.03	8.01	1.65	0.23	0.20	0.85	99.87	76.3	3
	SR0964-4.30[M]	44.70	1.08	5.91		12.34	0.17	29.07	5.23	0.80	0.08	0.11	1.47	99.49	83.8	3
Mauna Loa																
	ML-2-50[M]	48.44	1.40	9.46	11.26		0.17	19.92	7.38	1.54	0.22	0.12		99.91	77.8	1
	ML KAH-1	47.81	1.53	8.83	11.47		0.18	21.66	6.68	1.47	0.25	0.15		100.03	78.9	1
	ML 1868-9	47.96	1.37	8.88	11.37		0.18	21.48	6.82	1.46	0.26	0.14		99.92	78.9	1
HSDP-1	R128-0.45	45.33	1.06	7.55		12.29	0.17	26.12	5.70	0.10	1.29	0.10		99.71	82.4	2
HSDP-2	SR0036-1.22	46.37	1.16	7.35		12.52	0.18	24.24	6.41	1.13	0.21	0.14	-0.32	99.71	81.0	3
	SR0040-1.07	45.54	1.00	6.31		12.58	0.17	27.28	5.54	0.97	0.20	0.12	-0.37	99.71	82.7	3
	SR0066-0.00	44.35	1.02	6.46		12.84	0.18	28.99	4.92	0.81	0.08	0.10	0.12	99.74	83.3	3
	SR0098-2.00	47.22	1.46	9.02		12.33	0.17	20.77	7.20	1.31	0.23	0.14	-0.38	99.85	78.8	3
	SR0117-4.00	46.70	1.69	9.85		13.05	0.18	19.42	7.41	1.44	0.08	0.18	0.24	100.00	76.6	3
Hualalai[M]																
	H-2	49.98	1.76	11.32	9.44	1.7	0.17	13.63	9.20	1.68	0.26	0.18	0.78	100.10	72.0	9
	H-5	49.70	1.67	11.09	11.12		0.18	14.93	8.71	1.71	0.26	0.15		99.52	72.7	1
	H-7[+]	50.21	1.86	12.18		11.93	0.17	11.23	9.76	1.92	0.30	0.17		99.73	67.5	4
	H-9[+]	50.18	1.87	12.15	9.47	1.52	0.17	11.30	9.84	1.85	0.29	0.18	0.84	99.66	68.0	9
	H-11	49.93	1.74	11.46	10.98		0.17	13.67	9.02	1.86	0.27	0.16		99.26	71.2	1
	H-23	46.01	1.08	7.37	11.57		0.17	25.80	5.69	1.19	0.19	0.10		99.17	81.5	1
	H-27	49.16	1.70	11.01	9.29	2.1	0.17	14.91	8.88	1.64	0.25	0.17	0.79	100.07	74.1	9
	H-P	46.76	1.33	8.10		12.56	0.17	23.19	6.09	1.17	0.19	0.14	-0.34	99.36	80.3	9
Loihi[M]																
	LO-02-02	44.63	1.40	7.13	11.95		0.19	24.21	6.33	1.34	0.40	0.14		97.72	80.1	1
	LO-02-04	44.14	1.31	6.40	10.22	1.58	0.17	26.58	5.70	1.03	0.33	0.15	2.27	99.88	82.3	9
	158-9	46.32	2.20	9.54		12.98	0.17	16.57	8.97	1.79	0.66	0.23	0.15	99.43	73.8	5
	186-5	44.24	1.75	8.43		12.85	0.17	19.52	10.50	1.55	0.47	0.18	-0.13	99.66	77.0	5
	186-11	43.21	2.66	12.05		13.45	0.17	13.76	9.58	3.16	1.21	0.44	0.54	99.69	69.3	5
	187-1	42.93	1.33	7.08		13.31	0.18	25.16	7.58	1.28	0.38	0.14	-0.24	99.37	80.6	5
Kilauea																
	KIL-1-18[M]	49.35	2.03	11.22	11.33		0.18	13.80	9.14	1.64	0.39	0.17		99.25	70.7	1
	KIL-2-3[M]	46.23	1.62	8.30	9.38	2.03	0.16	22.36	6.83	1.23	0.27	0.16	0.73	99.30	81.0	9
	KIL-2-4[M]	46.32	1.61	8.29	9.52	1.81	0.16	22.55	6.79	1.21	0.27	0.17	0.77	99.47	80.9	9
	KIL-3-1[M]	47.62	1.97	9.42	9.92	1.73	0.17	19.24	7.24	1.44	0.35	0.22	0.62	99.94	77.6	9
	KIL 1840-2	49.32	2.11	11.38	11.22		0.18	14.27	9.19	1.79	0.37	0.19		100.02	71.6	1
Koolau																
	K98-08	46.77	1.78	10.25	10.12	1.63	0.18	17.78	8.36	1.54	0.23	0.17	1.24	100.05	75.8	9
	S497-6[M]	46.95	1.41	8.87	9.82	2.27	0.18	21.55	6.81	1.47	0.21	0.12	0.52	100.18	79.6	6
	S500-5B[M]	47.98	1.30	9.04	8.74	2.13	0.16	21.22	6.31	1.64	0.31	0.16	1.07	100.06	81.2	6
	S500-5B*[M]	45.26	1.36	8.11		13.26	1.62	21.21	5.85	1.20	0.26	0.22	1.57	99.92	77.9	9
Kohala[M]																
	KO-1-10	49.05	1.92	11.60	9.91	1.38	0.17	13.54	9.37	1.68	0.33	0.21	0.84	100.00	70.9	9
	KO-1-20[+]	50.14	2.28	12.88	9.17	1.94	0.18	9.60	10.19	2.09	0.41	0.27	0.92	100.07	65.1	9
	KOH-1-28	48.64	1.41	9.30	10.97		0.16	20.52	7.21	1.30	0.26	0.12		99.89	78.7	1
Lanai																
	LWAW-4	48.17	1.67	11.58		12.53	0.17	14.48	8.04	1.17	0.04	0.12	1.88	99.85	71.8	7
	LWAW-7[+]	49.24	1.96	12.80		12.82	0.17	11.69	8.91	1.46	0.10	0.17	1.00	100.32	66.8	7
Molokai[M]																
	S501-2	43.97	1.12	5.74	8.84	2.53	0.15	28.96	3.87	0.83	0.29	0.11	3.04	99.45	85.4	9

[1] Norman and Garcia, 1999 [2] Rhodes et al., 1996 [3] Rhodes et al., 2006 [4] Gurriet et al., 1995 [5] Garcia et al., 1995 [6] Tanaka et al., 2002 [7] West et al., 1992 [8] Chen et al., 1991 [9] this study

[+] tholeiitic basalt (MgO < 13 wt%)
[*] sample affected by Mn-crust alteration
[M] submarine sample
[†] total Fe reported as FeO or Fe_2O_3 unless values for both are present

Table 3.2: Average Olivine Core Chemistry for Hawaiian Picrites

Volcano	Sample Name	SiO$_2$ (wt%)	Al$_2$O$_3$	FeO	MnO	MgO	CaO	NiO	Cr$_2$O$_3$	CoO	SUM	Mg#$_{ol}$
Mauna Kea												
	MK-1-6	40.36	0.05	12.33	0.19	46.63	0.21	0.37	0.09	0.03	100.26	87.1
HSDP-2 *	SR0129-5.20[+]	39.29	0.05	17.72	0.24	42.53	0.31		0.03		100.21	81.1
	SR0450-3.55	40.44	0.05	13.57	0.19	45.82	0.23		0.08		100.43	85.7
	SR0502-4.85	36.95	0.07	12.97	0.19	48.45	0.23		0.12		98.99	86.9
	SR0683-5.75	40.51	0.08	11.90	0.16	46.86	0.25		0.09		99.86	87.5
	SR0714-11.55[+]	39.16	0.03	16.79	0.21	44.12	0.27	0.24	0.05		100.88	82.4
	SR0741-7.90	38.96	0.04	13.97	0.17	45.70	0.23	0.32			99.38	85.3
	SR0750-12.45	39.07	0.04	13.53	0.17	45.73	0.21	0.31			99.05	85.8
	SR0756-13.25	39.34	0.04	12.33	0.15	47.10	0.23	0.37			99.56	87.2
	SR0846-2.80[+]	39.44	0.79	15.48	0.20	43.88	0.27	0.30	0.06		100.43	83.5
	SR0891-15.10[M]	41.02	0.06	11.23	0.15	47.94	0.23	0.40	0.10		101.14	88.4
Mauna Loa												
	ML-2-50[M]	40.38	0.05	9.46	0.13	49.27	0.20	0.56	0.08	0.04	100.19	90.3
	ML KAH-1	40.51	0.05	9.54	0.14	49.34	0.20	0.49	0.10	0.03	100.40	90.2
	ML 1868-9	40.21	0.06	11.05	0.16	48.31	0.21	0.38	0.09	0.04	100.52	88.6
HSDP-2 *	SR0040-1.07	39.34	0.03	14.18	0.18	45.48	0.28		0.07		99.59	85.1
	SR0117-4.00	39.52	0.03	15.27	0.24	44.57	0.26		0.06		99.96	83.9
Hualalai[M]												
	H-2	40.42	0.06	10.97	0.16	47.97	0.21	0.39	0.08	0.03	100.30	88.6
	H-5	40.40	0.06	11.04	0.16	48.05	0.20	0.42	0.09	0.02	100.43	88.6
	H-7[+]	40.41	0.05	11.33	0.16	47.76	0.22	0.37	0.09	0.03	100.42	88.3
	H-9[+]	40.30	0.06	10.73	0.16	47.88	0.20	0.39	0.10	0.03	99.85	88.8
	H-11	40.32	0.06	11.69	0.16	47.29	0.21	0.36	0.08	0.03	100.19	87.8
	H-23	40.53	0.05	11.30	0.18	47.46	0.21	0.38	0.08	0.03	100.22	88.2
	H-27	40.58	0.06	10.64	0.15	48.29	0.21	0.41	0.09	0.03	100.46	89.0
	H-P	40.52	0.06	12.01	0.16	47.17	0.20	0.40	0.07	0.03	100.61	87.5
Loihi[M]												
	LO-02-02	40.33	0.04	11.68	0.17	47.31	0.28	0.34	0.08	0.04	100.27	87.8
	LO-02-04	40.23	0.05	12.76	0.20	46.29	0.32	0.32	0.06	0.03	100.26	86.6
	158-9	40.41	0.04	10.29	0.15	48.53	0.25	0.41	0.08	0.04	100.19	89.4
	186-5	40.03	0.05	12.30	0.19	46.67	0.32	0.26	0.05	0.03	99.91	87.1
	186-11	39.55		14.00	0.21	45.59		0.27			99.62	85.3
	187-1	40.24	0.05	11.84	0.17	47.36	0.30	0.30	0.07	0.04	100.35	87.7
Kilauea												
	KIL-1-18[M]	40.14	0.06	10.36	0.14	48.35	0.22	0.45	0.09	0.04	99.85	89.3
	KIL-2-3[M]	40.18	0.05	10.51	0.15	48.11	0.23	0.44	0.08	0.03	99.78	89.1
	KIL-2-4[M]	40.79	0.06	9.84	0.12	48.89	0.23	0.45	0.09	0.03	100.51	89.9
	KIL-3-1[M]	40.25	0.07	11.61	0.15	47.60	0.22	0.42	0.09	0.04	100.45	88.0
	KIL 1840-2	40.17	0.06	11.55	0.15	47.80	0.22	0.44	0.09	0.04	100.50	88.1
Koolau												
	K 98-08	40.11	0.04	14.06	0.19	45.74	0.22	0.36	0.06	0.04	100.81	85.3
	S497-6[M]	40.70	0.05	11.26	0.17	47.78	0.19	0.41	0.09	0.02	100.67	88.3
	S500-5B[M]	40.55	0.05	11.29	0.16	47.98	0.18	0.36	0.08	0.03	100.69	88.3
Kohala[M]												
	KO-1-10	40.49	0.04	12.47	0.20	46.95	0.23	0.30	0.05	0.05	100.79	87.0
	KO-1-20[+]	40.68	0.06	11.47	0.18	47.26	0.22	0.38	0.07	0.03	100.36	88.0
	KOH-1-28	40.88	0.05	10.68	0.18	48.37	0.20	0.41	0.08	0.02	100.86	89.0
Lanai												
	LWAW-4	39.33	0.04	15.40	0.19	44.87	0.18	0.46	0.05	0.04	100.57	83.9
	LWAW-7[+]	40.21	0.06	11.25	0.15	47.92	0.20	0.48	0.07	0.04	100.37	88.4
Molokai[M]												
	S501-2	40.64	0.06	10.90	0.17	48.05	0.22	0.36	0.09	0.03	100.51	88.7

* HSDP olivine analyses from Putirka *et al*., 2007

[+] tholeiitic basalt (MgO < 13 wt%)

[M] submarine sample

65

Table 3.3: HSE and ^{187}Os/^{188}Os data for Hawaiian Picrites

Volcano	Sample Name	Os (ppb)	Ir	Ru	Pt	Pd	Re	^{187}Os/^{188}Os
Mauna Kea								
	MK-1-6	0.736	0.476	1.444	1.254	1.572	0.353	0.12924
HSDP-1	R189-8.5B	1.240	0.494	1.787	1.217	1.588	0.046	0.12950
	R197-0.8B	1.089	0.442	1.570	1.039	1.310	0.083	0.12973
	R215-7.2B	0.893	0.456	1.843	1.265	1.189	0.076	0.12947
HSDP-2	SR0129-5.20[+]	0.026	0.193	0.067	1.569	1.383	0.318	0.12987
	SR0328-3.10	1.225	0.483	1.657	1.853	1.753	0.092	0.12970
	SR0346-5.60	0.411	0.301	0.912	1.402	1.487	0.128	0.12919
	SR0401-2.85	1.431	0.648	1.981	1.463	1.146	0.087	0.13073
	SR0450-3.55	1.240	0.781	1.746	1.977	2.386	0.256	0.12865
	SR0502-4.85	1.087	0.681	1.675	1.876	2.498	0.258	0.12920
	SR0683-5.75	1.005					0.262	0.12988
	SR0714-11.55[+]	0.152					0.679	0.12958
	SR0720-18.25	0.519	0.368	1.079	2.494	2.790	0.354	0.13053
	SR0741-7.90	0.241	0.133	0.481	1.004	1.149	0.407	0.12975
	SR0750-12.45	0.405					0.613	0.13032
	SR0756-13.25	1.493					0.467	0.12945
	SR0762-4.60	0.361					0.352	0.13056
	SR0846-2.80[+]	0.325					0.467	0.12982
	SR0891-15.10[M]	1.645	0.814	1.691	3.397	3.899	0.702	0.12987
	SR0940-18.35[M]	0.295	0.268	0.382	0.548	0.488	0.871	0.12951
	SR0954-8.00[M]	0.567	0.352	1.129	2.041	2.836	0.851	0.12870
	SR0964-4.30[M]	1.349	0.752	2.118	2.487	2.627	0.646	0.13067
Mauna Loa								
	ML-2-50[M]	0.902	0.515	1.474	2.373	1.426	0.324	0.13419
	ML-2-50 dup [M]	0.907	0.452	1.298	2.279	1.480	0.323	0.13457
	ML KAH-1	1.263	0.639	1.706	2.886	0.711	0.191	0.13395
	ML 1868-9	0.701	0.365	1.327	1.629	2.498	0.230	0.13491
HSDP-1	R128-0.45	1.320	0.374	1.459	1.690	1.020	0.075	0.13406
HSDP-2	SR0036-1.22	0.656	0.277	0.882	1.973	2.901	0.237	0.13442
	SR0040-1.07	1.138	0.513	1.528	2.956	3.473	0.171	0.13455
	SR0066-0.00	3.013	0.781	2.303	2.333	2.189	0.149	0.13358
	SR0098-2.00	0.873	0.470	1.555	2.154	1.990	0.152	0.13310
	SR0117-4.00	4.424	0.707	1.471	3.377	2.025	0.402	0.13377
Hualalai[M]								
	H-2	0.910	0.423	1.007	1.120	1.228	0.542	0.13685
	H-5	1.421	0.625	1.330	2.673	3.427	0.459	0.13413
	H-7[+]	0.792	0.402	0.876	2.810	3.659	0.769	0.13655
	H-9[+]	0.598	0.429	0.796	2.538	2.470	0.567	0.13624
	H-11	0.935	0.447	0.984	2.805	2.854	0.460	0.13425
	H-23	1.520	0.803	2.586	2.224	2.095	0.202	0.13472
	H-27	1.262	0.550	1.359	1.834	1.647	0.321	0.13437
	H-27 dup	1.144	0.493	1.517	1.786	1.244	0.308	0.13493
	H-P	1.201	0.548	1.823	1.359	2.090	0.174	0.13379
Loihi[M]								
	LO-02-02	0.984	0.836	1.689	5.825	7.301	0.679	0.13518
	LO-02-04	1.150	1.006	1.649	6.526	2.288	0.567	0.13377
	158-9	0.832	0.628	1.244	7.637	7.160	0.721	0.13336
	186-5	0.543	0.470	0.734	5.996	3.220	0.988	0.13102
	186-11	0.173	0.205	0.278	1.500	0.909	1.349	0.13569
	186-11 dup	0.182	0.211	0.281	1.753	0.949	1.338	0.13543
	187-1	1.212	0.879	1.827	6.068	5.863	0.674	0.13062
Kilauea								
	KIL-1-18[M]	0.572	0.558	0.991	2.564	1.672	0.813	0.13113
	KIL-1-18 dup[M]	0.574	0.454	0.995	2.579	1.667	0.824	0.13071
	KIL-2-3[M]	1.007	0.431	1.412	1.101	2.765	0.212	0.13139
	KIL-2-4[M]	0.827	0.439	1.613	1.733	5.882	0.361	0.13149
	KIL-3-1[M]	0.733	0.434	1.182	1.975	2.128	0.215	0.13031
	KIL 1840-2	1.129	0.373	0.984	1.807	2.384	0.171	0.13086
Koolau								
	K 98-08	0.800	0.440	1.156	0.640	0.541	0.216	0.13175
	S497-6[M]	1.124	0.582	1.714	2.618	1.599	0.108	0.13574
	S500-5B[M]	0.950	0.756	2.008	8.634	2.269	0.185	0.26209
	S500-5B dup[M]	0.940	0.657	2.074	8.652	2.168	0.198	0.26139
Kohala[M]								
	KO-1-10	0.368	0.373	0.651	2.219	2.425	0.261	0.13323
	KO-1-20[+]	0.358	0.160	0.356	1.695	1.695	0.392	0.14310
	KOH-1-28	1.052	0.376	1.321	1.929	1.896	0.282	0.13294
	KOH-1-28 dup	0.855	0.362	1.265	1.980	1.917	0.262	0.13310
Lanai								
	LWAW-4	0.827	0.522	1.129	4.171	2.281	0.236	0.13843
	LWAW-7[+]	0.349	0.344	0.568	4.234	2.701	0.221	0.13760
Molokai[M]								
	S501-2	1.857	0.792	2.672	3.383	4.033	0.229	0.13158
PUM								
	PUM*	3.9	3.5	7	7.6	7.1	0.35	0.1296
CI Chondrite								
	Orgueil[#]	459	456	650	859	563	38	0.1270

* Becker et al., 2007
# Horan et al., 2003
[+] tholeiitic basalt (MgO < 13 wt%)
[M] submarine sample

between Fo_{85} and Fo_{90}, with the Fo content typically remaining consistent for multiple grains in the same thin section. More evolved samples (SR0129-5.20, SR0714-11.55, SR0846-2.80 and LWAW-4) generally contain olivine with lower Fo contents (81 to 85).

The HSE and $^{187}Os/^{188}Os$ data are reported in Table 3.3. Absolute abundances of HSE in all of the picrites are generally greater than MORB, and in some cases approach the concentrations observed in peridotites and komatiites (Figure 3.1; 3.8). With the exception of Re, concentrations of HSE in all samples are less than estimates for primitive upper mantle (PUM; Becker *et al*., 2006; Figure 3.1). The HSE concentrations in the Hawaiian picrites are generally consistent with abundances reported for other picrites worldwide (Bennett et al., 2000; Rehkämper et al., 1999; Momme et al., 2003).

Two general types of HSE patterns are observed in CI chondrite-normalized HSE diagrams (Figure 3.1). Type-1 patterns are roughly similar to the shape of the PUM pattern, albeit with lower overall HSE abundances and higher relative and absolute abundances of Re. This pattern is characterized by lower Pt/Ir and Pd/Ir ratios than Type-2 samples, as well as a highly reproducible Os-Ir-Ru pattern.   It is best observed in most Mauna Kea samples, but is also observed in picrites from all volcanic centers except Loihi and Lanai. Subaerially erupted samples have substantially lower Re abundances.

Type-2 HSE patterns are comparatively flat for Os, Ir, and Ru, but have higher absolute and relative abundances of Pt, Pd and Re. This type of pattern is best observed for Loihi samples, but is also observed in all volcanic centers (except

67

Molokai) and all of the lower MgO tholeiitic basalts. It is characterized by more highly fractionated Pt/Ir and Pd/Ir ratios than Type-1 samples. All of the lower MgO tholeiitic basalts display this type of pattern. This pattern shape is broadly similar to that for MORB and Pacific oceanic crust, although absolute Os, Ir, Ru, Pt and Pd abundances are much higher in the picrites (Tatsumi, 2003; Peucker-Ehrenbrink et al., 2003).

When considering data for the entire picrite suite, Os, Ir and Ru are positively correlated with MgO (Figure 3.2). These correlations are clearly defined for picrites from most individual volcanic centers. Data for these elements generally plot within the range of compositions defined by samples from the Kilauea Iki lava lake, which originated as a differentiation sequence of ponded lava with an initial MgO content of ~15 wt% (Wright, 1973; Pitcher et al., in revision). Extensive differentiation processes at Kilauea Iki produced rocks with <5 to nearly 30 wt% MgO (Helz, 1987). In our picrite suite, Pt, Pd and Re generally show slightly negative correlations with MgO (Figure 3.2), but with significant scatter. Again, most data overlap with the range of concentrations present in samples of Kilauea Iki. Notable inter-volcanic differences include higher Os abundances in Hualalai and higher Pt, Pd and Re abundances in Loihi samples.

Variations in $^{187}Os/^{188}Os$ ratios are modest within most volcanic centers (maximum variations of ~ 3.5%); however, there are significant differences between the volcanic centers (Figure 3.3). Our results are consistent with those previously reported (Martin et al., 1994; Bennett et al., 1996; Hauri et al., 1996; Hauri and Kurz, 1997; Lassiter and Hauri, 1998; Brandon et al., 1999; Bennett et al., 2000; Bryce et
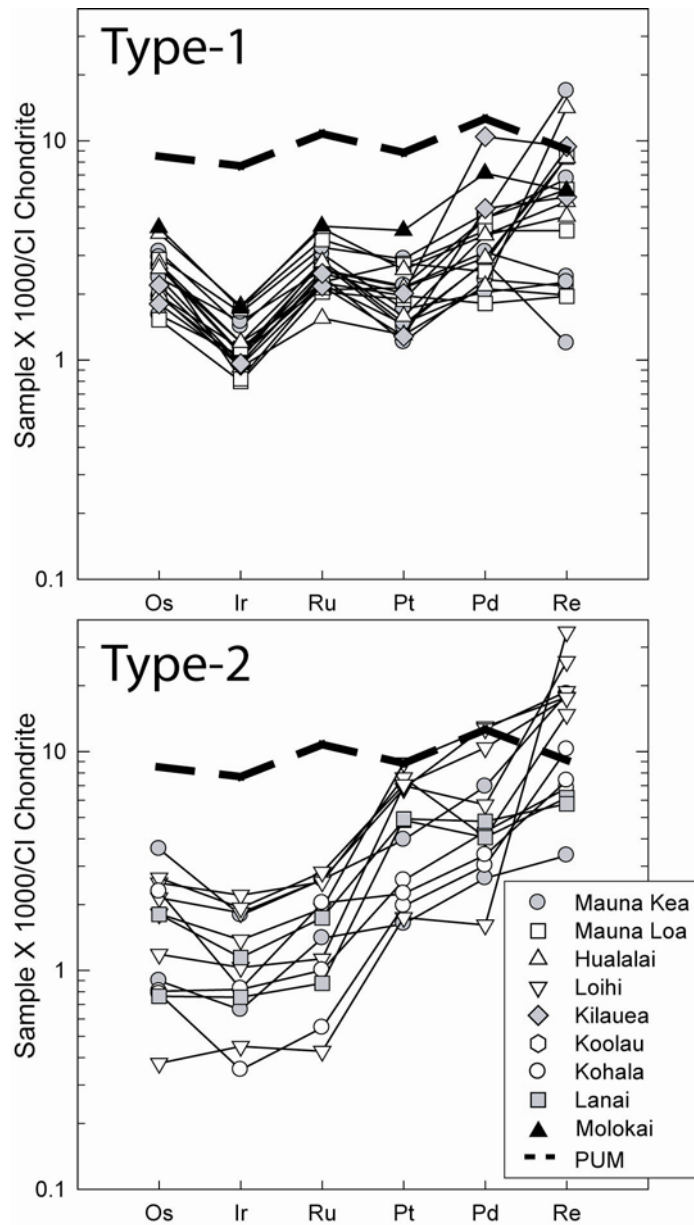
Figure 3.1: HSE patterns for the Hawaiian picrites. Type-1 picrites differ from Type-2 in having lower Pd/Ir and Pt/Ir ratios. Type-1 picrites also tend to have higher Os/Ir and Ru/Ir ratios. PUM is thought to be representative of fertile peridotites, prior to the removal of material from the upper mantle (Becker et al., 2006).
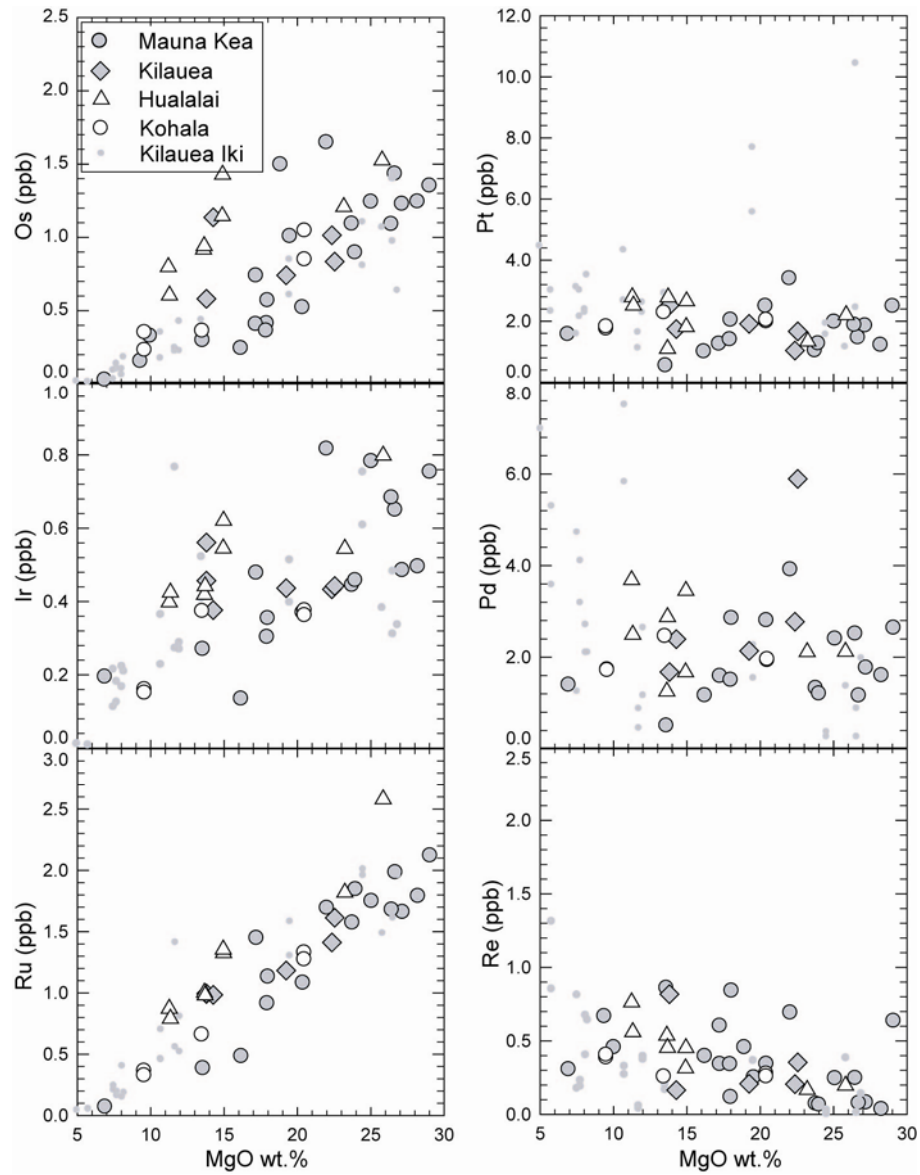
Figure 3.2a: HSE-MgO trends for all volcanoes analyzed in this study. Small gray symbols are from Kilauea Iki Lava Lake (Pitcher et al., 2009).
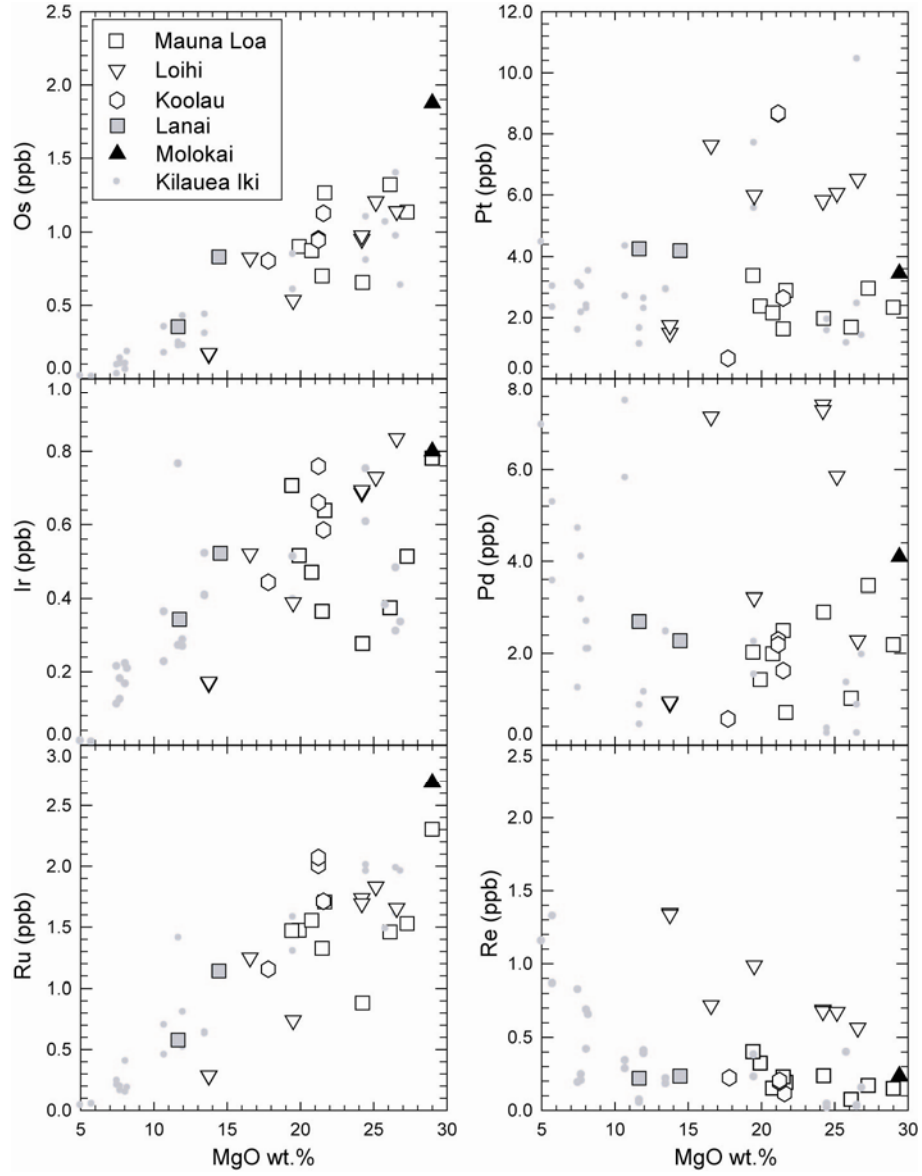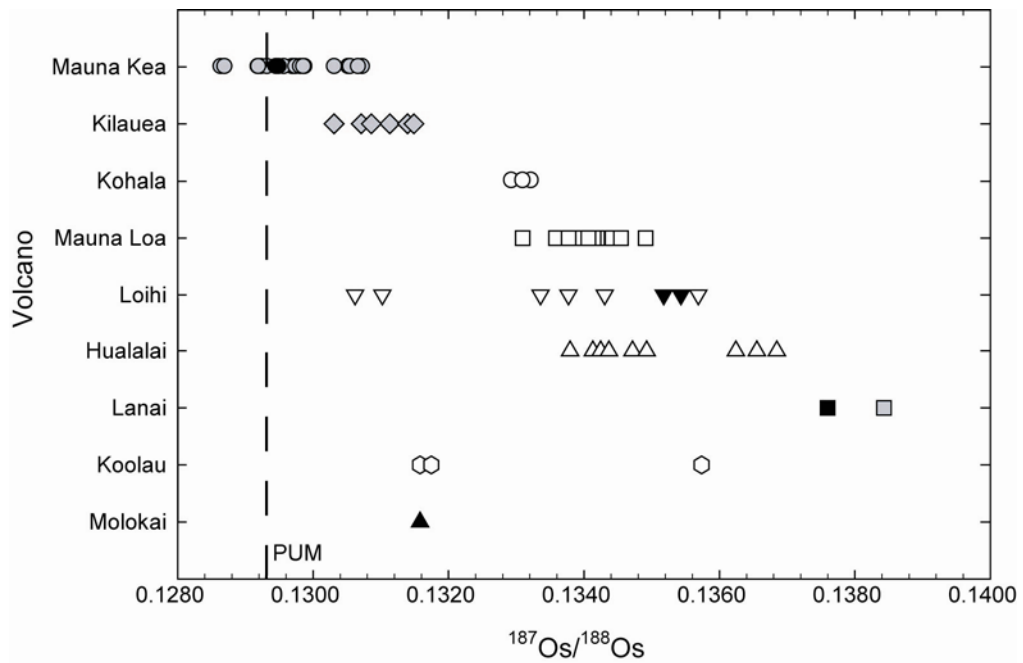
Figure 3.2b: HSE-MgO trends for all volcanoes analyzed in this study. Small gray symbols are from Kilauea Iki Lava Lake (Pitcher et al., 2009).

Figure 3.3: Range of $^{187}Os/^{188}Os$ ratios for each volcanic center. Mauna Kea and Kilauea are characterized by lower $^{187}Os/^{188}Os$ ratios, whereas Mauna Loa, Loihi and Hualalai are more radiogenic. Black symbols denote tholeiitic basalts (MgO < 13 wt%). Error bars for $^{187}Os/^{188}Os$ ratios are approximately the same size as the symbol. PUM estimate is from Meisel et al. (2001).

al., 2005). Of note, Mauna Kea samples have the lowest $^{187}Os/^{188}Os$ ratios spanning a narrow range from 0.1287 to 0.1307. Mauna Loa, Hualalai, Loihi and Lanai all have significantly more radiogenic $^{187}Os/^{188}Os$ ratios with an upper limit (with one exception) of 0.1384 for sample LWAW-4 from Lanai. There are no correlations between $^{187}Os/^{188}Os$ ratios and MgO content within volcanic centers.

Sample S500-5B from the Koolau volcano, has a very strong enrichment in Pt (~8 ppb) relative to the other samples, as well as a significantly elevated $^{187}Os/^{188}Os$ (~0.26). This sample also has an elevated MnO content (1.62 wt%), suggesting that Mn-crust material was present as a contaminant.

3.5 Discussion

Absolute and relative abundances of HSE in the Hawaiian picrite suite vary within and among each volcanic center (Table 3.3; Figure 3.1, 3.2). A major objective of this study is, therefore, to assess whether these variations are all process-related or reflect source heterogeneities. Processes such as crystal-liquid fractionation, during both partial melting and crystallization, and crustal contamination are major controls on HSE abundances in mafic through ultramafic systems (Barnes et al., 1985; Crocket and McRae, 1996; Brügmann et al., 1987; Barnes and Picard, 1993; Rehkämper et al., 1997; Rehkämper et al., 1999; Crocket, 2000; Puchtel and Humayun, 2001; Maier et al., 2003; Momme et al., 2003; Bockrath et al., 2004; Maier and Barnes, 2004; Puchtel et al., 2004; Ballhaus et al., 2006). Volatile losses in subaerial and shallow submarine flows can also affect abundances of Re and perhaps Ir (Zoller, 1983; Sun et al., 2003; Lassiter et al., 2003; Norman et

al., 2004). The effects of these processes must first be considered prior to a search for heterogeneities in the sources of these rocks.

3.5.1 Estimation of parental melt composition

Estimation of a parental melt composition can be helpful in trying to deconvolve the effects of crystal-liquid fractionation on HSE abundances. The parental melt represents the most primitive magma that was produced directly from the melting of the source region. Samples that have major element compositions that approach the estimated parental melt compositions are presumed to have experienced limited crystal-liquid fractionation following separation from their mantle sources (Norman and Garcia, 1999). Consequently, these samples may best preserve the HSE composition of the parental melt. Samples that deviate from the parental melt composition likely have experienced variable amounts of crystal-liquid fractionation or crustal contamination.

3.5.1.1 Parental melt composition and olivine fractionation

Norman and Garcia (1999) analyzed a subset of samples from the current study, including samples from Mauna Kea, Mauna Loa, Hualalai, Loihi, Kilauea and Kohala. They concluded that the parental melt compositions of the Hawaiian picrites for all volcanic centers in their sample suite likely contained at least 13-17 wt% MgO. Considering that olivine is the only major liquidus phase in these rocks, samples with higher MgO (up to 29.6 wt%) contents were presumed to have incorporated cumulate olivine, and samples with lower MgO contents were presumed to have lost olivine. A

log-log variation diagram of Al_2O_3 (an incompatible element in olivine) versus MgO (a compatible element in olivine; Figure 3.4) was used by Norman and Garcia (1999) to discriminate between samples related by olivine accumulation versus fractional crystallization. A break in slope for their entire sample suite was present at ~15 to 16 wt% MgO and ~10 wt% Al_2O_3, which roughly marks the estimated composition of the parental melt (Norman and Garcia, 1999). Our new data, for all volcanic centers, indicates a similar break in slope at ~16 wt% MgO and ~11 wt% Al_2O_3 which is generally consistent with this previous result. Although it would be advantageous to examine this relationship for samples from each volcanic center, there are either not enough samples, or insufficient spread in MgO contents within a suite, to make individual estimates of parental melt composition.

Parental melt compositions can also be inferred from the Fo contents of olivine phenocrysts. Assuming that $\frac{(Fe/Mg)_{ol}}{(Fe/Mg)_{wr}} = 0.3$ (Roeder and Emslie, 1970; Putirka, 2005) and 10% Fe^{3+} (relative to total Fe) for the whole rock (Rhodes and Vollinger, 2005), the MgO content of a melt in equilibrium with olivine can be estimated. High Fo content olivine (Fo_{86-90}) would be in equilibrium with melts that contain approximately 13-16% MgO. Several of the picrites we studied have MgO contents within this range and probably approximate the parental melts of the picrites. Samples that fall within this range of MgO, and that are also in equilibrium with associated olivine core compositions, include samples H-2, H-5, H-9, H-11, H-27, Lo 158-9 and Kil 1-18 (Figure 3.5).
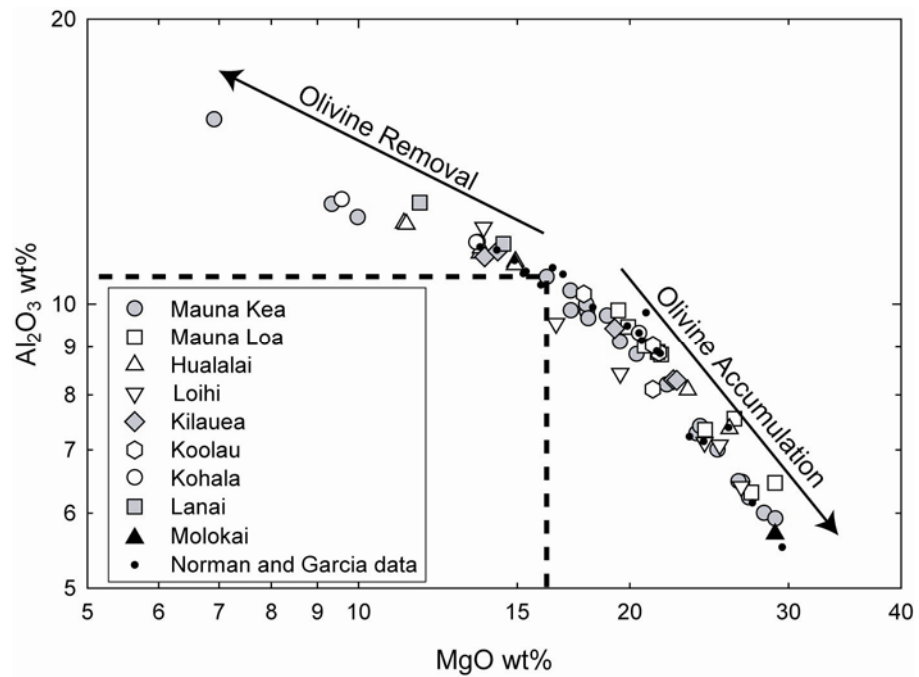
Figure 3.4: Log-Log variation diagram of Al_2O_3 vs. MgO. The break in slope at ~16
wt% MgO and ~11 wt% Al_2O_3 marks the estimated parental melt composition.
Samples with >16 wt% MgO are presumed to have accumulated olivine, whereas
samples with <16 wt% MgO have had olivine removed. Small black symbols are
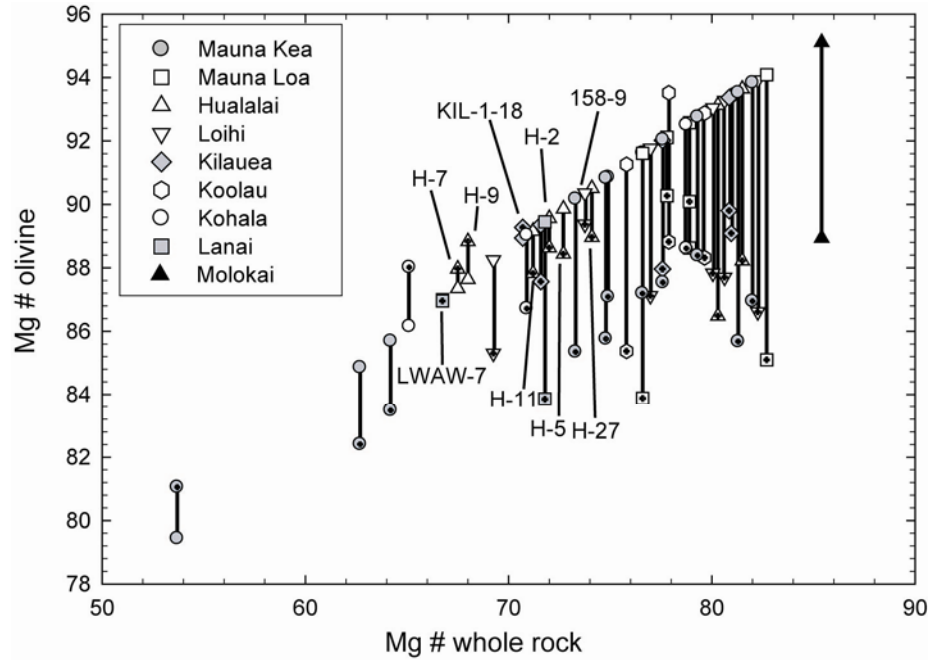samples from Norman and Garcia (1999).

Figure 3.5: A plot comparing measured olivine Mg# (crossed symbols) to the calculated Mg# of olivine in equilibrium with the whole rock (open symbols). Samples that have measured olivine that is close to equilibrium with the whole rock may approximate the parental melt composition for the picrites. Samples that have a whole rock composition that is in equilibrium with included olivine phenocrysts are H-2, H-5, H-7, H-9, H-11, H-27, Lo 158-9, Kil 1-18 and LWAW-7. Large deviations between the Mg# of the measured and calculated olivine denote those samples whose whole rock composition is not in equilibrium with olivine present in the sample. These samples have experienced variable amounts of olivine removal or accumulation.

Table 3.4: Estimated Percentages of Olivine Removal and Accumulation

Volcano	Number of Samples	MgO low	MgO high	Maximum Removal	Maximum Accumumlation
Mauna Kea	22	6.93	29.07	37.1	26.7
Mauna Loa	9	19.42	28.99	n/a	26.5
Hualalai	8	11.23	25.8	10.6	20.0
Loihi	6	13.76	26.58	8.3	21.6
Kilauea	5	13.80	22.55	4.9	13.4
Koolau	3	17.78	21.55	n/a	11.3
Kohala	3	9.60	20.52	14.2	9.2
Lanai	2	11.69	14.48	12.5	n/a
Molokai	1	28.96	28.96	n/a	26.5

Despite evidence that some whole rock samples may record primary magma compositions, it is also clear that variable proportions of olivine accumulation and removal have played an important role in the generation of these picrites. An estimate of the maximum amounts of olivine accumulation and removal for the remaining samples was deduced from the primary magma calculations above, assuming that parental melts contain 16 wt% MgO (Table 3.4). For samples believed to have lost olivine via fractional crystallization, equilibrium olivine was mathematically added in 0.1% increments until the calculated olivine composition corresponded to the most magnesian olivine in the sample suite, following the procedure outlined by Danyushevsky *et al*. (2000). We chose Fo_{90} because this olivine composition corresponds to the most magnesian olivine present in the sample suite, and is in equilibrium with a whole rock MgO content of 16 wt%. From this calculation, the maximum percentage of olivine removal is estimated to be ~37% (sample SR0129-5.20 from Mauna Kea, with a MgO content of 6.9 wt.%). For samples that have accumulated olivine, the amount of accumulation was estimated by mathematically subtracting Fo_{90} from the sample. This procedure was repeated until the sample composition calculated was in equilibrium with olivine of this composition (Fo_{90}). The maximum percentage of olivine accumulation is estimated to be 27% (sample SR0964-4.30 from Mauna Kea, with a MgO content of 29.1 wt%).

Hereafter, the parental melts for all the Hawaiian shield volcanoes included in this study are assumed to contain 16 wt% MgO. It is important to note, however, that this estimate is based on a data array for all the shield volcanoes analyzed in this study.

There may be small differences in the MgO content of parental melts between individual volcanoes.

3.5.1.2 Volatile loss of Re

The volatile loss of Re during magma degassing in subaerially erupted lavas has previously been recognized in arc magmas (Sun et al., 2003) and in Hawaiian lavas (Lassiter, 2003; Norman et al., 2004). This same effect might be observed in the chondrite-normalized HSE patterns for Mauna Kea and, to a lesser extent, for Mauna Loa. In general, the chondrite-normalized HSE patterns for the picritic suite show sharp enrichments of Re. However, in the subaerially and shallow submarine erupted lavas from the HSDP drill core for Mauna Kea (R189-8.5B, R197-0.8B, R215-7.2B, SR0328-3.10 and SR0401-2.85), the chondrite-normalized HSE patterns show relative depletions of Re, consistent with loss from the flows. The picrites from the Mauna Loa portion of the HSDP samples do not show such dramatic depletions in Re abundances, but likely effects can be observed in samples SR0066-0.00 and SR0098-2.00. Lavas that were erupted in deep submarine settings (> 2000 m below sea level) do not show obvious depletions in Re abundances and are presumed to have retained most or all of the Re from the melt (Table 3.1). Based on the depth of recovery of dredged samples, samples from Hualalai, Loihi, Kilauea (with the exception of subaerial erupted Kil 1840-2) and Koolau are presumed to have retained Re. Samples with significant Re volatile loss are not considered in the following section, where the Re abundances of the parental melts for each volcanic center are estimated.

80

Iridium abundances in Mauna Kea and Mauna Loa were also found to be somewhat variable with respect to MgO. Some of this variability may be due to minor volatile loss of Ir in subaerially erupted samples (Zoller et al., 1983). Apparent Ir depletions are most clearly observed for subaerially erupted Mauna Loa samples (ML 1868-9, R128-0.45, SR0036-1.22 and SR0040-1.07).

3.5.1.3 HSE characteristics of the parental melt

Removal and accumulation of olivine (and/or co-precipitated phases) have been shown to cause major effects on the absolute and relative abundances of HSE in mafic and ultramafic systems (Barnes et al., 1985; Brügmann et al, 1987; Rehkämper et al., 1999; Puchtel and Humayun, 2001; Bockrath et al., 2004; Maier and Barnes, 2004; Ballhaus et al., 2006.). The effects of crystal-liquid fractionation processes are evident in plots of HSE abundances versus MgO for each volcanic center in the Hawaiian suite (Figure 3.2). For those plots which show generally linear trends of HSE versus MgO, linear regression of the trends provides a means for estimating the HSE composition of the parental melt for each volcanic center. The intersections of the trends with the estimated parental melt composition of 16 wt% MgO are used to define the primary HSE abundances of the parental melts (Figure 3.6; Table 3.5). Osmium, Ir, Ru and Re contents of the parental melts were estimated in this manner for all volcanic centers from which greater than three samples were collected. Platinum and Pd exhibited much more scatter on the HSE versus MgO plots, so the parental melt composition for these two elements was not estimated for all volcanic centers. Platinum contents were estimated for Mauna Kea, Mauna Loa, Hualalai and
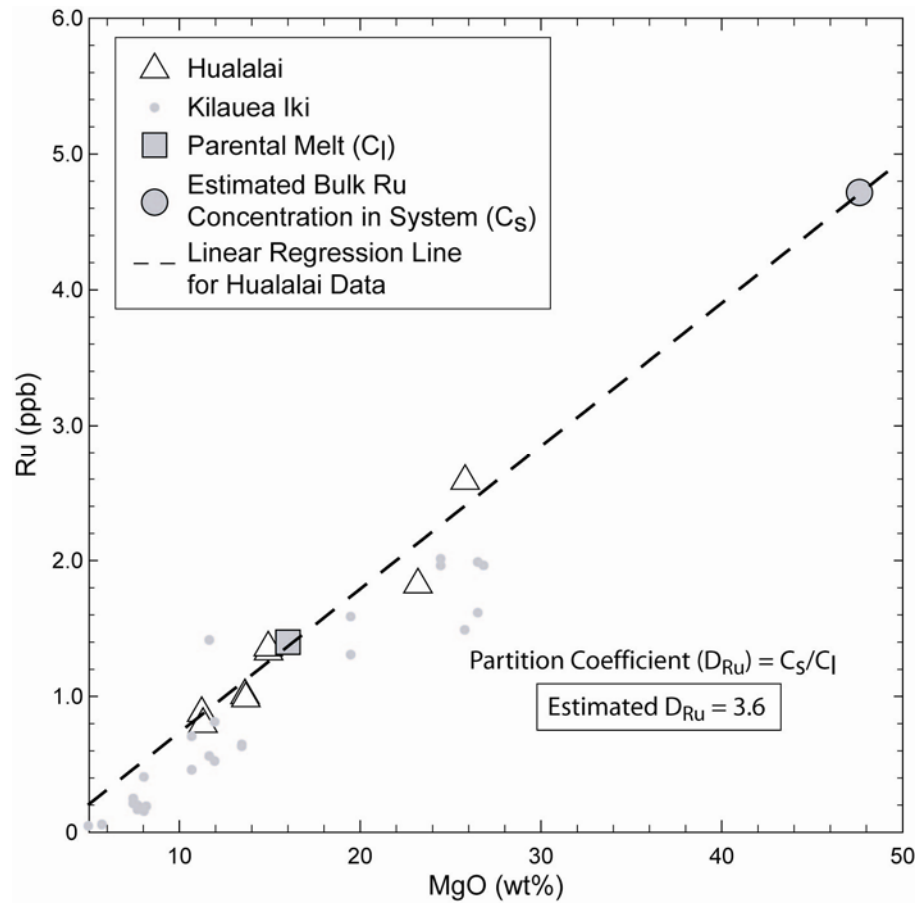
Figure 3.6: Example for how the HSE content in a parental melt and the partition coefficient were estimated, using Ru abundances from Hualalai. The parental melt is assumed to contain 16 wt% MgO, and its Ru abundance is determined by the linear regression of the data. To estimate the partition coefficient, the linear regression line was extrapolated to the MgO content of co-existing olivine. This MgO content is presumed to give the bulk HSE concentration present in the crystal phases.
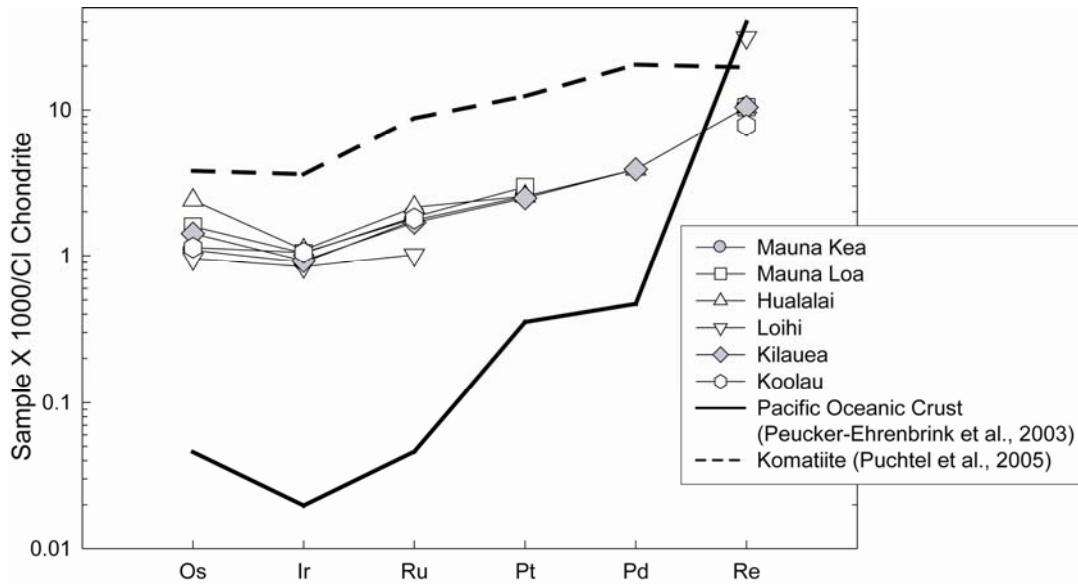
Figure 3.7: A chondrite-normalized HSE pattern plot showing the estimated parental melt compositions for all Hawaiian volcanic centers with greater than 3 samples. Also shown are the HSE patterns for a typical MORB (Peucker-Ehrenbrink et al., 2003) and a komatiite (Puchtel et al., 2005). Note that the HSE abundances for the Hawaiian parental melts are intermediate between a low-degree melt (MORB) and a high-degree melt (komatiite).

83

Table 3.5: Estimated Bulk Partition Coefficients and HSE Abundances in Picritic Parental Melts

Volcano		Ni	Os	Ir	Ru	Pt	Pd	Re	Average ^{187}Os/^{188}Os	Re/Os	Pt/Os
Mauna Kea	parental melt	688	0.50	0.41	1.14	2.20	-	0.40	0.1297	0.80	4.40
	2σ		0.03	0.09	0.13	0.45	-	0.02		0.04	0.65
	D	4.1	5.4	2.3	2.8	-	-	-			
Mauna Loa	parental melt	416	0.73	0.48	1.20	2.55	-	0.40	0.1341	0.55	3.50
	2σ		0.17	0.11	0.16	0.33	-	0.04		0.13	0.81
	D	7.5	2.6	1.3	2.5	0.7	-	-			
Hualalai	parental melt	782	1.00	0.50	1.40	2.20	2.20	0.40	0.1351	0.40	2.20
	2σ		0.01	0.00	0.01	0.03	0.04	0.04		0.05	0.40
	D	3.9	2.2	2.2	3.4	0.2	-	-			
Loihi	parental melt	728	0.44	0.38	0.66	-	-	1.20	0.1336	2.74	-
	2σ		0.07	0.04	0.12	-	-	0.07		0.45	-
	D	3.1	6.3	5.6	6.3	-	-	-			
Kilauea	parental melt	754	0.65	0.42	1.10	2.13	2.20	0.40	0.1310	0.61	3.28
	2σ		0.07	0.02	0.03	0.11	0.36	0.08		0.12	0.28
	D	4.7	2.9	1.2	2.7	-	-	-			
Koolau	parental melt	665	0.52	0.48	1.17	-	-	0.30	0.1337	0.57	-
	2σ		0.13	0.12	0.31	-	-	0.03		0.11	-
	D	4.5	7.1	2.8	4.4	-	-	-			

Kilauea; whereas, Pd contents, which exhibited the most scatter on the HSE versus MgO plots, were estimated only for Hualalai and Kilauea. Samples with nearly 16 wt% MgO and that are also in equilibrium with associated olivines approximate parental melt compositions, as discussed above. The HSE data for these samples (H-2, H-5, H-9, H-11, H-27, Lo 158-9 and Kil 1-18) tend to cluster close to the linear regression lines, consistent with our approach.

The estimated parental melt HSE abundances (where possible) for all volcanic centers are generally similar (Figure 3.7). Osmium, Ir, Ru and Re abundances in the majority of parental melts are 0.5 ± 0.2 ppb, 0.45 ± 0.05 ppb, 1.2 ± 0.2 ppb and 0.35 ± 0.05 ppb respectively. Likewise, estimated Pt abundances in the parental melt are similar at 2.3 ± 0.2 ppb. Notable exceptions include the estimated Os content of the Hualalai parental melt, which is higher at 1.0 ppb. The parental melt for Loihi is estimated to have the lowest abundances of Os, Ir and Ru, as well as the highest Re content (1.2 ppb). Although linear trends between Pt and Pd with MgO were not observed, Loihi picrites also have strong enrichments in these elements.

3.5.1.4 Estimated bulk distribution coefficients

For those elements that show good linear correlations with MgO, linear regressions of the trends can also be used to estimate bulk solid/melt partition coefficients (i.e. D values; Puchtel and Humayun, 2001). To do this, the linear HSE-MgO trends were extrapolated to the average MgO content of co-precipitating olivine for each shield volcano, the primary Mg-containing liquidus phase. This permits estimation of the bulk concentration of the HSE in the co-precipitating solid phases

(i.e., olivine, chromite; Table 3.5; Figure 3.6). The HSE concentrations calculated in the solid (olivine) were then related to those of the parental melts to obtain D values. Estimated D values for Os (2.2 to 7.1), Ir (1.2 to 5.6) and Ru (2.5 to 6.3) indicate that these elements all behaved compatibly in the picrites from each volcanic center. The estimated D values for Pt (0.2 to 0.7) indicate that it behaved incompatibly. Palladium does not display a meaningful linear correlation with MgO in any of the volcanic centers, indicating that olivine fractionation may have had little control on Pd. These D values compare favorably to other studies of HSE in high MgO Hawaiian rocks from Kohala (Jamais et al., 2008) and Kilauea Iki Lava Lake (Pitcher et al., in revision).

For Hawaiian picrites, we conclude that Os, Ir and Ru behaved compatibly, during crystal-liquid fractionation with their abundances directly related to the amount of olivine present. It is likely, however, that these elements are sited in chromite and sulfide inclusions present within the olivine grains, rather than structurally bound within the olivine (Yi et al., 2000; Puchtel and Humayun, 2001; Brenan et al., 2003; 2005). Platinum, Pd and Re behaved incompatibly and are evidently contained primarily in the matrix phases.

3.5.2 Additional processes potentially affecting HSE in parental melts

3.5.2.1 Crustal assimilation

Assimilation of crustal material by mantle-derived magmas as they ascend through the oceanic crust has the potential to alter the HSE characteristics and Os isotopic composition of a melt (Martin et al., 1994; Marcantonio et al., 1995; Roy-

Barman et al., 1995; Widom and Shirey, 1996; Lassiter and Hauri, 1998; Yi et al, 2000; Gaffney et al., 2005; Bizimis et al., 2007). Oceanic crust tends to have high Re/Os ratios due to the differences in compatibility between Re and Os during mantle melting. Over time, this leads to the development of highly radiogenic $^{187}Os/^{188}Os$ ratios. Assimilation of highly radiogenic oceanic crust by a picritic melt may, thus, result in an increase in $^{187}Os/^{188}Os$. This effect can be highly significant for basaltic melts with very low Os contents, or during the late stages of shield-building.

For Hawaiian shield volcanoes, assimilation of oceanic crust has been suggested for late shield-stage lavas from West Maui (Gaffney et al., 2005) as well as for samples from Mauna Kea (Lassiter and Hauri, 1998) and Haleakala (Martin et al., 1994) to explain radiogenic $^{187}Os/^{188}Os$ ratios. However, bulk oceanic crust contains much lower absolute abundances of the HSE (except Re) than the picrites analyzed in the present study (Peucker-Ehrenbrink et al., 2003). Bulk assimilation of the oceanic crust should, therefore, result in lower abundances of the HSE.

To quantitatively examine this possibility we consider the effects of bulk assimilation by modeling the addition of ~100 Ma Pacific oceanic crust that underlies Hawaii ($^{187}Os/^{188}Os$ = 0.9; Os = 0.02 ppb; Re = 1.5 ppb; Ir = 0.009 ppb; Ru = 0.03 ppb; Pt = 0.3 ppb and Pd = 0.3 ppb; Tatsumi, 2003; Peucker-Ehrenbrink et al., 2003) to a representative parental melt for the Hawaiian picrites. The Kilauea parental melt was chosen for the Hawaiian picrite end-member because it has the least radiogenic $^{187}Os/^{188}Os$ ratios (0.130) and has typical HSE abundances for Hawaiian picrites (Os = 0.7 ppb; Re = 0.4 ppb; Ir = 0.4 ppb; Ru = 1.1 ppb; Pt = 2.0 ppb and Pd = 1.5 ppb).

Calculations show that simple mixing of 1% to 20% proportions of a crustal assimilant similar to a Kilauea-like parental melt would have a limited, mostly dilutional effect, on the concentrations and relative abundances of the HSE in a picrite parental melt. For example, addition of 20% of oceanic crust would result in a decrease in Os, Ir, Ru, Pt and Pd abundances of ~19%. At the same time, Re would be enriched by ~30% (Figure 3.8) and $^{187}Os/^{188}Os$ ratios would be raised by ~4% (0.130 to 0.135). Such large amounts of assimilation, however, are inconsistent with the major element compositions of the picrites, because the addition of large amounts of basaltic material to a picritic melt would dilute the MgO content such that the melt would no longer be picritic and would likely result in equilibration with olivine of different composition than Fo_{90}. Additions of more geologically feasible proportions of <5% would not be resolvable within the variations present in the HSE abundance data. In a hypothetical mixture of the Kilauea parental melt with 5% crustal contamination, the $^{187}Os/^{188}Os$ ratio of the resulting melt would increase by only ~1%. Once again, this limited effect would not be resolvable in Os isotopic data for Kilauea. The limited variation in $^{187}Os/^{188}Os$ within volcanic centers suggests that variable amounts of bulk assimilation had little effect on the Os isotopic composition and HSE abundances in the picritic suite.

If crustal sulfide could be selectively assimilated by the picritic magmas during transport through the crust, as opposed to bulk assimilation, the HSE budget of the rising magma might be changed without having a significant effect on the major element composition. For example, Yi et al. (2000) suggested that the sulfides present in Loihi picrites (including sample 187-1) may represent assimilated crustal
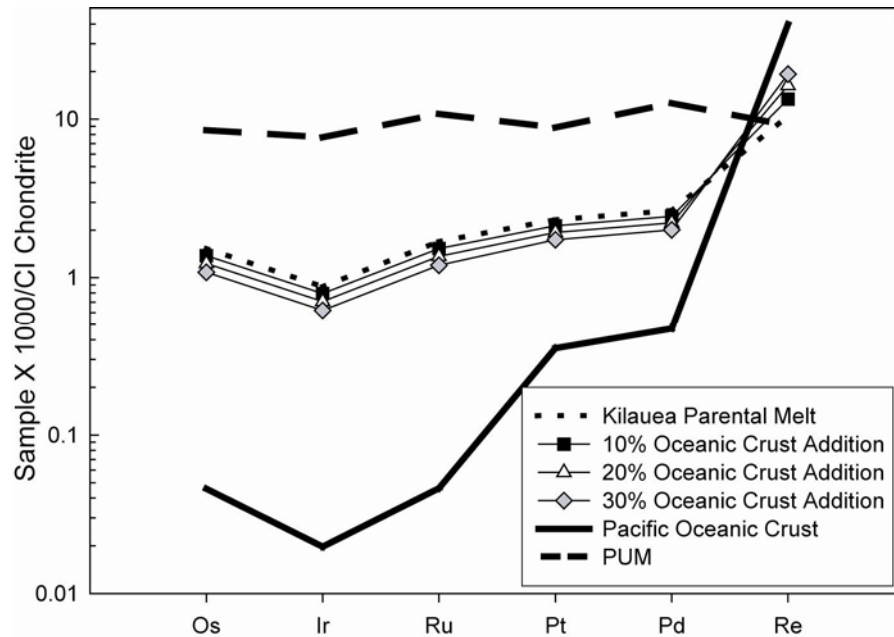
Figure 3.8: Example of how differing amounts of crustal contamination can affect

the HSE systematics of a sample. Crustal contamination has a diluting effect on

absolute HSE abundances, but no effect on relative abundances. Small to large

additions (0-20%) of oceanic crust to a magma results in a small decrease in the HSE

abundances in the magma, however, crustal material is highly radiogenic, making the

addition of large proportions of crust to a magma untenable.

sulfide, as well as sulfide that co-precipitated with olivine during olivine accumulation. However, the similar HSE patterns and narrow range in $^{187}Os/^{188}Os$ ratios found for each shield volcano (Figure 3.1; 3.3) argue against variable crustal sulfide assimilation being a major process for Hawaiian picrites. Crustal sulfides are likely to be highly variable in composition, possessing a wide range in HSE abundances and varying Re/Os ratios (Peucker-Ehrenbrink et al., 2003). The range of Re/Os ratios, coupled with different residence times within the crust, would lead to a broad range in $^{187}Os/^{188}Os$ ratios. Given the variability in these crustal sulfides, it would be unlikely for samples from the same volcanic center to inherit such similar HSE patterns and $^{187}Os/^{188}Os$ ratios. We conclude that assimilation of sulfides is unlikely to have significantly affected the HSE abundances in these rocks. However, it is a process worth further investigation, especially via analysis of S isotopes.

3.5.2.2 Fe-Mn crust contamination

The addition of Fe-Mn rich materials, including crusts, umbers and nodules, into mafic magmas have been suggested as a potential means to affect the HSE and Os isotopic characteristics of putative plume-derived magmas, as these materials tend to scavenge HSE, particularly Pt, from seawater (Smith, 2003; Baker et al., 2004; Schersten et al., 2004). Previous studies have argued that these materials can be recycled into the mantle sources of plumes during the subduction process. Here we examine the affect of Fe-Mn contamination of a sample on the seafloor.

Sample S500-5B permits examination of the effects that Fe-Mn alteration can have on HSE abundances in the picrites. The Mn content of our piece of S500-5B is 1.62 wt%, compared to a maximum of 0.18 wt% for all other samples (Table 3.1). The high Mn concentration of this sample indicates incorporation of ~5% of Mn-crust material (Mn = 25 wt%; Schersten et al., 2004). The absolute and relative abundances of Os, Ir, Ru, Pd and Re are similar to other Hawaiian picrites, and do not appear to be affected by major Mn deposition. A significant enrichment is observed for Pt, however, consistent with its addition during the alteration (Figure 3.9). Further, the alteration was evidently also accompanied by a dramatic increase in the $^{187}Os/^{188}Os$ ratio of the sample (0.260). Although seafloor alteration, resulting in the addition of Mn-rich materials to the picrites, can evidently cause Pt enrichment and an increase in $^{187}Os/^{188}Os$, it appears to have had no effect on the other HSE and on the remaining samples which have normal Mn contents.

Of all of the picritic suites studied here, only samples from Loihi show appreciable enrichments in Pt abundances, with up to three times more Pt (average = 6.4 ppb) than picrites from other volcanic centers (average = 2.0 ppb). Loihi picrites, however, also have elevated Pd and Re abundances, as well as low Mn abundances (0.17 to 0.19 wt%). Consequently, we conclude that the Pt enrichment was not caused by seafloor alteration or the presence of recycled seafloor precipitates in their mantle source.
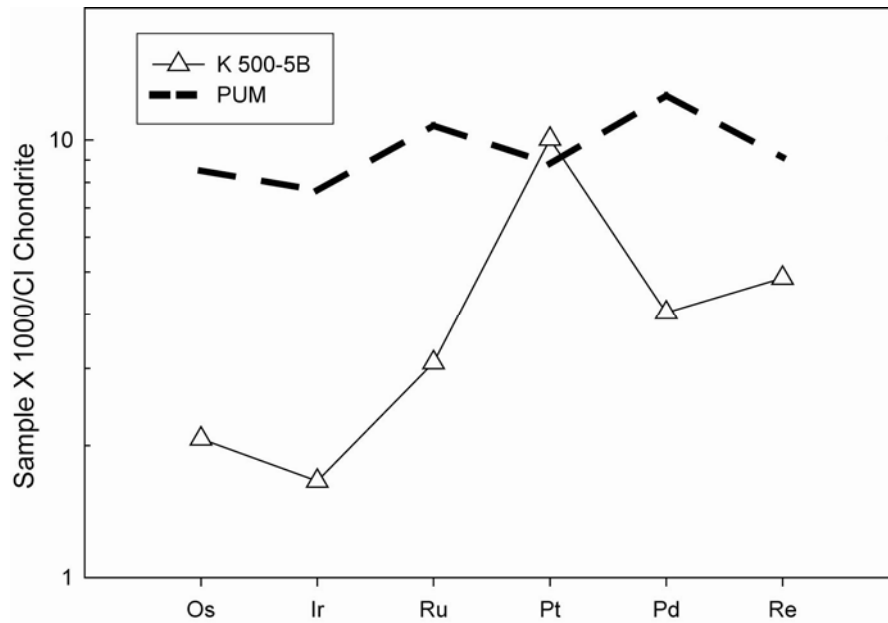
Figure 3.9: Sample S500-5B from Koolau, which has been pervasively altered by Mn-rich material. The HSE pattern for this sample is consistent with other volcanic centers, with the exception of Pt, which shows a marked enrichment.

3.5.2.3 Effects of partial melting and crystal-liquid fractionation

Partial melting can cause significant HSE fractionation (Barnes et al., 1985; Barnes et al., 1993; Rehkämper et al., 1999; Momme et al., 2003; Bockrath et al., 2004; Maier and Barnes, 2004). The effects of partial melting can most clearly be observed by a comparison between the HSE content of a high degree partial melt, such as some komatiites (Puchtel et al., 2004; 2005), and a lower degree melt, such as a typical MORB (Tatsumi, 2003; Peucker-Ehrenbrink et al., 2003).

The HSE abundances of a primary mantle melt are primarily controlled by the presence or absence of trace phases in the melt residue. Sulfides, in particular, are important carriers of the HSE in the mantle, although the IPGE (Os, Ir and Ru) are also hosted by other phases including Os-Ir-Ru alloys (Maier and Barnes, 2003; Bockrath et al., 2004; Ballhaus et al., 2006; Luguet et al., 2007). The IPGE are typically incorporated into Mss (mono-sulfide solid solution), which is frequently included in silicate phases (Maier and Barnes, 2003; Bockrath et al., 2004; Ballhaus et al., 2006; Luguet et al., 2007). The PPGE (Pt and Pd) are commonly hosted by Cu-sulfides which are usually found as interstitial phases (Alard et al., 2000; Maier and Barnes, 2003). Rhenium, on the other hand, is not evidently controlled by this inter-sulfide partitioning. It typically remains moderately incompatible during mantle melting and may be controlled by silicate partitioning. Thus, a strong Re enrichment is a common feature of most mantle-derived melts (e.g., Tatsumi, 2003; Peucker-Ehrenbrink et al., 2003)

Higher degree partial melts (>20%), such as some komatiites, are commonly S-undersaturated. Consequently the HSE can be efficiently removed from the source,

as the hosting sulfides are entirely incorporated into the melt. Such melts tend to have relatively flat chondrite-normalized HSE patterns (approaching chondritic Pd/Ir ratios), as well as higher absolute abundances of these elements, relative to other mafic melts (Puchtel et al., 2004; 2005). Conversely, lower degree partial melts (<20%), such as most basalts, tend to be S-saturated, resulting in incomplete dissolution of sulfide in the mantle source. In these cases the PPGE can be effectively fractionated from the IPGE as the interstitial Cu-rich sulfides melt out before Mss, resulting in magmas with high Pd/Ir ratios. In a similar manner, incongruent melting of mixed sulfide phases may also result in a residue containing Mss (Maier and Barnes, 2003; Ballhaus et al., 2006).

The picritic samples analyzed in this study have estimated parental melt concentrations of the HSE that fall between those of komatiites and Pacific MORB (Figure 3.7). Norman and Garcia (1999) concluded that the degree of partial melting necessary to generate the Hawaiian picrites was ~ 4 to 10%, indicating that these samples were sulfur-saturated at the time of melting. However, as a melt ascends, sulfide can be eliminated by decompression, causing the melt to become sulfur-undersaturated (Ballhaus et al., 2006). Although these picrites represent similar degrees of partial melting as MORB, the difference in HSE abundances might be attributed to late-stage sulfide fractionation processes. MORB are generally much more evolved than OIB, and have, therefore, lost HSE due to sulfide fractionation (Ballhaus et al., 2006). The partial melting estimates were used by Bennett et al. (2000) to argue for the presence of variable amounts of residual sulfide in the Hawaiian plume source. These authors postulated that the observed variations in the

HSE abundances likely did not reflect large differences in the HSE composition of the source regions of the volcanoes, but rather the presence of variable proportions of residual sulfides in the mantle sources of each volcanic center. For a given mantle source, lower degrees of partial melting may result in larger amounts of residual sulfide, which would lead to lower absolute abundances of the HSE in the resulting melt. The HSE patterns of the picrites analyzed by Bennett et al. (2000) are similar to the Type-2 pattern observed in the present study. Samples with Type-2 patterns tend to have higher average abundances of Pt and Pd than samples with Type-1 patterns, resulting in elevated Pd/Ir and Pt/Ir ratios. We note that these two pattern types are observed within a single volcanic center and are not correlated with MgO content (i.e. samples with similar MgO contents can exhibit either pattern). If the Type-2 samples result from lower degrees of partial melting, the source region may retain more of the PPGE-hosting interstitial Cu-rich sulfide relative to the Type-1 samples. Thus, if the difference between the two HSE patterns is due to significant differences in the degree of partial melting, it should be reflected in the ratios of trace elements that would be sensitive to this process (e.g., La/Yb, Rb/Sr), as well as in the MgO content of the parental melts (Norman and Garcia, 1999). However, with the exception of Loihi, there is no discernible difference between the two HSE trends in terms of incompatible element ratios indicative of partial melting (Figure 3.10).

Slight differences in the degree of partial melting, however, may account for some of the inter-volcano differences. Samples from Loihi possess higher abundances of Pt, Pd and Re than the other volcanic centers. Norman and Garcia (1999) inferred from trace element modeling that Loihi magmas formed from the lowest degrees of partial
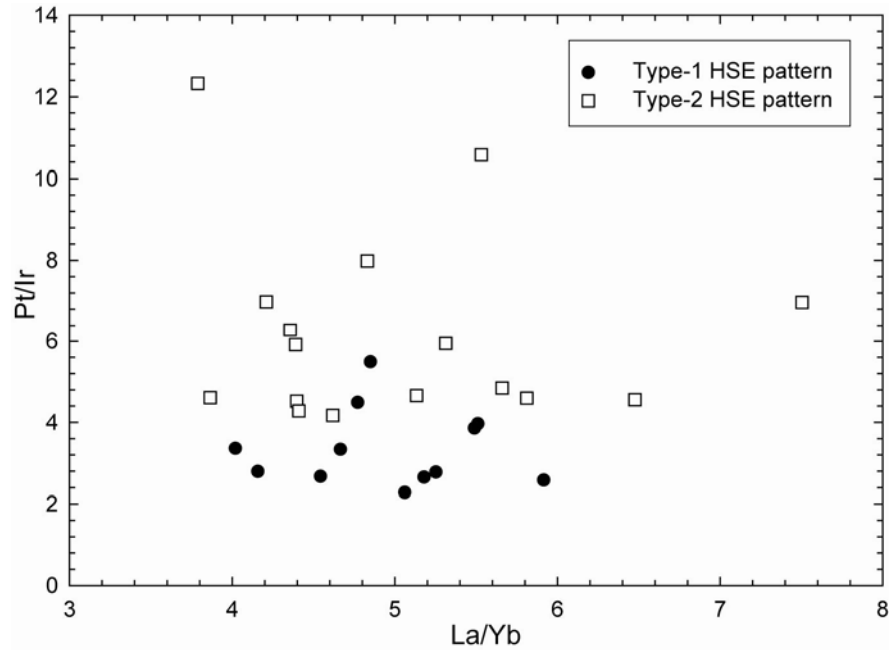
95

Figure 3.10: A plot of Pt/Ir versus La/Yb. La/Yb is a trace element ratio that is not affected by olivine crystallization and varies with the degree of partial melting. If the difference in Pt/Ir ratios between Type-1 and Type-2 HSE patterns was a result of different degrees of partial melting, a relationship between the two ratios would be expected. However, there is no correlation between the HSE patterns and La/Yb which indicates that partial melting was not the cause of the difference. La/Yb data are from Norman and Garcia (1999), Huang and Frey (2003) and Ireland et al. (2009).

melting among the Hawaiian volcanoes. This interpretation is supported by the present study, as Loihi has the highest concentrations of the more incompatible PPGE, as well as the highest La/Yb ratios in the sample suite. Differing degrees of partial melting can also have a bearing on the absolute abundances of the HSE in the sample suite, based on the proportion of residual sulfide that may be left in the mantle. However, this process alone may not produce the variations in relative abundances that are observed between Type-1 and Type-2 HSE patterns.

By process of elimination, we speculate that the variations between Type-1 and Type-2 samples mainly relate to slight differences in the degree of partial melting and the sulfide mineralogy of the residual mantle, coupled with minor dissimilarities in the crystal-liquid fractionation process for each volcanic suite. This hypothesis may be best observed in samples H-2 (Type-1 HSE pattern) and H-11 (Type-2 HSE pattern) from Hualalai, both of which contain ~13.6 wt% MgO and have olivine in equilibrium with the whole rock. These samples are from the same volcanic center and have similar La/Yb ratios, so they likely do not reflect a change in the degree of partial melting. The different HSE patterns instead most probably reflect minor differences in the crystal-liquid fractionation process, which could result from slightly different magma evolution histories. Chromite fractionation in a PGE-chromite saturated (but sulfide-undersaturated) melt may result in the direct removal of the IPGE as a magma ascends, as chromite may act as a nucleation point for IPGE alloys (Ballhaus et al., 2006). This process can further fractionate the IPGE from the PPGE, as a magma ascends through the mantle or as a magma sits in a high level magma chamber. Removal of Mss from an immiscible sulfide liquid could also fractionate

the IPGE from the PPGE. We speculate that sample H-11 lost Os, Ir and Ru relative to Pt and Pd due to the direct removal of IPGE phases (i.e. Mss or chromite-associated IPGE alloys) during magma ascent or through the removal of cumulate phases in a higher-level magma chamber. The retention of chromite-associated IPGE alloys could also potentially explain the reproducibility of the Os-Ir-Ru relative abundances observed in the Type-1 HSE pattern.

3.5.3 Source heterogeneities

In order to account for variations in $^{187}Os/^{188}Os$ ratios, a parameter not affected by crystal-liquid fractionation or variable partial melting, some level of HSE heterogeneity must be present in the Hawaiian mantle plume. These isotopic variations require long-term differences in the Re/Os ratios of the source regions for the Hawaiian volcanic centers (Lassiter and Hauri, 1996; Brandon et al., 1999; Bennett et al., 2000; Bryce et al., 2007). Previous authors have attributed the $^{187}Os/^{188}Os$ variations to the presence of recycled oceanic mafic crust and/or sediments in the plume source for Hawaiian volcanoes (e.g., Lassiter and Hauri, 1998). A role for core-mantle interaction has also been proposed to account for some of the ^{187}Os enrichment (and corresponding ^{186}Os enrichment) observed in some volcanic centers (Brandon et al., 1999).

Currently, precisely extrapolating mantle source HSE abundances from parental melt compositions is impossible because of the compatible to slightly incompatible nature of these elements. However, given similar melting conditions, the assumption

can be made that large scale variations in absolute and relative HSE abundances in the mantle sources would be reflected in the parental melt compositions.

Relative and absolute HSE abundances in the picrites show no correlation with variations in $^{187}Os/^{188}Os$ ratios (Figure 3.11), suggesting either insufficient resolution, or that relatively recent processes have led to a decoupling between these geochemical parameters. To consider the required level of resolution necessary, we use the mixing model of Lassiter and Hauri (1998). They concluded that the addition of ~30% of 1.8 Ga recycled oceanic crust, comprising a mixture of 97% basalt and 3% sediment, to the mantle source for the Hawaiian plume could produce the most radiogenic observed basalts ($^{187}Os/^{188}Os$ ratios of 0.148 for Koolau). Following the parameters of their modeling, the Re/Os ratio of their hybrid mantle source would increase by a factor of ~2. If the increased Re/Os ratio of the source is also reflected in the parental melts, it would provide a direct link between the $^{187}Os/^{188}Os$ isotopic composition and the HSE characteristics of the picrites and the source. However, although the Re/Os ratios of the estimated parental melts in this study also vary by a factor of 2, the variation is in the opposite direction predicted by oceanic crust recycling. For example, the parental melt for Hualalai, which has the highest average $^{187}Os/^{188}Os$ ratio in this suite, is estimated to have the lowest Re/Os ratio; whereas, the estimated parental melt for Mauna Kea has the lowest average $^{187}Os/^{188}Os$ ratio, but the highest Re/Os (Table 3.5; Figure 3.11). This result suggests that either the Re/Os of parental melts do no accurately reflect the Re/Os of the mantle source, or that relatively recent processes have affected the Re/Os ratios of the sources, and caused a decoupling of ^{187}Os and Re/Os.

One clue to the lack of correlation may be the Os enrichment in Hualalai lavas (Figure 3.2a). The parental melts for Hualalai have a higher estimated Os abundance (~1.0 ppb) than estimates for the other volcanic centers (0.5±0.2 ppb). This increase in Os abundance is accompanied by estimated Ir and Ru contents that fall on the high end of the Hawaiian spectrum, but not significantly greater than the other estimated parental melts. The enrichment in Os, relative to Ir and Ru, could be the result of melt percolation processes, which have been shown to fractionate Os from the other IPGE.

For example, Büchl et al. (2002; 2004a; 2004b) reported that melt percolation processes occurring in the Troodos Ophiolite on Cyprus, resulted in the fractionation of Os from Ir and Ru. Fractionation occurs as these elements become mobilized, and behave incompatibly, contrary to their behaviour during partial melting processes. Troodos harzburgite samples, which Büchl et al. (2002) concluded formed by low melt/rock ratios, have higher Os/Ir ratios than associated dunites (high melt/rock ratios). These harzburgites were interpreted to have undergone open-system melting, which resulted in an up to ~6-fold increase in Os/Ir relative to the dunites, yet retained the $^{187}Os/^{188}Os$ ratio of the mantle source. If such a melt percolation process occurred for Hualalai, at low melt/rock ratios, a modified source region with higher Os/Ir and Os/Ru ratios could have been formed. Partial melting of this modified source would result in a parental melt with higher Os/Ir and Os/Ru rations. An added consequence of this style of melt percolation would be a lowering of the Re/Os ratio, which is observed for the estimated Hualalai parental melt (Re/Os = 0.4). If the interpretation of this process is correct, the enriched $^{187}Os/^{188}Os$ at Hualalai

100

requires that it was a relatively recent event because the lower Re/Os ratio would ultimately lead to a retardation in the ^{187}Os/^{188}Os ratio. However, the high Os/Ir ratios in the harzburgites did not result from enrichments in Os, but rather depletions in Ir.

Becker et al. (2001) documented enriched Os concentrations in pyroxenitic precipitates caused by the melt percolation of a Mg-rich silicate melt through dunite channels from the Bohemian massif. They indicated that the Os budget of the pyroxenite was dominated by Os that was originally derived from mantle peridotite, which provides a means to increase the Os abundance of a melt if this pyroxenitic material can be incorporated into later melting events. Recently, Sobolev et al. (2005; 2007) suggested that recent melt percolation events have occurred in the mantle source region of the Hawaiian plume, resulting in a mixed pyroxenite-peridotite source, which provides a means to decouple HSE abundances and ^{187}Os isotopic compositions of Hawaiian parental melts. At this time, however, it is difficult to assess the effects of the peridotite to pyroxenite conversion on HSE abundances because the partitioning of these elements between these two phases is unknown. Such processing will have to be further examined via experimental techniques.

Some studies have also noted coupled enrichments between both ^{187}Os/^{188}Os and ^{186}Os/^{188}Os (^{190}Pt$\rightarrow$^{186}Os + α; $\lambda = 1.417 \times 10^{-12}$ yr^{-1}) in Hawaiian picrites and komatiites from Gorgona Island (Brandon et al., 1999; Brandon et al., 2003). Recent models attempting to reconcile these data have appealed to mixed pyroxenite-peridotite sources and redistribution of base-metal sulfides (BMS) to explain the co-
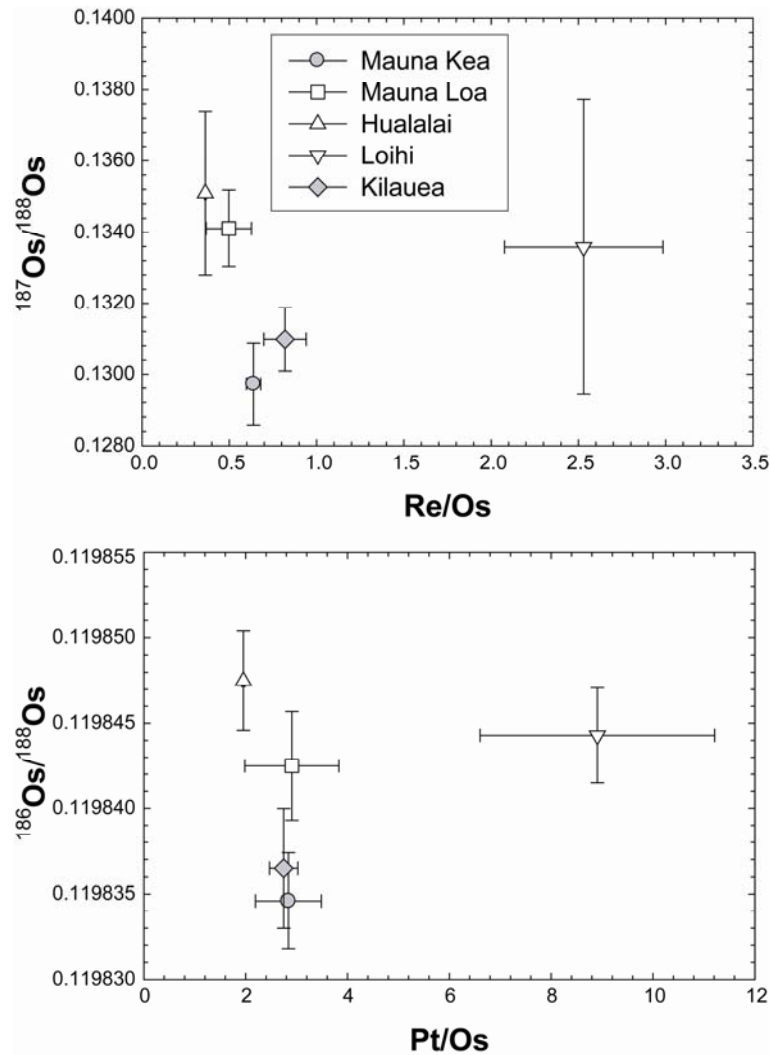
Figure 3.11: Plots of Os isotopic composition versus Re/Os and Pt/Os ratios. There is no correlation between these parameters, suggesting that either recent events have modified the Re/Os and Pt/Os characteristics of the mantle sources, or that parental melt HSE abundances are decoupled from those of their mantle source. [186]Os/[188]Os data from Brandon et al. (1999).

variations (Bockrath et al., 2004; Ballhaus et al., 2006; Luguet et al., 2008), consistent with claims of a pyroxenitic source for Hawaiian lavas (Sobolev et al., 2005; 2007). Some of these models suggest that peridotitic mantle sources can be hybridized by the addition of melts with high Pt/Os and Re/Os ratios, which are originally derived from subducted oceanic crust. Base-metal sulfides, which concentrate the HSE, may also be transferred into the hybridized source.

To consider this interpretation, we model the addition of ~0.8% of the most radiogenic BMS discussed in the Luguet et al. (2008) study to a peridotite source and assess the effect of this addition on $^{187}Os/^{188}Os$ ratios and HSE abundances. If such a process can physically occur, the resulting hybridized mantle would have an $^{187}Os/^{188}Os$ ratio of ~0.14, consistent with data for Lanai. A consequence of the addition of this sulfide, however, is a substantial increase in the Pt abundance of the mantle source from ~5 ppb to 17 ppb, accompanied by a 3-fold increase in the Pt/Os ratio. The increase in Pt abundances and Pt/Os ratios should be resolvable within the HSE data reported here, assuming that the increase in the source is reflected in the parental melt. This type of Pt enrichment is not observed in the more ^{187}Os or ^{186}Os enriched picrites from Hualalai (Brandon et al., 1999). Moreover, the estimated Pt abundances and Pt/Os ratios of the parental melts for the Hawaiian volcanoes are similar (Figure 3.11). These estimates suggest that hybridization of the mantle source with a pyroxenitic melt, and its associated BMS, either may not have played a major role in producing the trends observed between $^{187}Os/^{188}Os$ and $^{186}Os/^{188}Os$ ratios in the Hawaiian suite, or that the enriched Pt abundances in the source region somehow was not transferred to the parental melts for the picrites (Luguet et al., 2008).

3.6 Conclusions

1) The absolute HSE abundances of the Hawaiian picrites are intermediate between komatiites and typical MORB basalts. Osmium, Ir, and Ru behaved compatibly in the Hawaiian picrites, whereas Pt, Pd and Re generally behaved slightly incompatibly and became concentrated in the melt, although the behaviour of these elements was variable. The relative abundances of the HSE fall into two distinct groups that are not specific to a volcanic center. Type-1 patterns, when normalized to chondrites, are characterized by lower Pt/Ir, Pd/Ir and Pt/Pd than Type-2 samples.

2) The picrites analyzed in this study experienced variable amounts of olivine removal or accumulation, although some approximate a parental melt. This parental melt is estimated to contain ~16 wt% MgO and ~11 wt% Al_2O_3. The HSE characteristics of the various parental melts were generally similar (containing 0.5 ± 0.2 ppb Os, 0.45 ± 0.05 ppb Ir, 1.2 ± 0.2 ppb Ru, 2.3 ± 0.2 ppb Pt, and 0.35 ± 0.05 ppb Re). The estimated parental melt for Hualalai has a higher Os content at 1.0 ppb. The Loihi parental melt contained lower abundances of Os, Ir and Ru, but higher Pt, Pd and Re contents.

3) Crustal processes probably had only a minor affect on the Hawaiian picrites. Volatile loss of Re (and perhaps Ir) may have occurred in some subaerially erupted lavas. If crustal contamination occurred, it had a minor effect on the absolute HSE abundances of the picritic suite.

4) The complex relationship between the degree of partial melting and crystal-liquid fractionation appears to be the dominant control on the observed HSE abundances in

the samples.   Type-1 and Type-2 HSE patterns reflect minor differences in residual sulfides left in the mantle source and/or the loss of IPGE during magma ascent or in the cumulate zones of higher-level magma chambers associated with chromite crystallization. Minor variations in the degree of partial melting can explain some of the differences in the absolute abundances of the HSE between volcanic centers (e.g. Loihi).

5) There are source heterogeneities among the Hawaiian volcanic centers that are reflected in the ^{187}Os/^{188}Os ratios observed. However, ^{187}Os/^{188}Os variations are a result of ancient processes and are decoupled from HSE abundances in parental melts. Any HSE heterogeneities in the mantle sources for the various Hawaiian volcanic centers are probably small and have been obscured by the partial melting and crystal-liquid fractionation processes. Melt percolation events may play a small role in the relative fractionation of Os, Ir and Ru and may be able to explain high Os/Ir and Os/Ru for Hualalai. These melt percolation events would have had to occur recently, so as not to disturb the long-term Re/Os and ^{187}Os/^{188}Os ratios of the system.

Chapter 4: ^{186}Os systematics of Hawaiian picrites

Abstract

Nineteen Hawaiian picrites (MgO > 13 wt.%), as well as three related basalts, were analyzed for their ^{186}Os/^{188}Os and ^{187}Os/^{188}Os compositions. Variations in these ratios reflect long-term Pt/Os and Re/Os differences in the mantle source regions of the Hawaiian volcanoes. ^{187}Os/^{188}Os ratios vary from 0.1290534 ± 19 to 0.1361215 ± 16 ($2\sigma_m$), within the range defined by previous studies. ^{186}Os/^{188}Os ratios vary from 0.1198332 ± 26 to 0.1198480 ± 19 ($2\sigma_m$), with some compositions clearly resolved from current estimates of the ambient upper mantle (0.1198365 ± 55 2σ). Earlier studies of Hawaiian picrites reported coupled enrichments between ^{186}Os/^{188}Os and ^{187}Os/^{188}Os ratios that defined a well-correlated linear relationship. The trend was interpreted to imply that there is a homogenous, common Os reservoir contributing radiogenic ^{186}Os and ^{187}Os to the Hawaiian plume, possibly the outer core. The incorporation of recycled oceanic crust and Fe-Mn crusts, as well as enrichment in base-metal sulfides have also been proposed as mechanisms for generating correlated enrichments in ^{186}Os and ^{187}Os.

The new, much larger ^{186}Os-^{187}Os database does not define a single linear trend. Addition of ancient portions of recycled oceanic crust can produce observed variations in ^{187}Os/^{188}Os, however, are not likely to generate substantial ^{186}Os/^{188}Os

variations. Two scenarios are evaluated to explain the new data. 1) The first

considers the mixing of a common Os enriched (COs) reservoir with the two

dominant, geochemically distinct Hawaiian sources, represented by so-called Kea-

and Loa-trend lavas. The presence of two source components that dominate

lithophile element compositions is consistent with previous observations based on Sr,

Nd and Pb isotopes. The higher $^{87}Sr/^{86}Sr$ and $^{187}Os/^{188}Os$, and lower $^{143}Nd/^{144}Nd$ of

Loa-trend sources have been attributed to the presence of a recycled oceanic crust

component. A third component, the COs reservoir, is characterized by both elevated

$^{186}Os/^{188}Os$ and $^{187}Os/^{188}Os$ ratios. Mixing between these three components would

produce a field of Os isotopic data outlined by two linear mixing trends between the

COs reservoir and the Kea- and Loa-trend sources. The new data are broadly

consistent with this. Interpretation of the COs component as the outer core, however,

faces major challenges. 2) The second scenario involves the incorporation of variably

Pt, Re and/or ^{186}Os- and ^{187}Os-enriched base-metal sulfides (BMS) into the Hawaiian

source during a hybridization process. Variable and selective transport of BMS into

the source regions during metasomatism of the mantle source could produce the

observed trends. Correlations between Pt/Os and $^{186}Os/^{188}Os$ in Hualalai may provide

support for this interpretation. It too, however, can not account for all of the

characteristics imposed by Os isotopes and highly siderophile element abundances.

Keywords: highly siderophile elements; platinum group elements; Os isotopes;

Hawaii; core-mantle interaction; pyroxenites; base-metal sulfides

4.1 Introduction

The ^{190}Pt-^{186}Os isotopic system (^{190}Pt $\rightarrow$ ^{186}Os + α; λ=1.48x10^{-12} yr^{-1}; Walker et al., 1997) is a potentially powerful tool to characterize the nature of the mantle sources of ocean island basalt (OIB) volcanism, as well as to possibly constrain the depths of origin of OIB (Walker et al., 1995, 1997; Brandon et al., 1998, 1999, 2003, 2007; Puchtel et al., 2004, 2005). The long half-life of ^{190}Pt (t$_{1/2}$ = 469 Ga), combined with its low natural abundance (~0.01296%; Walker et al., 1997), results in an isotopic system that is relatively insensitive to most geologic processes. Only those processes that result in long term and large fractionations in Pt/Os ratios will produce measurable differences in ^{186}Os/^{188}Os.

Platinum and Os are highly siderophile elements (HSE; Os, Ir, Ru, Pt, Pd and Re), meaning that they have a high affinity for metallic Fe (Barnes et al., 1995; Walker, 2000). Consequently, mass balance calculations suggest that core segregation resulted in the nearly quantitative removal of these elements from the mantle. At present ~98% of the terrestrial budget of the HSE resides in the core (McDonough, 2003). Although the mantle is depleted in HSE relative to the core, these elements occur in roughly chondritic proportions in the upper mantle (Meisel et al., 2001; Becker et al., 2006). Thus, the upper mantle has evolved with an approximately chondritic Pt/Os ratio over time (Brandon et al., 2006), and has an ^{186}Os/^{188}Os ratio within the range of chondrites (Brandon et al., 2006; Yokoyama et al., 2007).

Enrichments in ^{186}Os/^{188}Os, relative to the ambient upper mantle, have been documented in three putative plume systems, including Hawaii, Gorgona Island and an ore sample from Noril'sk that is related to the Siberian Traps (Walker et al., 1997;

Brandon et al., 1998; 1999; 2003). Accompanying these [186]Os enrichments are observed excesses in [187]Os relative to ambient upper mantle. [187]Os is the daughter product of [187]Re (β^- decay; $\lambda=1.67 \times 10^{-11}$ yr^{-1}; Smoliar et al., 1996) and comprises a complementary isotopic system to the Pt-Os decay scheme (Walker et al., 1997; Shirey and Walker, 1998; Brandon et al., 1999, 2003; Puchtel et al., 2004, 2005). Well-correlated coupled enrichments in both [186]Os and [187]Os were interpreted to suggest that there may be a common process and/or mixing component (common Os component, or COs) that is responsible for producing the coupled enrichments between [186]Os and [187]Os (Brandon et al., 1998, 1999, 2003; Brandon and Walker, 2005).

Several previous studies have concluded that the outer core is the most likely COs source (Brandon et al., 1998, 1999, 2003). The core-mantle interaction hypothesis purports that crystallization of the Earth's inner core may have caused the fractionation of Pt and Re from Os, resulting in an outer core that has elevated Pt/Os and Re/Os relative to chondrites. Fractionations of the necessary magnitudes are observed in experimental and natural low pressure solid metal-liquid metal systems (e.g., Malvin et al., 1986; Fleet and Stone, 1991; Cook et al., 2004), as well as some higher pressure and temperature experimental systems (e.g., Lauer and Jones, 1998; Walker, 2000). Given predicted changes in parent-daughter ratios, the outer core would have evolved to suprachondritic [186]Os/[188]Os and [187]Os/[188]Os over time. This isotopically distinct metal may be sparingly sampled by plumes that rise from the core-mantle boundary. The core contaminated portion of the plume may contribute melt to lavas that are transported to the surface (Walker et al., 1997; Brandon et al.,

1998, 1999, 2003). The interpretation that the outer core can serve as the COs component in the Hawaiian system, however, has several significant challenges. First, some experimental partitioning work done at high pressures and temperatures is not consistent with the production of the necessary fractionations of the HSE (van Orman et al., 2008). Also, given plausible limits on the extent of fractionation that can be caused by crystallization of the inner core, early (within <1 Ga of the formation of the Earth) and rapid crystallization of the inner core, is required to produce the requisite elevated Os isotopic compositions (Brandon et al., 2003). Such early inner core formation is contrary to several recent thermal evolution and geodynamo power models (Buffett et al., 1996; Labrosse et al., 2001, 2003; Lassiter, 2006). Finally, collateral geochemical effects that might be expected to be present in mantle sources contaminated by outer core metal, such as raised overall HSE abundances, have not been observed (e.g., Bennett et al., 1999; Ireland et al., 2009a).

Several alternative hypotheses for the coupled ^{186}Os-^{187}Os enrichments have been suggested, and generally involve the recycling of different types of materials via subduction processes. For example, the presence of recycled oceanic crustal component, characterized by high Pt/Os and Re/Os ratios, in some OIB sources may also lead to coupled Os isotope systematics (Smith, 2003; Meibom et al., 2004; Luguet et al., 2008). Luguet et al. (2008), for example, highlighted one pyroxenite sample, presumed to be derived from an oceanic crust protolith, from the Beni Bousera massif that had Pt/Os and Re/Os ratios that could produce a mixing trend consistent with the Hawaiian observations; however, such compositions may be atypical of recycled oceanic crust (Luguet et al., 2008; van Acken et al., 2009).

Alternatively, Mn-crusts and nodules with high Pt/Os and Re/Os ratios may be incorporated into an OIB source and could lead to enrichments in ^{186}Os and ^{187}Os (Ravizza et al., 2001; Smith, 2003; Baker and Jensen, 2004; Schersten et al., 2004).

A potential role for base-metal sulfides (BMS) has also been suggested as another means of producing a mantle source with elevated ^{186}Os and ^{187}Os, and/or elevated Pt/Os and Re/Os ratios (Bockrath et al., 2004; Alard et al., 2005; Ballhaus et al., 2006; Luguet et al., 2008). A BMS is broadly defined as a sulfide phase containing base metal cations (e.g., Fe, Cu, Zn, and Pb among others), and may be important, mobile carriers of the HSE, particularly Pt and Pd, in the mantle (Bockrath et al., 2004; Ballhaus et al., 2006; Luguet et al., 2008). The HSE and Os isotopic compositions of BMS are highly variable, but due to typically high Pt/Os and Re/Os ratios in some of these grains, they may evolve to high ^{186}Os/^{188}Os and ^{187}Os/^{188}Os (Luguet et al., 2008). If such sulfides are selectively transported into a mantle domain during a mantle metasomatic event, eventual melting of the hybridized domain could produce a melt with coupled Os isotopic enrichments (Luguet et al., 2008).

Here we re-focus on the Hawaiian shield volcanoes and consider the ^{186}Os and ^{187}Os characteristics of a large suite of Hawaiian picrites and three related basalts, using high-precision thermal ionization mass spectrometric techniques. Hawaii represents a prototypical example of OIB volcanism, with the greatest mass buoyancy flux (Sleep, 1990) and the hottest mantle potential temperature (e.g., Putirka, 2008) of any modern OIB locality. Several geophysical studies have suggested that the source region of the Hawaiian shield volcanoes may extend to the core-mantle boundary

(CMB; e.g., Russell et al., 1998; Zhao, 2001; Courtillot et al., 2003; Montelli et al., 2004), in addition to the geochemical arguments made by Brandon et al. (1999) and possible complementary evidence provided by Fe/Mn ratios (Humayun et al., 2004). Previous HSE and ^{187}Os measurements of Hawaiian rocks suggested a variable role for residual sulfides in the plume source, which may buffer the absolute HSE abundances (Tatsumi, 1999; Bennett et al., 2000; Ireland et al., 2009a). ^{187}Os/^{188}Os ratios tend to have a narrow range within an individual volcanic center, but are variable between different volcanoes (Hauri et al., 1996; Lassiter and Hauri, 1998; Bennett et al., 2000; Bryce et al., 2005; Ireland et al., 2009a) suggesting long-term, discrete Re/Os variations in the Hawaiian mantle source regions.

The picritic sample suite analyzed here, which includes four samples from the original Brandon et al. (1999) study (Kil 1-18, ML 1868-9, Lo-02-02, Lo-02-04 and H-11), represents some of the most primitive melts from Hawaiian shield volcanoes, and thus, may be particularly useful in preserving information about the mantle source regions of the Hawaiian plume (Norman and Garcia, 1999). These specific samples have been previously investigated for HSE abundances and for ^{187}Os (Ireland et al., 2009a), with the suggestion that the Re/Os and Pt/Os ratios of the mantle sources are decoupled from those in the final lavas. In this study, we present high precision ^{186}Os/^{188}Os isotopic data for the Hawaiian picritic suite, along with Pt/Os and ^{187}Os/^{188}Os ratios, and attempt to reconcile these data with the processes that may be affecting the mantle source regions of the Hawaiian shield volcanoes.

4.2 Samples

The sample suite analyzed in this study were predominately main-shield stage picrites (MgO>13 wt.%; n=19), with two related tholeiitic basalts (MgO<12 wt.%) from Hualalai (H-7, H-9) and a pre-shield stage basalt from Loihi (158-9. Major element and HSE data were previously reported for all of these rocks (Ireland et al., 2009a and references therein). The picrites are derived from high density melts that erupted on the flanks of the main-stage shield volcanoes, and likely bypassed the summit reservoirs (Garcia, 1995). Therefore, these rocks are less likely to have been affected by crystal-liquid fractionation processes that may operate in high-level magma chambers (Norman and Garcia, 1999). Thus, these are likely among the best samples available to constrain the nature of the mantle source regions of the Hawaiian volcanoes.

Six volcanic centers, which span approximately 3 Myr of eruption history, are represented in the study: Mauna Kea, Mauna Loa, Hualalai, Loihi, Kilauea and Koolau. Samples were obtained from submersible dives and submarine dredge hauls from the submerged flanks of the Hawaiian volcanoes, subaerial flows and from the Hawaiian Scientific Drilling Project (HSDP-2) hole (Table 1). The samples were selected based on previously collected Os abundance and ^{187}Os isotopic data (Ireland et al., 2009a) in order to cover a wide range in ^{187}Os/^{188}Os ratios, as well as high concentrations of Os, in order to facilitate the ^{186}Os analysis.

4.3 Analytical procedures

Samples were generally collected as multiple 100 to 400 g hand-sized masses, although some of the HSDP samples were obtained as rock chips and powders. Visibly weathered surfaces on large hand samples were removed using a diamond rock saw, and polished using SiC sandpaper to remove the saw marks. Samples were broken in to cm-sized chips using a high-tensile strength alloy mortar and pestle or with a ceramic-faced jaw crusher. These chips were screened again for weathered pieces and any potential metal contamination, and then ground into a fine powder and homogenized using an agate shatterbox.

The procedures used for the separation of Pt, Re and Os are outlined in Ireland et al. (2009). In brief, the sample powder was digested, along with appropriate amounts of spike solutions, in a mixture of 3 g of Teflon-distilled concentrated HCl, and 6 g of Teflon-distilled concentrated HNO_3, inside sealed Pyrex Carius tubes and heating at $240°C$ for about 48 hours. Osmium was separated using a solvent extraction technique, purified by a microdistillation step (Birck et al., 1997) and then analyzed using a single collector NBS-style TIMS (thermal ionization mass spectrometer) at the University of Maryland. The remaining HSE were purified using anion exchange chromatography and analyzed using a Nu Plasma ICP-MS (inductively coupled plasma mass spectrometer).

Unspiked aliquots of the sample powders were processed following the methods described in Brandon et al. (1999, 2000, 2003). Generally, 150 to 500 g of sample powder were fused using a NiS fire assay method (Hoffman, 1978) in order to pre-concentrate the Os and to obtain ~100 to 200 ng of Os for isotopic analysis. The

114

fusions were performed at 1100ºC for 90 minutes, using sodium tetraborate as a flux, in a sample:nickel:sulfur:flux weight ratio of 10:1:0.5:20. This procedure resulted in the formation of an immiscible NiS bead that concentrated the Os, and permitted extraction from the fusion glass. These NiS beads were dissolved in 6N HCl, and insoluble Os-sulfide was trapped on cellulose paper by filtering the HCl solution. The Os-bearing filter paper was dissolved in a Pyrex Carius tube using 4 mL of Teflon-distilled concentrated HCl and 8 mL of Teflon-distilled concentrated HNO_3, and was then heated at $240°C$ for about 48 hours. Osmium was separated from the aqueous phase using a carbon tetrachloride solvent extraction technique, and then back-extracted into concentrated HBr (Cohen and Water, 1996). A final microdistillation step further purified the sample (Birck et al., 1997). Prior to isotopic analysis, the purified Os was dissolved in 2μL of concentrated HCl for filament loading. The total Os yields from the fusion process were measured by equilibrating small aliquots (~2-3%) of the purified Os with a spike solution, and varied from 40 to 80%, with the majority of sample fusions resulting in a 50 to 60% yield.

High-precision Os isotope data for unspiked aliquots of the samples were obtained by negative thermal ionization mass spectrometry (NTIMS) using a Thermo Electron Triton mass spectrometer at the University of Maryland, with the exception of four samples analyzed at the Johnson Space Center (Mauna Kea samples SR0450-3.55, SR0720-18.25, SR0954-8.00) also using a Thermo Election Triton mass spectrometer. Data were collected in static mode using nine Faraday collectors with signal intensities of >100 mV on mass 234 ($^{186}Os^{16}O_3^-$) and 235 ($^{187}Os^{16}O_3^-$) generated for ≥180 ratios (17 s integration time per ratio) to reach an in-run precision

of ± 25 ppm ($2\sigma_m$) or better for the $^{186}Os/^{188}Os$ ratio. The oxygen pressure for all runs was maintained between 1 to 2×10^{-7} mbar. Oxygen corrections were carried out using $^{17}O/^{16}O$ of 0.000375 and $^{18}O/^{16}O$ of 0.002044 (Nier, 1950), followed by instrumental mass fractionation corrections using the exponential law and a $^{192}Os/^{188}Os$ ratio of 3.083.

During the analytical campaign, 30 runs of a Johnson Matthey Os internal standard were conducted at the University of Maryland with an average $^{186}Os/^{188}Os$ ratio of 0.1198437 $\pm$ 20 and a $^{187}Os/^{188}Os$ ratio of 0.1137826 $\pm$ 25 ($2\sigma_{pop}$). The average of these ratios for 10 runs at the Johnson Space Center was 0.1198459 $\pm$ 20 and 0.1137907 $\pm$ 25 ($2\sigma_{pop}$) respectively. Previous measurements of the Johnson-Matthey Os standard conducted at the University of Maryland on a VG Sector-54 mass spectrometer and on the Triton at the Johnson Space Center averaged 0.1198475 (Walker et al., 1997; Brandon et al., 1998, 1999, 2000, 2003, 2006; Puchtel et al., 2004, 2005; Walker et al., 2005). For the sake of direct data comparison, all Hawaiian and other ^{186}Os data reported here are corrected to the average Johnson-Matthey Os standard $^{186}Os/^{188}Os$ of 0.1198475 obtained in earlier studies. A correction factor of 1.0000319 was applied to samples run at the University of Maryland and 1.0000136 for samples run at the Johnson Space Center. A well-characterized Os-rich alloy from SW Oregon (OSUM8) was run as a secondary standard multiple times during the analytical campaign (n=23). These runs had a corrected $^{186}Os/^{188}Os$ ratio of 0.1198399 $\pm$ 20 and an $^{187}Os/^{188}Os$ ratio of 0.1314618 $\pm$ 20 respectively ($2\sigma_{pop}$), in good agreement with previous measurements of the same sample (Lamellae 4: $^{186}Os/^{188}Os$=0.1198388 $\pm$ 17, $^{187}Os/^{188}Os$=0.1314672 $\pm$ 24 $2\sigma_m$;

Walker et al., 2005). Sample uncertainties are cited as $2\sigma_m$ of the run statistics for individual samples, and as the $2\sigma_m$ of duplicate analyses for samples that were measured multiple times. No age-correction is applied to the isotopic data since the samples are all relatively young.

4.3.1 Potential Analytical Concerns

Luguet et al. (2008) outlined several potential analytical issues with the high precision/accuracy measurement of Os isotopes via NTIMS. These issues mainly involve the identification and removal of different polyatomic mass interferences and oxygen isotope interferences. In addition to these concerns, the analytical blank and its potential impact on measured $^{186}Os/^{188}Os$ ratios is also discussed in the next section.

Os Blank:

Three measurements of the analytical blank produced by the fusion process have been made, two by Brandon et al. (1999) and one in the present study. Osmium contributions from the blank are 0.44, 0.70 (this study) and 1.0 pg/g of fused sample, and have an average $^{186}Os/^{188}Os$ ratio of 0.1199 ± 2. To assess the impact of the analytical blank on the measured $^{186}Os/^{188}Os$ ratio of a sample, the deviation in $^{186}Os/^{188}Os$ ratios was modeled as a function of the sample to blank ratio (Figure 4.1). For this modeling, a hypothetical blank of 1.5 pg/g Os (50% higher than the maximum observed), and with $^{186}Os/^{188}Os$ ratios of 0.1199 and 0.1201, was applied in order to estimate a maximum blank impact. This blank was mathematically added to a hypothetical sample with a composition identical to that of the upper mantle ($^{186}Os/^{188}Os = 0.1198365$), with the sample to blank ratios mirroring the range

117

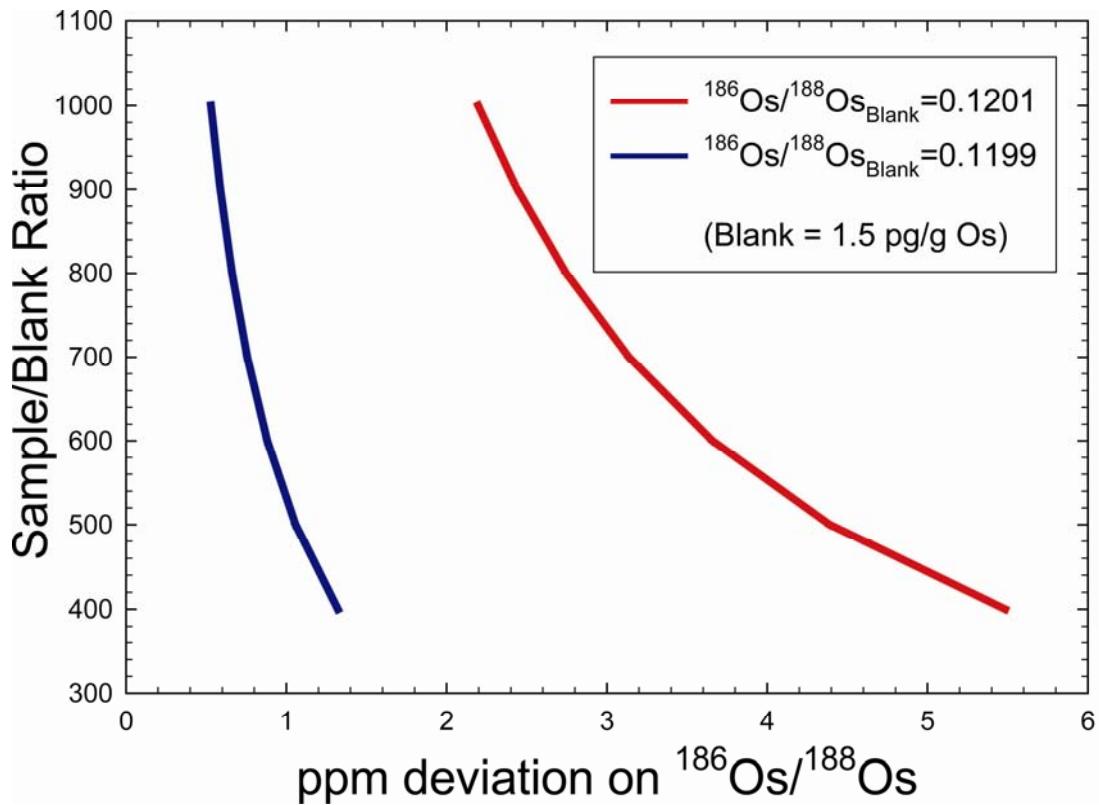**Figure 4.1:** The impact of the on the measured $^{186}Os/^{188}Os$ ratio. The blank is modeled at an Os concentration of 1.5 pg/g of fused sample (50% higher than the maximum measured blank) and at two different $^{186}Os/^{188}Os$ ratios. This blank was added to a hypothetical sample with an upper mantle-like $^{186}Os/^{188}Os$ ratio of 0.1198365, at differing sample:blank ratios.

observed in the dataset (~400 to 1000). The blank with the lower $^{186}Os/^{188}Os$ ratio

has a maximum impact of 1.3 ppm; whereas the blank with the higher $^{186}Os/^{188}Os$

ratio has a maximum effect of 5.5 ppm at a sample to blank ratio of 400. The effect

of the blank is less at the higher sample to blank ratios. Considering that the typical

precision of the measurements reported is $\pm$ 25 ppm and that the hypothetical blank

modeled here is likely larger than the real blank, the blank effect is relatively minor

and uncertainties in the blank do not affect any interpretations.

<u>Mass Interferences</u>:

Several potential polyatomic mass interferences on the various Os isotopes,

typically involving oxides of Pt, Re and W, have been outlined by previous studies

(e.g., Brandon et al., 1999, Luguet et al., 2008) and are summarized in Table 4.1 for

the Os isotopes of interest in this study (^{186}Os, ^{187}Os, ^{188}Os and ^{192}Os). For example,

mass 234 ($^{186}Os^{16}O_3^-$) can be potentially affected by both $^{198}Pt^{18}O_2^-$ and $^{186}W^{16}O_3^-$.

For PtO_3^-, a mass interference that could impact $^{192}Os^{16}O_3^-$ (an atom used for mass

fractionation corrections), post-run mass scans up to mass 250 were monitored and

showed no evidence for PtO_3^- signals. Likewise, monitoring of $^{198}Pt^{16}O_2^-$ (mass 230)

allowed for an assessment of the $^{198}Pt^{18}O_2^-$ affect on $^{186}Os^{16}O_3^-$ (mass 234)

measurement. The effect of this interference is very minor, given the low count rates

on mass 230 (typically <25,000 cps) and the lower isotopic abundance of ^{18}O relative

to ^{16}O. For example, a 25,000 cps signal on mass 230 would translate to ~0.1 cps on

mass 234, equivalent to a 0.002 μV signal, which would have a ~0.02 ppm effect on

the $^{186}Os/^{188}Os$ ratio. For these reasons, no correction for PtO_2^- interference was

Table 4.1: Mass interferences on Os masses during NTIMS analysis

Mass	Os isotope	Polyatomic Interference[a]	Oxygen Interference[b]
234	$^{186}Os^{16}O_3^-$	$^{186}W^{16}O_3^-$ $^{198}Pt^{18}O_2^-$	$^{184}Os^{16}O_2^{18}O^-$
235	$^{187}Os^{16}O_3^-$	$^{187}Re^{16}O_3^-$	$^{186}Os^{16}O_2^{17}O^-$
236	$^{188}Os^{16}O_3^-$		$^{187}Os^{16}O_2^{17}O^-$ $^{186}Os^{16}O_2^{18}O^-$
240	$^{192}Os^{16}O_3^-$	$^{192}Pt^{16}O_3^-$	$^{190}Os^{16}O_2^{18}O^-$

[a] only polyatomic oxide interferences are listed here
[b] only oxygen interferences with two ^{16}O are listed here, because of the low probability of multiples of ^{17}O or ^{18}O

made in this study, although $^{198}Pt^{16}O^{18}O^-$ may be a significant interference on $^{184}Os^{16}O_3^-$ (mass 232).

A potential isobaric interference on $^{186}Os^{16}O_3^-$ by $^{186}W^{16}O_3^-$ was monitored by measuring $^{184}Os^{16}O_3^-$ (mass 232: $^{184}W^{16}O_3^-$), and was not observed during the course of the analyses. Luguet et al. (2008) noted that monitoring W interferences in this manner may not uniquely identify presence of an $^{184}W^{16}O_3^-$ interference due to the potential presence of $^{198}Pt^{16}O_2^-$. As an alternative, $^{183}W^{16}O_3^-$ (mass 231) was also measured on ion counters following each run with count rates typically <30 cps, indicating that the effects of this interference are negligible at the typical run voltages, which is in good agreement with the conclusion of previous studies (Brandon et al., 1999, 2003; Meibom et al., 2004; Walker et al. 2005; Luguet et al., 2008).

The interference of $^{187}Re^{16}O_3^-$ on $^{187}Os^{16}O_3^-$ (mass 235) was monitored by observing the size of the mass 233 ($^{185}Re^{16}O_3^-$) peak on the ion counters immediately following each analysis. This is a maximum estimate for Re interferences because most Re is ionized as ReO_4^-. Count rates on mass 233 were typically lower than 100 cps, which translates to a maximum ~2.7 µV signal on mass 235 ($^{187}Re^{16}O_3^-$). Luguet et al. (2008) noted that correcting the $^{187}Os^{16}O_3^-$ ratio for this interference will lower the resulting $^{187}Os/^{188}Os$ ratio by ~13 ppm, which is within the 2σ precision of our measurements. No corrections for these interference were made.

Oxygen Isotopic Composition

Oxygen isotope interferences on the various OsO_3^- ions need to be accounted for as well, since the interferences caused by ^{17}O and ^{18}O affects the measurements of heavier Os isotopes. For this study, O corrections were carried out using the O

isotopic composition of Nier (1950; $^{17}O/^{16}O$=0.000375 and $^{18}O/^{16}O$= 0.002044).

However, some recent studies have suggested that the isotopic composition of O

combining with Os in the mass spectrometer may not be constant during the course of

an individual run (Liu et al., 1998; Luguet et al., 2008). These studies have advocated

measuring the O isotopic composition in-run through the monitoring of the different

O isotopes on $^{192}OsO_3^-$, since ^{192}Os is the most abundant Os isotope, and correcting

each line of measurements individually (Luguet et al., 2008). Luguet et al. (2008)

reported that the maximum variation of the in-run $^{18}O/^{16}O$ ratios was 500 ppm (2σ),

but was typically smaller. However, this study did not consider the precision of an

individual $^{18}O/^{16}O$ ratio measurement, which is calculated here to be larger than the

overall variation in $^{18}O/^{16}O$ ratios reported for an entire run. For example, a 3V signal

on mass 240 ($^{192}Os^{16}O_3^-$) equates to a 0.00612V (370,000 cps) signal on mass 242

($^{192}Os^{16}O_2^{18}O^-$). A 4s integration time of this signal, as applied by Luguet et al.

(2008), would detect ~1.5 million ions. Assuming Poisson's counting statistics, the

best-case scenario for the precision on a single $^{18}O/^{16}O$ ratio is therefore ~ ±800 ppm,

which is larger than the maximum 500 ppm variation observed over the course of an

entire run by Luguet et al. (2008). The precision on $^{17}O/^{16}O$ is even worse since ^{17}O

is less abundant than ^{18}O. Thus, the in-run O correction, as employed by Luguet et al.

(2008) can not be as precise as implied in that study and its application here is not

justified, given the likely minor changes in O isotopic composition that may occur

during analysis.

The results of the ^{186}Os and ^{187}Os analyses are presented in Table 4.2, along with

previously reported Os, Pt, Re abundance data from Ireland et al. (2009a). The

^{186}Os/^{188}Os ratios of the samples range from 0.1198332 ± 26 for Mauna Kea sample

SR0502-4.85 to a high value of 0.1198480 ± 19 for sample H-9 from Hualalai. This

overall range is nearly identical to that observed in previous studies of Hawaiian

picrites (Brandon et al., 1998, 1999). ^{187}Os/^{188}Os ratios span a narrow range within

each volcanic center, which is typical of Hawaiian volcanism, and have an overall

range of 0.1290534 ± 19 to 0.1361215 ± 16, consistent with many previous analyses

of Hawaiian basalts and picrites (Martin et al., 1994; Hauri et al., 1996; Hauri and

Kurz, 1997; Lassiter and Hauri, 1998; Brandon et al., 1999; Bennett et al., 2000;

Bryce et al., 2005; Ireland et al., 2009a). The Os isotopic compositions of the three

related basalts fall into the range defined by the picrites, although these samples

typically have higher Pt/Os ratios.

There is generally good agreement in ^{186}Os/^{188}Os and ^{187}Os/^{188}Os ratios between

the samples analyzed by both the Brandon et al. (1999) study and the current work

(Figure 4.2; ML1868-9, H-11, Lo-02-02, Lo-02-04, Kil-1-18). Samples ML1868-9,

Kil-1-18, Lo-02-02 and Lo-02-04 have ^{186}Os/^{188}Os ratios that are within analytical

uncertainty of the previous measurements. Sample H-11, which had the highest

^{186}Os/^{188}Os ratio in the Brandon et al. (1999) study (0.1198475 ± 50), however, is

slightly outside (lower) of the uncertainty of the newly measured ratio ($0.1198410 \pm$

11). ^{187}Os/^{188}Os measurements are also generally comparable between studies,

although Lo-02-02 and ML1868-9 are outside of uncertainty. The minor differences

Table 4.2: Os, Pt, Re and Os isotopic data for the Hawaiian Picrites

Volcano	Sample Name	Os[a]	Pt[a]	Re[a]	Pt/Os	Re/Os	$^{184}Os/^{188}Os$[b]	$^{186}Os/^{188}Os$[b]	$\varepsilon^{186}Os$[c]	$^{187}Os/^{188}Os$[b]
Mauna Kea										
	SR0328-3.10	1.225	1.853	0.092	1.513	0.08	0.0013018 (14)	0.1198378 (18)	0.23	0.1298756 (20)
	SR0401-2.85	1.431	1.463	0.087	1.022	0.06	0.0013065 (17)	0.1198365 (20)	0.13	0.1306505 (21)
	SR0450-3.55[d]	1.240	1.977	0.256	1.594	0.21	0.0013058 (22)	0.1198392 (29)	0.35	0.1291371 (32)
	SR0502-4.85	1.087	1.876	0.258	1.726	0.24	0.0013041 (18)	0.1198332 (26)	-0.15	0.1298523 (28)
	SR0720-18.25 fusion 1[de]	0.519	2.494	0.354	4.805	0.68	0.0013074 (9)	0.1198418 (15)		0.1295643 (14)
	SR0720-18.25 fusion 1 rep[d]						0.0013105 (14)	0.1198427 (20)		0.1295628 (20)
	average (2σ_m)						0.0013089 (31)	0.1198423 (9)	0.61	0.1295636 (15)
	SR0954-8.00[d]	0.567	2.041	0.851	3.600	1.50	0.0013111 (13)	0.1198409 (18)	0.49	0.1290534 (19)
	SR0964-4.30 fusion 1	1.349	2.487	0.646	1.844	0.48	0.0013053 (6)	0.1198399 (10)		0.1295229 (11)
	SR0964-4.30 fusion 1 rep						0.0013042 (8)	0.1198404 (11)		0.1295229 (12)
	SR0964-4.30 fusion 1 rep2						0.0013049 (11)	0.1198414 (14)		0.1295234 (17)
	average (2σ_m)						.0013048 (6)	0.1198405 (9)	0.46	0.1295231 (3)
Mauna Loa										
	ML1868-9	0.701	1.629	0.230	2.324	0.33	0.0013050 (18)	0.1198428 (16)	0.65	0.1361215 (16)
	MLKAH-1	1.263	2.886	0.191	2.285	0.15	0.0013060 (10)	0.1198379 (26)	0.24	0.1345942 (26)
Hualalai										
	H-2	0.910	1.120	0.542	1.231	0.60	0.0013060 (13)	0.1198396 (18)	0.38	0.1346768 (16)
	H-7[f]	0.792	2.810	0.769	3.548	0.97	0.0012983 (31)	0.1198469 (36)	0.99	0.1364480 (36)
	H-9[f]	0.598	2.538	0.567	4.244	0.95	0.0013054 (14)	0.1198480 (19)	1.08	0.1354806 (19)
	H-11 fusion 1	0.935	2.805	0.460	3.000	0.49	0.0013083 (12)	0.1198401 (27)		0.1343229 (31)
	H-11 fusion 2						0.0012947 (31)	0.1198420 (15)		0.1345852 (18)
	H-11 fusion 3						0.0013090 (22)	0.1198408 (29)		0.1346474 (28)
	average (2σ_m)						0.0013040 (93)	0.1198410 (11)	0.50	0.1345185 (199)
	H-27	1.144	1.786	0.308	1.561	0.27	0.0013084 (13)	0.1198388 (17)	0.32	0.1347176 (19)
Loihi										
	Lo-02-02 fusion 1	0.984	5.825	0.679	5.920	0.69	0.0013071 (23)	0.1198434 (25)		0.1343226 (32)
	Lo-02-02 fusion 2						0.0013014 (13)	0.1198412 (20)		0.1347297 (18)
	Lo-02-02 fusion 2 rep						0.0012989 (29)	0.1198415 (33)		0.1347274 (39)
	average (2σ_m)						0.0013024 (49)	0.1198421 (22)	0.59	0.1345932 (271)
	Lo-02-04 fusion 1	1.150	6.526	0.567	5.675	0.49	0.0012975 (13)	0.1198435 (18)		0.1341483 (18)
	Lo-02-04 fusion 2						0.0013042 (12)	0.1198440 (19)		0.1341559 (21)
	Lo-02-04 fusion 3						0.0013054 (12)	0.1198405 (16)		0.1341942 (19)
	average (2σ_m)						0.0013024 (49)	0.1198427 (22)	0.64	0.1341661 (284)
	158-9 fusion 1[f]	0.832	7.637	0.721	9.179	0.87	0.0013031 (10)	0.1198407 (14)		0.1337556 (15)
	158-9 fusion 1 rep						0.0013049 (12)	0.1198421 (16)		0.1337570 (17)
	average (2σ_m)						0.0013040 (18)	0.1198414 (15)	0.53	0.1337563 (14)
Kilauea										
	Kil 1-18	0.572	2.564	0.813	4.483	1.42	0.0013076 (10)	0.1198361 (13)	0.09	0.1323272 (16)
	Kil 2-4	0.827	1.733	0.361	2.096	0.44	0.0013067 (19)	0.1198474 (19)	1.03	0.1319908 (30)
	Kil 3-1 fusion 1	0.733	1.975	0.215	2.694	0.29	0.0013061 (12)	0.1198468 (17)		0.1302953 (17)
	Kil 3-1 fusion 2						0.0013030 (15)	0.1198454 (19)		0.1302866 (19)
	average (2σ_m)						0.0013045 (31)	0.1198461 (14)	0.93	0.1302909 (87)
Koolau										
	S500-5B fusion 1	0.950	8.634	0.185	9.088	0.19	0.0013042 (10)	0.1198381 (17)		0.1395647 (14)
	S500-5B fusion 1 rep						0.0013006 (20)	0.1198376 (21)		0.1395621 (22)
	average (2σ_m)						0.0013024 (36)	0.1198379 (5)	0.24	0.1395634 (22)
	OSUM8 (n=23)						0.0013067 (33)	0.1198399 (20)		0.1314618 (20)
	Johnson-Matthey Standard (n=30)						0.0013057 (30)	0.1198437 (20)		0.1137826 (25)

[a] concentrations of Os, Pt and Re are in ng/g and from Ireland et al., 2009a

[b] Os isotopic compositions from unspiked aliquots

[c] $\varepsilon^{186}Os=[(^{186}Os/^{188}Os)_{sam}/(^{186}Os/^{188}Os)_{chon}-1]*10000$; where the present day $^{186}Os/^{188}Os_{chon}$ is 0.1198350 (Yokoyama et al., 2007)

[d] samples were analyzed at the Johnson Space Center. All other samples were analyzed at the University of Maryland

[e] samples for which different aliquots of powder were fused separately are numbered sequentially (e.g., fusion 1, 2 …)

[f] tholeiitic basalts (H-7 and H-9) and pre-shield stage basalt (158-9)

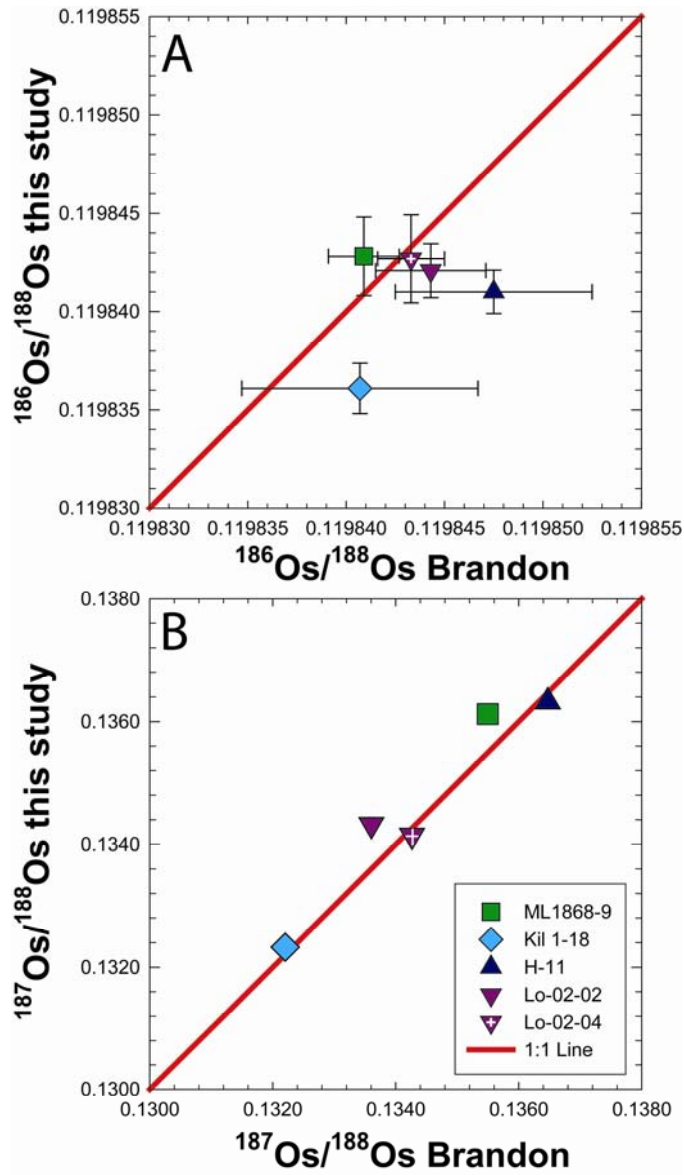rep: indicates a repeat run of the same filament on the mass spectrometer

Figure 4.2: Data comparison of A) $^{186}Os/^{188}Os$ and B) $^{187}Os/^{188}Os$ for samples

analyzed by both Brandon et al. (1999) and this study. For $^{186}Os/^{188}Os$ ratios, all

samples are within analytical uncertainty of each other, except for sample H-11. For

$^{187}Os/^{188}Os$ ratios, three out of five samples are within analytical uncertainty. Note

that error bars on $^{187}Os/^{188}Os$ measurements are smaller than the size of the symbols.

in $^{187}Os/^{188}Os$ may reflect the fact that sample powders for the different studies were made from different pieces of the rock (as sampled by submersible). These differences do not affect the interpretations of this study.

The relationship between $^{186}Os/^{188}Os$ and $^{187}Os/^{188}Os$ ratios for the picritic suite is presented in Figure 4.3. The majority of the samples have $^{186}Os/^{188}Os$ ratios that overlap the upper mantle average (0.1198365; Brandon et al., 2006). However, several samples (H-7, H-9, Kil-2-4 and Kil-3-1) have $^{186}Os/^{188}Os$ that are well above the upper mantle average. Also, although most volcanic centers are defined by a modest range in $^{187}Os/^{188}Os$ ratios, $^{186}Os/^{188}Os$ data for picrites from each of the Mauna Kea, Kilauea and Hualalai systems span nearly the range of $^{186}Os/^{188}Os$ ratios for the entire Hawaiian suite.   In general, the well-correlated ^{186}Os-^{187}Os trend observed in the earlier Hawaiian study (Brandon et al., 1999) is not apparent when considering the new, complete dataset.

Sample S500-5B from Koolau, which shows evidence for a Mn-crust contaminant (Ireland et al., 2009a), has an elevated $^{187}Os/^{188}Os$ ratio of 0.1395647 ± 14 and an anomalously high Pt/Os ratio (9.09). However, this sample shows no corresponding enrichment in $^{186}Os/^{188}Os$ (0.1198379 ± 5), and is within the range of the upper mantle average.

4.5 Discussion

4.5.1 $^{186}Os/^{188}Os$ composition of ambient upper mantle

When discussing enrichments in $^{186}Os/^{188}Os$ in Hawaiian picrites, a useful point of comparison is to the $^{186}Os/^{188}Os$ of the ambient upper mantle. Precisely defining

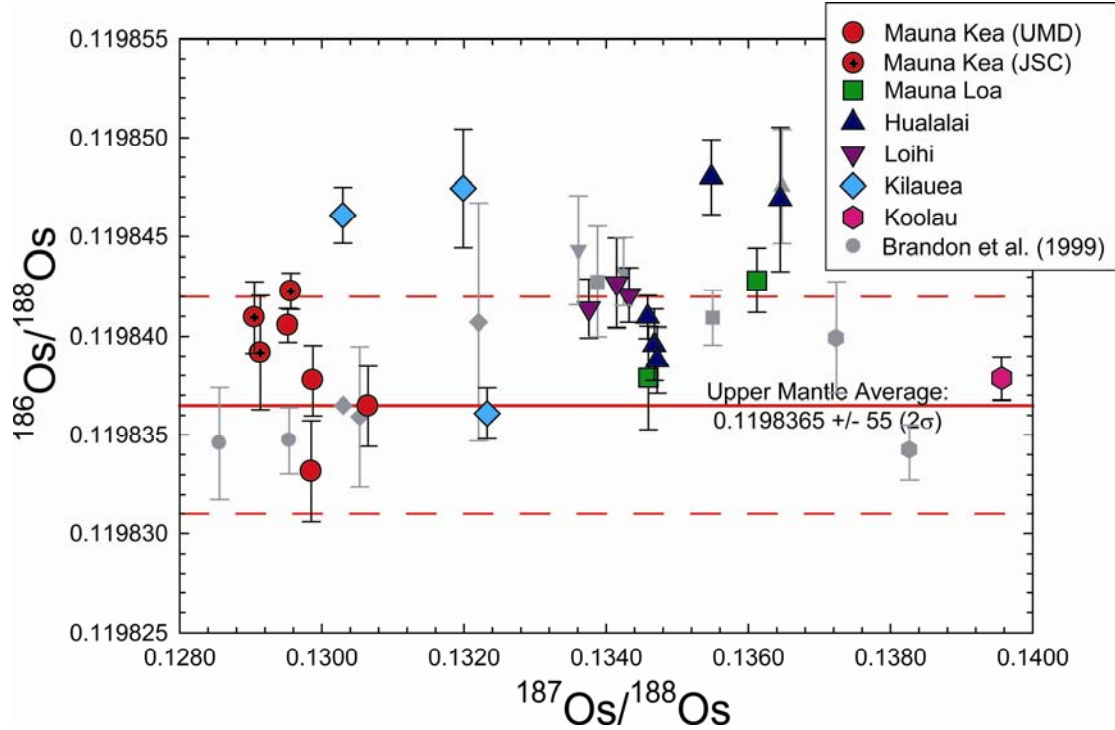**Figure 4.3:** $^{186}Os/^{188}Os$ versus $^{187}Os/^{188}Os$ for the Hawaiian picrites. Solid and dashed red lines represent the upper mantle $^{186}Os/^{188}Os$ average and 2σ respectively (0.1198365 ± 55; Brandon et al., 2006). Grey symbols denote samples from Brandon et al., (1999), where symbol shapes reflect volcanic center as per the new data. Sample S500-5B from Koolau has experience Fe-Mn alteration on the seafloor and has an elevated $^{187}Os/^{188}Os$ ratio, but a $^{186}Os/^{188}Os$ ratio similar to the upper mantle.

the ^{186}Os/^{188}Os ratio of the ambient upper mantle, however, has proven difficult and requires a careful consideration of the types of materials that may be present in the upper mantle, as well as knowledge about Pt and Os abundances in the silicate Earth. Previous studies have suggested that Os-rich alloy grains are viable samples for constraining the ^{186}Os/^{188}Os ratio of the ambient upper mantle, due to their high Os concentrations (e.g., Walker et al., 1997; Brandon et al., 2006). Such grains are predominately composed of Os, Ir and Ru, and are often found as inclusions in chromite or in placer deposits from ultramafic massifs (Cabri et al., 1996; Walker et al., 2005; Brandon et al., 2006). These grains have very low Pt/Os and Re/Os ratios, so ingrowth of ^{186}Os and ^{187}Os stopped when the grains formed. Thus, these materials record the ^{186}Os/^{188}Os, ^{187}Os/^{188}Os and the long term Pt/Os and Re/Os compositions of their mantle sources (Walker et al., 1997; Bird et al., 1999; Meibom et al., 2004; Walker et al., 2005; Brandon et al., 2006). Brandon et al. (2006) analyzed 14 Os-rich alloy grains from various locations for ^{186}Os/^{188}Os, and combined these data with published ^{186}Os/^{188}Os data for an additional 14 Os-rich alloy grains from SW Oregon (Walker et al., 2005). They reported an average of 0.1198382 ± 28 (2σ) and suggested that this value may be representative of the upper mantle. The global applicability of this average, however, may be limited because 18 of the 28 Os-rich alloy grains combined in that study are from a single location in southwest Oregon.

Another type of material that may be useful to constrain the upper mantle ^{186}Os/^{188}Os ratio are abyssal peridotites, which are believed to be the residues of recent partial melting of MORB-source mantle (Snow et al., 1994; Niu et al., 1997).

Analyses of abyssal peridotites from the Kane Fracture Zone on the mid-Atlantic ridge gave an average $^{186}Os/^{188}Os$ ratio of 0.1198353 ± 7 (2σ) for 7 samples (Brandon et al., 2000), which is within uncertainty of the average for the Os-rich alloys. Combining the data from these two studies, along with $^{186}Os/^{188}Os$ data for three ophiolite-derived chromitites from Saudi Arabia (Brandon et al., 1998), gives an overall average $^{186}Os/^{188}Os$ for upper mantle-derived samples of 0.1198365 ± 55 (2σ), which we take to currently be the best estimate for the ambient upper mantle.

This value for the upper mantle is in good agreement with the chondritic $^{186}Os/^{188}Os$ average of 0.1198350 ± 119 (2σ; Yokoyama et al., 2007). The large variance on this average value is due to a few chondritic samples with substantially lower $^{186}Os/^{188}Os$ ratios, outside of the range of the majority of chondrite data. Similarly, Brandon et al. (2006) noted that H-group ordinary chondrites had relatively uniform $^{186}Os/^{188}Os$ ratios with an average of 0.1198398 ± 16 (2σ). Collectively, the chondrite data are in good agreement with the ambient upper mantle defined above. These comparisons imply that the upper mantle has evolved with chondritic values for Pt/Os and $^{186}Os/^{188}Os$ ratios. Correspondingly, it has been suggested that the long-term Pt/Os ratio of the ambient upper mantle is comparable (within $\pm10\%$; Brandon et al., 2006) to that of chondrites at a Pt/Os ratio of $\sim2.0 \pm 0.2$.

4.5.2 Generation of high $^{186}Os/^{188}Os$ ratios

The long half-life of ^{190}Pt (469 Ga) and the low abundance of this isotope (0.01296%), makes the Pt-Os system relatively insensitive to most geologic processes (Walker et al., 1997; Brandon et al., 1999, 2003, 2006; McDaniel et al., 2004). Large

fractionations between Pt and Os over long periods of time are required to produce resolvable variations in $^{186}Os/^{188}Os$ ratios. Hypothetical age progressions of $\varepsilon^{186}Os$ at varying Pt/Os ratios are illustrated in Figure 4.4, where $\varepsilon^{186}Os$ represents:

$$\varepsilon^{186}Os = \left(\frac{\left(^{186}Os/^{188}Os\right)_{sample}}{\left(^{186}Os/^{188}Os\right)_{chondrite}} - 1 \right) *10000$$

For example, given the present-day chondritic $^{186}Os/^{188}Os$ ratio of 0.1198350 (Yokoyama et al., 2007), and the most radiogenic sample analyzed here (H-9; $^{186}Os/^{188}Os=0.1198480 \pm 19$), an $\varepsilon^{186}Os$ of +1.08 is calculated. Given a reservoir with an initially chondritic $^{186}Os/^{188}Os$ ratio and a Pt/Os ratio of 5, it would take ~3 Ga to evolve to the $\varepsilon^{186}Os$ value of sample H-9.

In the following sections, different mechanisms for generating variations in both $^{186}Os/^{188}Os$ and $^{187}Os/^{188}Os$ ratios are considered. These mechanisms include the recycling of materials with variable Pt-Re-Os compositions, mixing of Hawaiian source regions with a COs component, and the addition of BMS to a mantle source via mantle metasomatism.

4.5.3 Fe-Mn alteration/recycling

It has been suggested that the addition of Fe-Mn rich materials, including altered crust, umbers and nodules, into the sources of putative plume-derived magmas has the potential to affect the HSE and Os isotopic composition because these materials tend to scavenge the HSE, particularly Pt, from seawater (Ravizza et al., 2001; Smith, 2003; Baker and Jensen. 2004; McDaniel et al., 2004; Scherstén et al., 2004). Young, Fe-Mn rich materials, formed during seafloor alteration, tend to
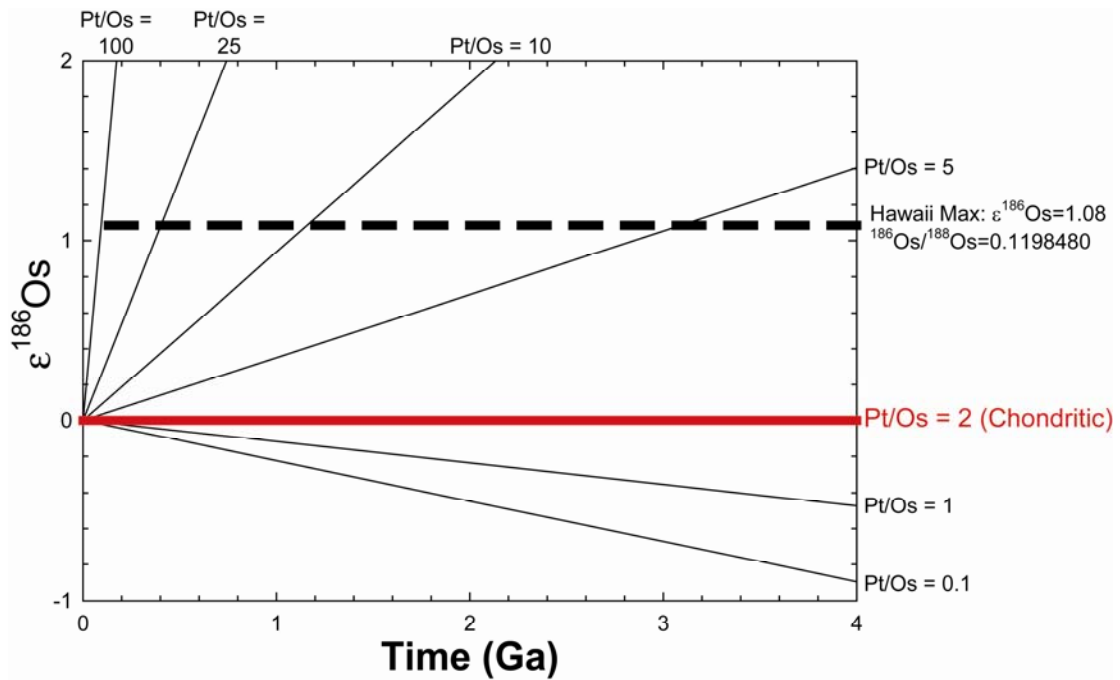
Figure 4.4: A time progression of ε^{186}Os at varying Pt/Os ratios, where ε^{186}Os is the

deviation in parts per 10000 of the sample relative to chondrites (0.1198350 and

Pt/Os=2; Brandon et al., 2006 Yokoyama et al., 2007).

have highly radiogenic $^{187}Os/^{188}Os$ ratios (>0.95), but generally chondritic $^{186}Os/^{188}Os$ ratios, which reflect their relatively recent derivation from seawater ($^{187}Os/^{188}Os$ of ~1.05 and $^{186}Os/^{188}Os$ of 0.119829 ± 11 $2\sigma_{pop}$; McDaniel et al., 2004). Over time, the elevated Pt abundances relative to Os, will produce enrichments in ^{186}Os.

As reported in Ireland et al. (2009a), sample S500-5B from Koolau experienced recent Fe-Mn alteration on the sea floor. The alteration of S500-5B resulted in a large increase in the $^{187}Os/^{188}Os$ ratio (0.1395634 ± 22) relative to other samples, due to the incorporation of seawater Os. This ^{187}Os enrichment is smaller than reported by Ireland et al. (2009a) because more powder was produced for this sample, which resulted in diluting the effect of the Fe-Mn crust contamination. S500-5B has an elevated Pt/Os ratio (9.09) relative to other samples, due to the addition of Pt ([Pt]=8.6 ng/g). The alteration, however, did not affect any of the other HSE abundances. The $^{186}Os/^{188}Os$ of this sample (0.1198379 ± 5) is similar to that of the present-day upper mantle, which indicates that the Fe-Mn alteration had no detectable effect on this ratio. With the passing of time, this sample would evolve to more radiogenic $^{186}Os/^{188}Os$ and $^{187}Os/^{188}Os$ ratios, and it can serve as a proxy for actual subducted Fe-Mn rich materials to evaluate how these materials may affect the growth in $^{186}Os/^{188}Os$ and $^{187}Os/^{188}Os$ ratios of a mantle source region.

For example, if this sample is aged for 2 Ga from its current ^{186}Os isotopic composition, the $^{186}Os/^{188}Os$ ratio would rise to 0.1198597 (an $\varepsilon^{186}Os$ value of 1.26 at 2 Ga from present), which is higher than any observed plume sample. If such Fe-Mn rich material is subducted along with oceanic crust into an OIB mantle source, it could be a potential cause of ^{186}Os and ^{187}Os enrichments in plume magmas (Ravizza

et al., 2001; Smith, 2003; Baker and Jensen. 2004; Scherstén et al., 2004). Based on

the composition of S500-5B, however, unreasonable quantities (~75%) of Fe-Mn rich

material would need to be added to the Hawaiian mantle source region to produce the

most ^{186}Os-enriched sample, with a corresponding elevation in ^{187}Os/^{188}Os (up to

0.18) that is much greater than that observed in the sample set. The addition of such a

large proportion of Fe-Mn rich material should also result in the transfer of high Mn

contents to the mantle source regions, which is not observed in these particular

samples. Furthermore, Brandon and Walker (2005) contended that Fe-Mn rich

materials are not present in sufficient quantities (< 3 wt.% of the uppermost 1 m^3 of

oceanic crust) to have an impact on the overall Pt and Os budget of the oceanic crust.

Thus, we consider it unlikely that these types of materials can produce the observed

^{186}Os/^{188}Os and ^{187}Os/^{188}Os relationships.

4.5.4 Oceanic crust and pyroxenite recycling – potential effects on ^{186}Os/^{188}Os and

^{187}Os/^{188}Os

    Previous studies have reported isotopic differences in ^{87}Sr/^{86}Sr, ^{143}Nd/^{144}Nd and

Pb isotopes between two geochemically distinct trends observed in Hawaiian

volcanoes, termed the Kea- and Loa-trends (e.g., Frey and Rhodes, 1993; Hauri,

1996; Lassiter et al., 1996; Huang et al., 2005; Ren et al., 2005). Kea-trend

volcanoes, represented by Mauna Kea and Kilauea in this study, are characterized by

^{87}Sr/^{86}Sr and ^{143}Nd/^{144}Nd isotopic ratios that span a range from a DMM-like (depleted

MORB mantle) signature to slightly more evolved compositions. It has been

suggested that this component is dominated by a DMM-like mantle isotopic

composition (Huang et al., 2005). In contrast, the Loa-trend volcanoes, as represented here by Mauna Loa, Hualalai and Loihi, are characterized by the highest $^{87}Sr/^{86}Sr$ and the lowest $^{143}Nd/^{144}Nd$ ratios among the Hawaiian volcanoes (Huang et al., 2005). The mantle source regions of the Loa-trend volcanoes have been postulated to contain a recycled oceanic crust and sediment component, consistent with the observation that oceanic crust typically has higher Rb/Sr and lower Sm/Nd ratios than the mantle, and can, thus, contribute to the observed isotopic characteristics over time (West et al., 1987; Roden et al., 1994; Eiler et al., 1996; Hauri, 1996; Lassiter and Hauri, 1998; Huang and Frey, 2005; Huang et al., 2005).

Variations in $^{187}Os/^{188}Os$ ratios between Kea- and Loa-trend volcanoes have been documented by previous studies (Bennett et al., 1996, 2000; Lassiter and Hauri, 1998; Bryce et al., 2005; Ireland et al., 2009a). These studies observed a limited range of $^{187}Os/^{188}Os$ ratios within individual volcanic centers, but with a notable difference between Kea- (lower $^{187}Os/^{188}Os$ ratios: approximate range of 0.1280 to 0.1320) and Loa-trend lavas (higher $^{187}Os/^{188}Os$ ratios: approximate range of 0.1330 to 0.1400). Our new data are also consistent with this observation. Lassiter and Hauri (1998) attributed these variations to the incorporation of up to 30% of an ancient (1.8 Ga) subducted oceanic basalt plus sediment package (97% oceanic basalt and 3% sediment) into the mantle source regions of Loa-trend volcanoes to account for the ^{187}Os enrichments. Little to no subducted component was projected for the sources of the Kea-trend volcanoes. Their model subducted component has a high Re/Os ratio of 17 ([Re]=0.93 ng/g, [Os]=0.055 ng/g), which, if formed at 1.8 Ga, would evolve to a present day $^{187}Os/^{188}Os$ ratio of 2.74. Recent addition of 30% of this component to

134

a chondritic mantle reservoir ([Os]=3.1 ng/g, $^{187}Os/^{188}Os$ of 0.1270; Shirey and

Walker, 1998) would raise the $^{187}Os/^{188}Os$ ratio to 0.1416, consistent with the most

radiogenic samples observed at Hawaii (Koolau; Lassiter and Hauri, 1998). Thus,

oceanic crustal recycling is likely involved in at least some of the variations in

$^{187}Os/^{188}Os$ observed in our data. Lassiter and Hauri (1998), however, did not

consider the collateral effects of crustal recycling on Pt abundances or $^{186}Os/^{188}Os$

ratios of the mantle source regions.

More recent studies have considered the effects of recycled materials on Pt/Os

and $^{186}Os/^{188}Os$ systematics in the sources of OIB. For example, the incorporation of

a recycled oceanic crust, in the form of a pyroxenite component, has been suggested

to be capable of producing enriched $^{186}Os/^{188}Os$ and $^{187}Os/^{188}Os$ ratios (Smith, 2003;

Meibom et al., 2004; Luguet et al., 2008). Although HSE and Os isotopic data for

pyroxenites are sparse, some of these materials may have the requisite long-term high

Pt/Os and Re/Os ratios necessary to produce the observed levels of enrichment in

both ^{186}Os and ^{187}Os (Smith, 2003; Meibom et al., 2004; Luguet et al., 2008; van

Acken et al., 2009). Such materials may also be present in considerable quantities in

the upper mantle (up to 5 wt.%; Hirschmann and Stolper, 1996).

For example, Smith (2003) noted a Pt-rich pyroxenite from the Bay of Islands

ophiolite that had the requisite high Pt/Os and Re/Os ratios to produce coupled ^{186}Os

and ^{187}Os enrichments similar to those observed in the most radiogenic Hawaiian

samples (Table 4.3). Luguet et al. (2008) analyzed a suite of pyroxenites from the

Beni Bousera orogenic massif that were interpreted to have been derived from an

oceanic crustal protolith (Pearson et al., 2004). These authors measured the Pt, Re

and Os abundances of these samples, and calculated the corresponding $^{186}Os/^{188}Os$

and $^{187}Os/^{188}Os$ ratios based on an assumed age of 1.2 Ga. The measurements and

calculations demonstrated that these pyroxenites have highly variable Pt/Os and

Re/Os ratios that, over time, would have evolved variable $^{186}Os/^{188}Os$ and $^{187}Os/^{188}Os$

compositions ranging from similar to ambient upper mantle to highly radiogenic

(equivalent present day ratio of up to 0.1198642 and 0.92007, respectively). Using

the highest calculated $^{186}Os/^{188}Os$ ratios derived from two pyroxenite samples, Luguet

et al. (2008) proposed that the most ^{186}Os-enriched Hawaiian samples could be

produced by the bulk mixing of 50 to 90% of a pyroxenite component with mantle

peridotite (Figure 4.5).

Only pyroxenites with the most highly fractionated Pt/Os can be mixed with

peridotites and generate melts with sufficiently radiogenic Os isotopic compositions.

These pyroxenites, however, tend to represent the most extreme compositions, which

may not be typical of pyroxenites in general. Van Acken et al. (2009) noted that most

pyroxenites for which HSE data are available have Pt/Re ratios that are much too low

to produce the appropriate ^{186}Os-^{187}Os enrichments for Hawaii and will develop

radiogenic $^{187}Os/^{188}Os$ too rapidly, relative to $^{186}Os/^{188}Os$, to account for the Hawaiian

data. In Figure 4.5, the bulk mixing of several pyroxenite compositions with a

peridotite component, calculated for 2 Ga of radiogenic ingrowth, are modeled

(compositions in Table 4.3). From this model, only the sample with the most extreme

composition from Luguet et al (2008), GP 87T, has the proper $^{186}Os/^{188}Os$ and

$^{187}Os/^{188}Os$ characteristics to approach the most radiogenic data for Hawaiian picrites.

Tabel 4.3: Pyroxenite mixing model parameters

Component	Os (ng/g)	Pt (ng/g)	Re (ng/g)	Pt/Os	Re/Os	Pt/Re	^{186}Os/^{188}Os[a]	^{187}Os/^{188}Os[a]
Peridotite	3.30	7.60	0.35	2.30	0.11	21.7	0.1198365	0.1296
Bay of Islands pyroxenite[b]	1.06	211.10	4.18	199	3.94	50.5	0.1204170	0.7751
GP 87T[c]	0.10	3.47	0.03	34.7	0.30	115.7	0.1199276	0.1625
Luguet Average[c]	0.51	2.79	1.17	5.43	2.28	2.4	0.1198496	0.4853
van Acken Average[d]	1.70	7.93	2.14	4.67	1.26	3.7	0.1198522	0.3325

[a] ^{186}Os/^{188}Os and ^{187}Os/^{188}Os ratios were calculated for a model age of 2 Ga, assuming that the material had chondritic ^{186}Os/^{188}Os and ^{187}Os/^{188}Os ratios at the time of formation (^{186}Os/^{188}Os(2Ga)=0.1198339; ^{187}Os/^{188}Os(2Ga)=0.11351; based on ^{186}Os/^{188}Os$_i$=0.1198269 and Pt/Os=1.999 (Brandon et al., 2006) and ^{187}Os/^{188}Os$_i$=0.09531 and Re/Os=0.083 (Shirey and Walker, 1998)

[b] Smith (2003)

[c] Luguet et al. (2008)
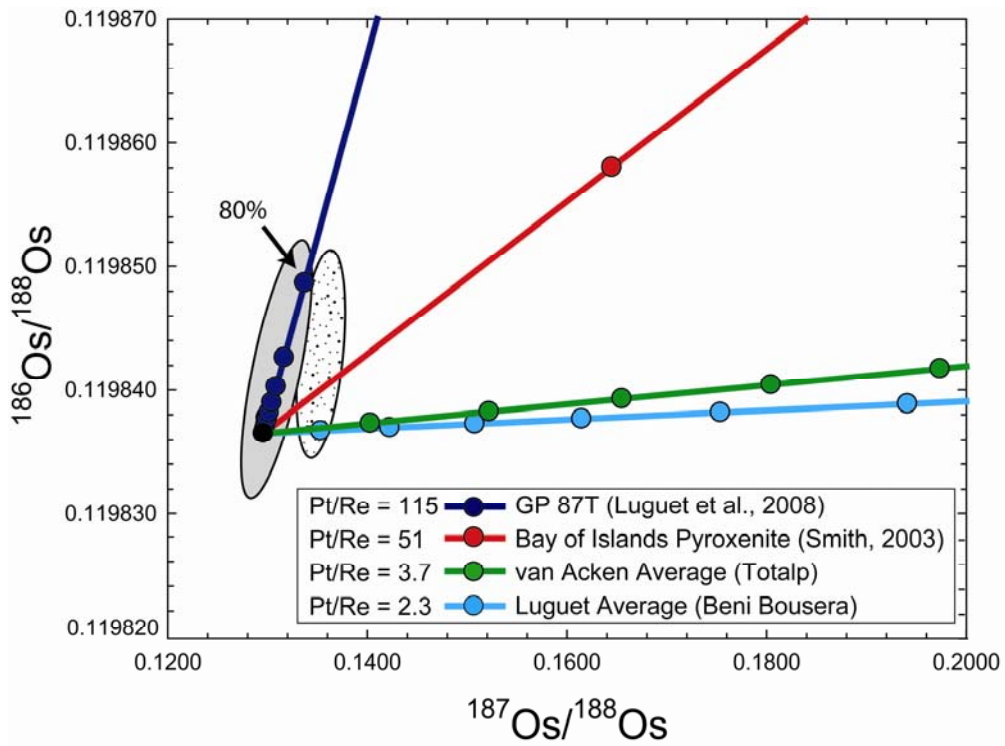
[d] van Acken et al. (2009)

Figure 4.5: Mixing model involving the addition of various pyroxenite compositions, aged for 2 Ga, into a mantle peridotite. Only one sample from Luguet et al. (2008) has the necessary Pt-Re-Os abundances to produce a trend similar to that observed at Hawaii. All other compositions produce enrichments in ^{187}Os too rapidly relative to ^{186}Os. Colored circles represent 10% increments of pyroxenite addition. The light gray field outlines Kea-trend samples, and the stippled field denotes Loa-trend samples. Mixing parameters are outlined in Table 4.3.

This type of model will also have collateral effects. For example, nearly 80% of this pyroxenite component would be needed to produce the most ^{186}Os enriched samples. Yet, most pyroxenites have low Os concentrations; thus, mixing large proportions of this component into a peridotite source will tend to dilute the Os concentration of the hybridized source, which would make it unlikely to produce some of the higher Os abundances that are observed in Hawaii. For example, a mixture of 80% of a pyroxenite with a composition of sample GP 87T ([Os]=0.1 ng/g) and mantle peridotite ([Os]=3.3 ng/g), would result in a hybrid source containing 0.7 ng/g Os. Some of the Hawaiian samples in this study have Os concentrations that are two times higher than this hybrid source estimate. Such high Os concentrations could not be produced from this source, unless the partitioning behaviour of Os switched from compatible to incompatible either during partial melting or subsequent fractionation. This is unlikely, however, given the compatible nature of Os, even at the higher degrees of partial melting required to produce some komatiites, where the melt/residue partition coefficient of Os may approach unity (Puchtel et al., 2004; Puchtel and Humayun, 2005). All other pyroxenite compositions considered (Bay of Islands pyroxenite, Luguet average, and van Acken average) have Pt/Re ratios that are too low to produce the observed ^{186}Os/^{188}Os and ^{187}Os/^{188}Os relationships at Hawaii.

For these reasons, the variable bulk mixing of a recycled oceanic component into the mantle sources of Hawaii is consistent with producing some of the ^{187}Os/^{188}Os variations between Kea- and Loa-trend volcanoes, however, this process likely cannot generate the variable observed ^{186}Os/^{188}Os ratios. An additional component or

mechanism is required to explain the ^{186}Os/^{188}Os characteristics of Hawaii. Two

possibilities for this are discussed.

4.5.5 Common Os isotopic reservoir (COs) hypothesis

The well-defined linearity of the correlations between ^{186}Os and ^{187}Os that were

observed in previous studies of Hawaiian picrites and Gorgona Island komatiites

(Brandon et al., 1998, 1999, 2003) has been the strongest evidence in support of a

COs model. These well-correlated trends suggest that there may be a single enriched

component that, when mixed into a mantle source region, can account for the coupled

enrichments in ^{186}Os and ^{187}Os in each sample suite. The linear trends intersect at a

region with elevated ^{186}Os/^{188}Os and ^{187}Os/^{188}Os, which may imply that there is a

homogenous, COs reservoir that is contributing to both volcanic systems (Brandon et

al., 2003; Brandon and Walker, 2005). The intersection region provides a possible

composition for this enriched component (^{186}Os/^{188}Os=0.119870 and

^{187}Os/^{188}Os=0.1492; Brandon et al., 2003; Brandon and Walker, 2005). Due to the

apparent ubiquity of the COs reservoir in these two putative plume systems,

combined with solid metal/liquid metal partitioning data for Pt, Re and Os from some

high pressure-temperature experiments, these authors attributed the coupled

enrichments to an outer core component.

The new data obtained in this study, when viewed collectively, do not show a

good correlation between ^{186}Os/^{188}Os and ^{187}Os/^{188}Os (Figure 4.3), apparently in

contradiction to the COs hypothesis. If considered separately, however, the data for

Kea and Loa-trend picrites define generally positive correlations between ^{186}Os/^{188}Os

and $^{187}Os/^{188}Os$ (Figure 4.6a,b). On a combined plot of $^{186}Os/^{188}Os$ versus

$^{187}Os/^{188}Os$, the Os isotopic data for Hawaii can be outlined by a triangular field

bounded by a COs component, and the projected Kea- and Loa- trend mantle sources

(Figure 4.6c). Three-component mixing between the Kea- and Loa-trend volcanoes

and a putative COs component would suggest that a minor amount of this COs

material (<0.5 wt.%), along with a recycled crustal component in the Loa-trend

mantle sources, could produce the general $^{186}Os/^{188}Os$ and $^{187}Os/^{188}Os$ relationships

that are observed. $^{186}Os/^{188}Os$ variations within a single volcanic center may either

result from variable interaction of the mantle source regions with the COs component,

or require an additional process. For example, Mauna Kea sample SR0964-4.30 may

reflect mixing of the COs component with the Kea-trend mantle component; whereas

Mauna Kea sample SR0401-2.85 would require mixing between a Kea- and Loa-

trend component (Figure 4.6c). The observation of some overlap in $^{87}Sr/^{86}Sr$,

$^{143}Nd/^{144}Nd$, and Pb isotopic data for Kea- and Loa-trend basalts supports this

interpretation (Huang et al., 2005).

    If it is assumed that the data reflect three-component mixing, including a COs

component, the mantle source $^{187}Os/^{188}Os$ composition of the Kea and Loa-trend

volcanoes can also be estimated from the intersections of the mixing lines with the

$^{186}Os/^{188}Os$ ratio of the upper mantle. The Kea-trend mantle source would have an

approximately chondritic $^{187}Os/^{188}Os$ ratio of 0.1270 prior to mixing with the COs. In

a similar manner, the Loa-trend mantle source would have a more radiogenic

$^{187}Os/^{188}Os$ ratio of 0.1320. The amount of the recycled component in Loa-trend

volcanoes can be constrained by using the parameters for the subducted oceanic crust
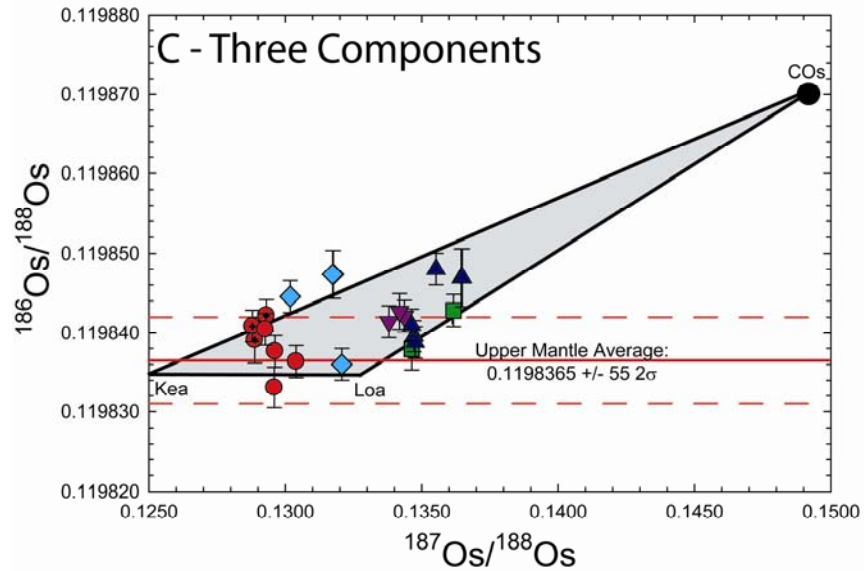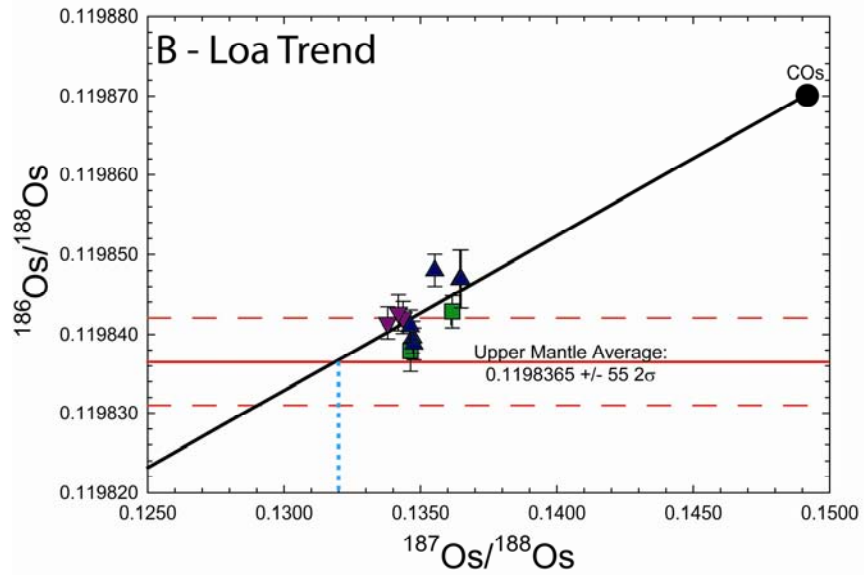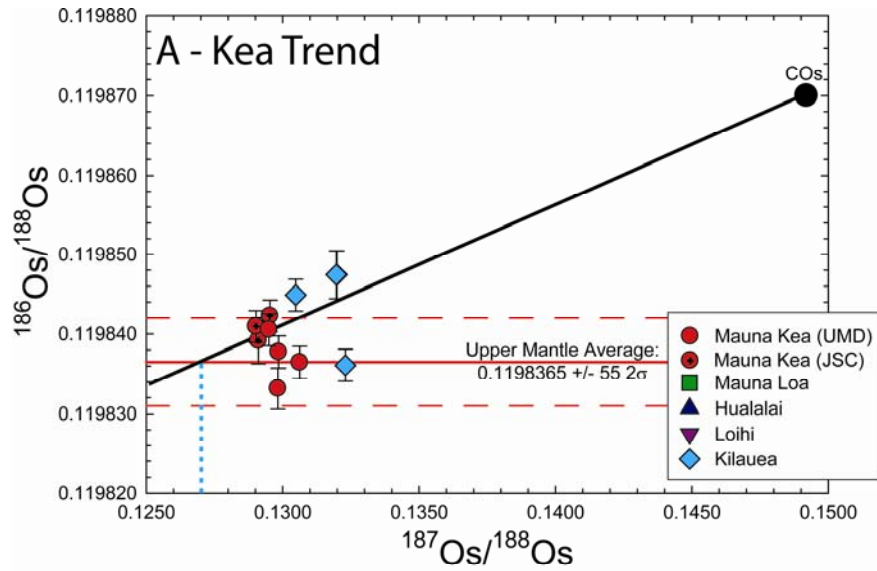
142

Figure 4.6: Mixing between a common Os reservoir (COs; $^{186}Os/^{188}Os$=0.119870, $^{187}Os/^{188}Os$=0.1492; Brandon et al., 2003) and the mantle source region for A) Kea-(Mauna Kea and Kilauea) and B) Loa-trend (Mauna Loa, Hualalai and Loihi) volcanoes respectively. The $^{187}Os/^{188}Os$ of the average mantle source for Kea- and Loa-trend volcanoes can be estimated from the intersection of the mixing trends and the upper mantle $^{186}Os/^{188}Os$. The average Kea-trend mantle source has an $^{187}Os/^{188}Os$ of 0.1270, while the average Loa-trend source region has an $^{187}Os/^{188}Os$ of 0.1320, which is denoted by the dotted blue line. The difference between the Kea- and Loa-trend sources may be explained by the addition of ~15% of a recycled crust and sediment component to the Loa-trend source ([Re]=0.93 ng/g, [Os]=0.05 ng/g, $^{187}Os/^{188}Os$=2.74; Lassiter and Hauri, 1998). The correlation lines are best fit regressions through the data. C) Three-component mixing of a COs component, with Kea- and Loa-trend components can potentially explain the range in both $^{186}Os/^{188}Os$ and $^{187}Os/^{188}Os$ data for the Hawaiian picrites. The bounding triangle was drawn to encompass all of the data.

component outlined above (Lassiter and Hauri, 1998). From the ^{187}Os/^{188}Os data collected here, the difference in the ^{187}Os/^{188}Os ratios between pure Kea- and Loa-trend mantle sources can be accounted for by the presence of ~15% of a recycled component in the Loa-trend source.

We conclude that the mixing of a COs component into the dominant Kea and Loa mantle sources of the Hawaiian shield volcanoes is a viable hypothesis for producing the ^{186}Os/^{188}Os and ^{187}Os/^{188}Os attributes of the Hawaiian picrites. In this scenario, the inter-volcano ^{187}Os/^{188}Os variations can largely be attributed to a recycled oceanic crust component that would have little effect on ^{186}Os/^{188}Os ratios. Variations in ^{186}Os/^{188}Os ratios would reflect variable interaction with the COs component, although the nature of the COs reservoir remains open to interpretation.

4.5.5.1 COs and the outer core

If a COs component is assumed to be derived from the outer core, as previously suggest (Brandon et al., 1999; 2003), there would be other collateral geochemical effects. For example, bulk mixing of the mantle with outer core metal would likely result in an increased concentration of the HSE in the plume source that would predictably be related to the ^{186}Os isotopic composition. Two previous studies that analyzed the absolute and relative abundances of the HSE in Hawaiian picrites, however, did not observe the predicted high HSE concentrations in lavas previously identified as having enriched ^{186}Os/^{188}Os (Bennett et al., 2000), or correlations between the Pt/Os ratio of an estimated parental melt with average volcano ^{186}Os/^{188}Os ratios (Ireland et al., 2009a). The new extended database allows

comparisons between Pt/Os and ^{186}Os/^{188}Os for individual samples within a volcanic

suite. A strong positive correlation is now observed between Pt/Os and ^{186}Os/^{188}Os

ratios for Hualalai (Figure 4.7). This trend is consistent with interaction with a COs

component and suggests that relative source Pt/Os variations may be transferred to a

partial melt, if the melting conditions and solid/melt partitioning behaviour of Pt and

Os are similar for each sample. A similar correlation is not, however, observed for

other volcanic suites (in some cases due to insufficient data) or between Re/Os and

^{187}Os/^{188}Os ratios (Figure 4.8), which is likely due to the different solid/melt

partitioning behaviour of Re (modestly incompatible) and Os (highly compatible)

during partial melting of the mantle (Shirey and Walker, 1998).

Tungsten isotopes, involving the decay of the extinct radionuclide ^{182}Hf to ^{182}W

($t_{1/2}$=9 Ma), have been suggested as a robust tracer of core-mantle interaction because

the silicate Earth is isotopically enriched in ^{182}W relative to chondrites (Scherstén

et al., 2004; Brandon and Walker, 2005; Hawkesworth and Scherstén, 2007; Takamasa

et al., 2009); hence, due to mass balance arguments, the Earth's core is presumed to

be depleted in ^{182}W relative to the silicate Earth by ~2 parts in 10000 (ε_W units;

Kleine et al., 2002). If core material was added to the Hawaiian source, it could have

led to a modest depletion in ^{182}W in the plume source, although this depends on the

abundance of W in the mantle source (Scherstén et al., 2004; Brandon and Walker,

2005; Hawkesworth and Scherstén, 2007; Arevalo and McDonough, 2008; Ireland et

al., 2009b). The estimated mantle source W composition for Hawaii (10 ng/g; Ireland

et al., 2009b) and a lack of depletions in ^{182}W of three Hawaiian samples with high

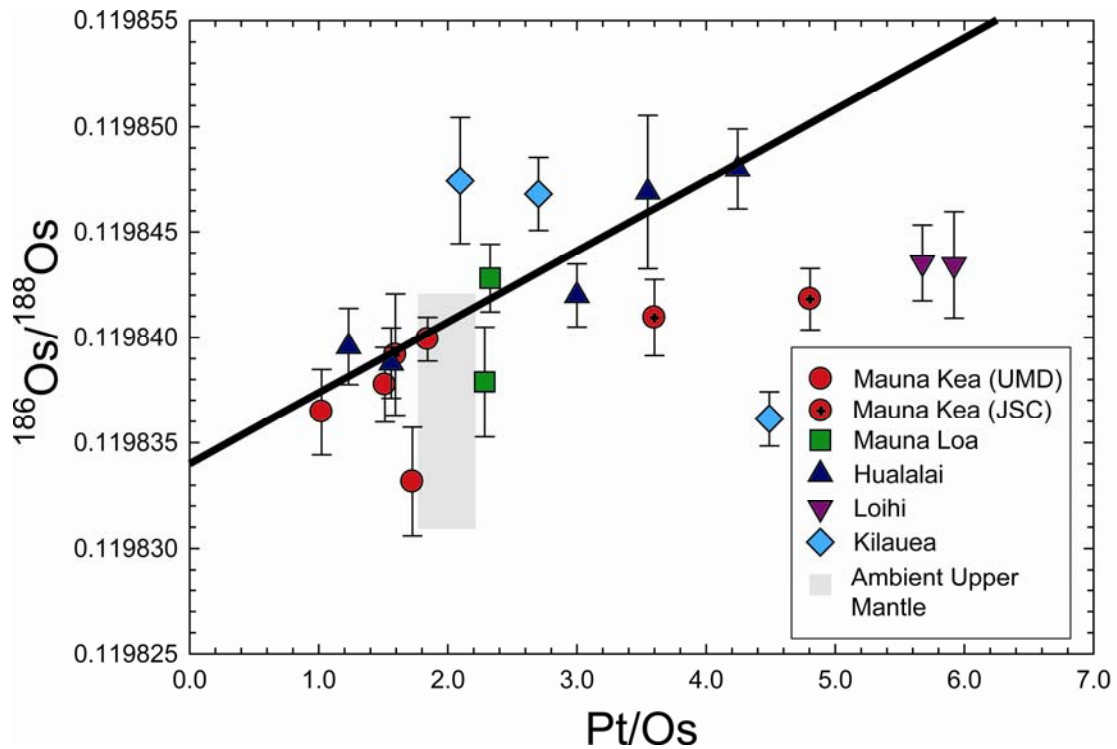^{186}Os/^{188}Os (H-11, Lo-02-02 and Lo-02-04; Scherstén et al., 2004) suggest that either

Figure 4.7: The relationship between $^{186}Os/^{188}Os$ and Pt/Os. A correlation for Hualalai samples (denoted by the solid black line) suggests that relative source Pt/Os heterogeneities may be transferred to a partial melt if the partitioning behaviour of Pt and Os are similar for most samples in the trend. All Loihi samples have an elevated Pt/Os ratio, which can be attributed to a lower degree of partial melting for Loihi, which may result in the fractionation of Pt from Os. A field for ambient upper mantle is also included ($^{186}Os/^{188}Os$=0.1198365 ± 55 2σ; Pt/Os=2.0 ± 0.2; Brandon et al., 2006).

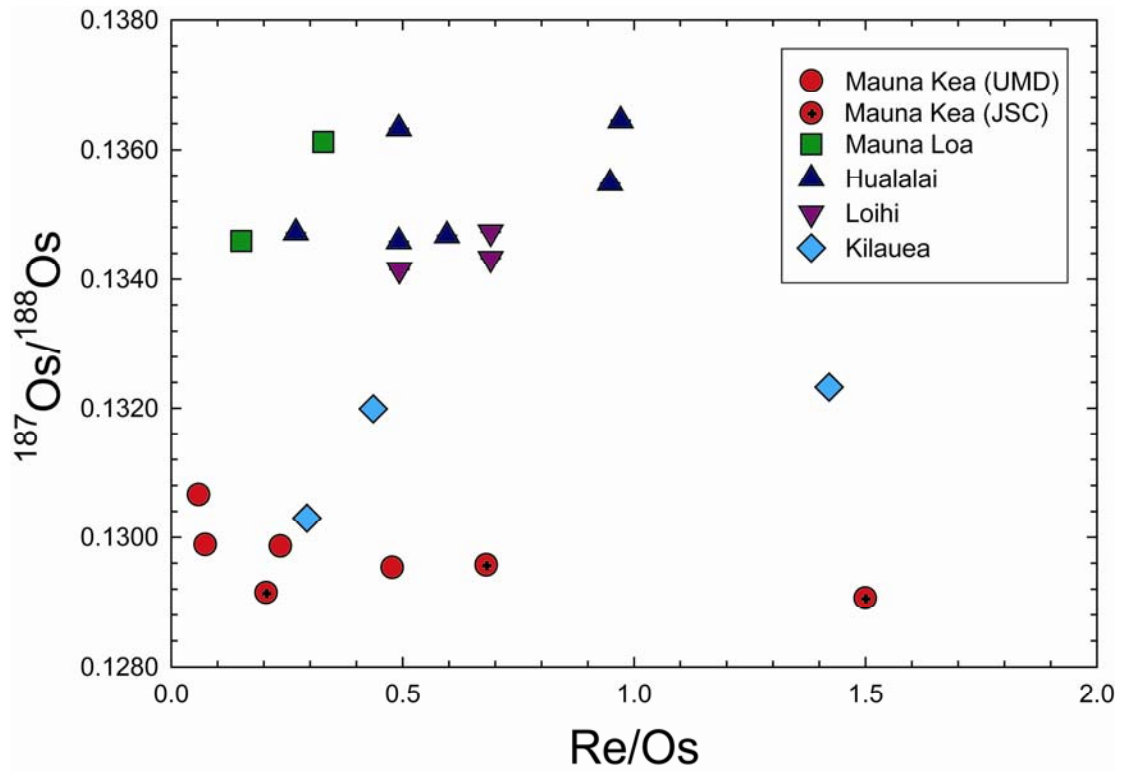**Figure 4.8:** The relationship between $^{187}Os/^{188}Os$ and Re/Os. There is no correlation observed between Re/Os ratios and ^{187}Os isotopic composition, likely due to the differing solid/melt partitioning behaviour of these two elements during partial melting of the mantle.

core-mantle interaction does not occur, involves smaller amounts of outer core material, or that mechanisms other than physical mixing, such as isotopic exchange, may operate at the core-mantle boundary (Puchtel and Humayun, 2000, 2005; Humayun et al., 2004).

Despite the challenges outlined above, the outer core cannot currently be ruled out as the COs component. Further experimental and geochemical work is required to better define the HSE and Os isotopic characteristics of COs, if such a component is present in OIB, and to relate this component to specific reservoirs.

4.5.6 Mantle metasomatism involving base-metal sulfides (BMS)

Although bulk mixing of pyroxenite into the mantle source regions of Hawaii is unlikely to be responsible for ^{186}Os variations, a more complex process involving a pyroxenite component has been proposed. Recently, Sobolev et al. (2005, 2007) suggested that the mantle source regions of the Hawaiian plume may be affected by mantle metasomatic events that resulted in the production of a hybrid pyroxenite-peridotite source. In this model, the pyroxenite component is generated via a two-stage process whereby recycled oceanic crust undergoes partial melting to form an eclogitic melt, which then infiltrates into, and reacts completely with mantle peridotite to form an olivine-free pyroxenite lithology. This hybridized pyroxenite-peridotite source region can then melt to form the observed lavas. The effect of such a two-stage process on the HSE abundances of the pyroxenite component is unclear because the partitioning behaviour of these elements during melting of subducted oceanic crust is still poorly constrained. Luguet et al. (2008), however, argued that

HSE abundances during metasomatic processes are largely controlled by movement of BMS, and therefore, can be modeled as a simple sulfide transport process.

BMS are often associated with recycled eclogite and pyroxenite (Luguet et al., 2001; Alard et al., 2005; Luguet et al., 2008), and may be capable of producing some of the Os isotopic characteristics observed for the Hawaiian suite. In mantle materials, Cu-bearing BMS may be important carriers of Pt and Pd, and are typically found as interstitial phases (Maier and Barnes, 2004). Osmium, Ir and Ru, however, are typically sited in Mss (mono-sulfide solid solution) phases, or alloys, that typically occur as inclusions in silicates, which may act as barriers to reaction (Maier et al., 2003; Bockrath et al., 2004; Ballhaus et al., 2006). During the melting of eclogite and the subsequent formation of a hybrid pyroxenite-peridotite source, BMS may be highly reactive (Luguet et al., 2001, 2004; Alard et al., 2005) given their typically lower melting temperatures relative to the silicate phases. In this scenario, the addition of BMS into a mantle source region would most likely represent a non-modal process, whereby the BMS preferentially become incorporated into the hybridized pyroxenite-peridotite source, relative to silicates present in the pyroxenite. At low melt fractions, this may result in the formation of a hybrid pyroxenite-peridotite source that is metasomatically enriched in BMS. These phases can have highly variable HSE and Os isotopic compositions, and may control the HSE budget of the hybridized source. Moreover, metasomatic reactions involving BMS in the mantle have been suggested as a mechanism to produce peridotites that have experienced Pt enrichment relative to Os (Buchl et al., 2002; Schulte et al., 2009), which may be related to the mobility of Pt-rich sulfide phases. Based on Pt-Re-Os

abundances, Luguet et al. (2008) calculated that individual BMS may evolve to much higher ^{186}Os/^{188}Os and ^{187}Os/^{188}Os than bulk pyroxenite. This observation led these authors to suggest that the addition of small proportions (0.035 to 1.5%) of BMS to a hybridized source may be capable of producing the ^{186}Os-^{187}Os characteristics observed in some plume-derived systems, although the estimated proportions are strongly dependent on the modeled age of the BMS.

Although the preferential incorporation of BMS-phases into a hybrid pyroxenite-peridotite source may be a practical alternative to the COs reservoir hypothesis to explain the ^{186}Os and ^{187}Os characteristics of the Hawaiian samples, there remain several important considerations that need to be addressed. A key issue is how the grain-scale HSE variations in BMS translate to larger scales, such as hand sample or mantle source domains. This may become a larger problem with regard to the partial melting process, which tends to average mantle compositions from a wide geographic area (Ribe and Christensen, 1999). Mass balance constraints of peridotite, pyroxenite and associated sulfides in a mantle source region must be thoroughly defined in order to expand from the grain to mantle source scale. Additional, comprehensive studies of the HSE abundances and Os isotopes in these materials, such as those by Luguet et al. (2008) and van Acken et al. (2009), are necessary to address these topics and to provide a global perspective of the compositions of these materials.

The metasomatic addition of BMS to peridotite may also result in an excess of Pt in the mantle source region (Luguet et al., 2008; Ireland et al., 2009a). For example, if 1.5% of BMS sample M2015-9 ([Pt]=1548 ng/g) from Luguet et al. (2008) is added to a mantle peridotite ([Pt]=7.6 ng/g), the hybridized source would contain ~30 ng/g

Pt, or about a three time increase in the mantle source Pt abundance relative to peridotite. One might expect that a partial melt of such a source would inherit a high absolute Pt concentration. Absolute Pt abundances, however, do not indicate a mantle source with an anomalously high Pt concentration (Ireland et al., 2009a), although a trend between $^{186}Os/^{188}Os$ and Pt/Os is observed for the Hualalai suite (Figure 4.7). This trend is consistent with the incorporation of BMS, and may reflect relative Pt/Os heterogeneities in the mantle source region if the solid/melt partitioning of Pt and Os, as well as melting conditions, are similar between samples. Luguet et al. (2008) further argued that Pt solubility in silicate melts is limited, and therefore absolute Pt abundances in a melt may be decoupled from the Os isotope signature. However, additional experimental work on the partitioning behaviour of Pt, as well as the other HSE, between BMS, pyroxenite, and peridotite during partial melting is necessary to elucidate this issue.

4.6 Conclusions

The suite of Hawaiian picrites analyzed here spans a range of $^{186}Os/^{188}Os$ ratios (0.1198332 ± 26 to 0.1198480 ± 19) similar to that reported by a previous study (Brandon et al., 1999). Likewise, these samples have $^{187}Os/^{188}Os$ characteristics that are consistent with previous observations (Martin et al., 1994; Hauri et al., 1996; Hauri and Kurz, 1997; Lassiter and Hauri, 1998; Brandon et al., 1999; Bennett et al., 2000; Bryce et al., 2005; Ireland et al., 2009a). However, in contrast to the well-defined linear correlations observed between $^{186}Os/^{188}Os$ and $^{187}Os/^{188}Os$ by Brandon

et al. (1999, 2003), the relationships between these two ratios in the current study are more complex.

The bulk recycling of oceanic crust and pyroxenites may be responsible for the dominant $^{187}Os/^{188}Os$ variations between volcanic centers, however, these materials are not likely to generate the $^{186}Os/^{188}Os$ variations observed. Two possibilities were considered:

1) COs reservoir: The mantle source regions of Kea- and Loa-trend volcanoes were modeled separately, based on the discrete $^{187}Os/^{188}Os$ characteristics of these trends. Three-component mixing with a COs reservoir may be able to explain the generally positive correlations between $^{186}Os/^{188}Os$ and $^{187}Os/^{188}Os$ ratios and is consistent with the incorporation of ≤0.5 wt.% COs component. This hypothesis generates a plausible model for the Hawaiian mantle sources, with the higher $^{187}Os/^{188}Os$ ratio of Loa-trend volcanoes, relative to the Kea-trend, possibly reflecting the addition of ~15% of a recycled oceanic crust and sediment package. The COs reservoir may be related to an outer core component, although the exact nature of this component is still open to interpretation.

2) Base-metal sulfides: A viable alternative is the preferential incorporation of a BMS component into a mantle source during metasomatism that produces a hybrid pyroxenite-peridotite source. The variable HSE abundances and Os isotopic compositions of BMS may account for the large intra-volcanic variations in $^{186}Os/^{188}Os$ ratios, and may be the most consistent with a correlation between Pt/Os and $^{186}Os/^{188}Os$ ratios observed for Hualalai. This hypothesis, however, requires further development, particularly with respect to how grain-scale BMS variations

152

translate to larger scales and to place mass balance constraints on the proportions of peridotites, pyroxenite and BMS that may be involved.

These two hypotheses are not mutually exclusive and both provide viable mechanisms that can potentially account for the observed ^{186}Os and ^{187}Os characteristics of the Hawaiian picrites. More detailed work, especially through direct measurements and experimental techniques, is needed to more thoroughly define the relationships between pyroxenite, peridotite and BMS, and to better characterize the nature of the COs component, if it is present.

Chapter 5: Summary

5.1 Overview of the Dissertation

The primary goal of this dissertation was to improve the understanding of the processes and materials that contribute to the mantle sources of Hawaiian volcanism. To accomplish this objective, a suite of elements comprised of W and the HSE (Os, Ir, Ru, Pt, Pd and Re), including two radioactive decay systems (Pt-Os and Re-Os), were evaluated in a well-characterized group of Hawaiian picrites. These picritic samples are among the most primitive samples produced from the Hawaiian main-shield stage volcanes. As such, they may preserve considerable information about the mantle source regions from which they were derived.

The absolute and relative abundances of the selected elements may be affected by mantle processes that include the incorporation of recycled oceanic crust and sediments, and mantle metasomatic events. Crystal-liquid fractionation processes may also have an effect on these elements in both the mantle source regions and in the crust. Furthermore, these elements may be suitable for addressing the role that core-mantle interaction has, if any, in modifying the mantle source regions of OIB, as the outer core is highly enriched in the moderately and highly siderophile elements relative to the mantle, and may also have a distinct Os isotopic composition.

The following section explores the contribution of the data gathered in each chapter to our overall comprehension of the processes and materials that may affect the Hawaiian mantle source regions, as well as the limitations for some of the interpretations provided.

5.2 Recycled components in Hawaiian mantle sources

5.2.1 Consistency of new ^{187}Os/^{188}Os data with previous studies of Hawaii

Prior geochemical studies of Hawaiian basalts identified two prominent trends, termed the Kea- and Loa-trends, for the Hawaiian shield volcanoes, which are defined by correlations between Sr, Nd, Pb and Hf isotopic data (Figure 1.5; e.g., Frey and Rhodes, 1993; Hauri, 1996; Lassiter et al., 1996; Huang et al., 2005; Ren et al., 2005). Earlier analyses of the Re-Os systematics of Hawaiian basalts also observed a similar distinction between Kea- and Loa-trend volcanic centers. These studies noted that there was limited ^{187}Os/^{188}Os variability within a single volcanic center, but significant variation between Kea- and Loa-trend shield volcanoes, with Loa-trend lavas characterized by systematically higher ^{187}Os/^{188}Os ratios relative to Kea-trend lavas (e.g., Bennett et al., 1996, 2000; Hauri, 1996; Lassiter and Hauri, 1998; Bryce et al., 2005). The primary interpretation of the Kea- and Loa-trend distinctions has generally been attributed to the mixing of an ancient subducted component, composed of oceanic basalt and sediment with high Re/Os, into the source regions of Loa-trend volcanoes. The Kea-trend mantle sources would contain little of this recycled material (Lassiter and Hauri, 1998; Huang et al., 2005).

The new ^{187}Os/^{188}Os data presented here (Chapter 3 and 4) are consistent with these previous observations, with significant differences observed between Kea- and Loa-trend lavas (Figure 3.3; Figure 4.3). Likewise, our evaluation of the data resulted in similar interpretations that were proposed by the previous studies. For example,

mixing of ~15% of a model subducted oceanic basalt and sediment package, which would have a high Re/Os ratio, into a peridotitic source is capable of generating the higher $^{187}Os/^{188}Os$ ratios observed in Loa-trend lavas (Figure 4.6a,b).

Similarly, a pyroxenitic component, which may be derived from subducted oceanic crust, has also been suggested as a way to produce Os isotopic variations in a mantle source (Smith, 2003; Luguet et al., 2008). Bulk mixing of pyroxenites into a mantle domain are also consistent the new $^{187}Os/^{188}Os$ data, because these materials tend to have variably elevated Re/Os ratios, which will evolve variable $^{187}Os/^{188}Os$ over time.

Thus, the variable bulk mixing of recycled components into a mantle source is considered a viable mechanism to produce some of the observed variations in $^{187}Os/^{188}Os$, and is consistent with the Hf, Sr, Nd and Pb isotopic differences between Kea- and Loa-trend sources. There are, however, some important limitations of recycling to account for the ^{186}Os-^{187}Os relations.

5.2.2 Limitations of recycled component

Luguet et al. (2008) assessed bulk mixing of peridotite and pyroxenite components as a primary mechanism to generate elevated $^{186}Os/^{188}Os$ ratios in some OIB. They noted that some pyroxenites may have the appropriate Pt-Re-Os characteristics to produce enrichments in ^{186}Os and ^{187}Os similar to those observed at Hawaii, however, these examples may not be representative of typical pyroxenites. A mixing model involving various pyroxenite compositions, aged for 2 Ga, and mantle peridotite established that average pyroxenites from two independent studies tend to

develop enrichments in ^{187}Os too rapidly, relative to ^{186}Os, to account for the Hawaiian data (Figure 4.5; Smith, 2003; Luguet et al., 2008; van Acken et al., 2009). For this reason, an additional component or mechanism is needed to account for the observed ^{186}Os/^{188}Os variations.

5.3 Mechanisms for producing variations in ^{186}Os/^{188}Os

5.3.1 COs component

5.3.1.1 Consistency of new ^{186}Os/^{188}Os data with previous studies of Hawaii

An earlier study of the two radiogenic Os isotopes in Hawaii observed a linear correlation between ^{186}Os/^{188}Os and ^{187}Os/^{188}Os ratios (Brandon et al., 1999). These authors attributed the trend to the mixing of a COs component into the mantle source (Brandon et al., 1999, 2003), which they related to the outer core. This COs component would be characterized by an enrichment in both ^{186}Os and ^{187}Os, reflecting long-term elevated Pt/Os and Re/Os ratios. This component would also have to be ubiquitous in the Hawaiian system.

Although the new data span a similar range in ^{186}Os/^{188}Os as the previous study, a single linear correlation with ^{187}Os/^{188}Os is not observed in the new dataset. Brandon et al. (1999) did not consider the ^{187}Os/^{188}Os distinction between Kea- and Loa-trend volcanic centers, and instead implied that both ^{186}Os and ^{187}Os variations were due to variable mixing with the COs component. In the previous section, however, a strong case was made for the role of a recycled component in producing some of the ^{187}Os/^{188}Os variations observed in Hawaii. If considered separately, ^{186}Os/^{188}Os and

$^{187}Os/^{188}Os$ data for the Kea- and Loa-trend picrites define generally positive trends (Figure 4.6a,b).

Despite these different interpretations, the combined ^{186}Os and ^{187}Os data from the current study may still be consistent with a COs component in the Hawaiian plume, with general HSE and Os isotopic characteristics similar to that modeled by Brandon et al. (1999; 2003). The combined ^{186}Os and ^{187}Os data presented in Chapter 4, are consistent with three-component mixing between Kea- and Loa-trend mantle sources and a COs component (Figure 4.6c). In this scenario, $^{187}Os/^{188}Os$ variations may still be related to the bulk addition of recycled materials, while variations in $^{186}Os/^{188}Os$ can be generated by variable interaction of the mantle source with the COs component. Although the data are consistent with a COs component, the nature of this reservoir is still open to interpretation.

5.3.1.2 COs and the outer core?

The outer core was suggested as the COs component by Brandon et al. (1999, 2003), based on solid metal/liquid metal partitioning data for Pt, Re and Os from some high pressure-temperature experiments (Lauer and Jones, 1998; Walker, 2000), that could potentially lead to elevated Pt/Os and Re/Os ratios in the outer core. Although the ^{186}Os-^{187}Os isotopic data may be consistent with the outer core representing the COs component, there would be some geochemical consequences of this relationship. The lack of corresponding enrichments in HSE abundances and the low estimated W source abundances, combined with a lack of ^{182}W anomalies in Hawaiian rocks, provide arguments against the outer core having a significant role in

the Hawaiian mantle source regions. Despite these issues, however, the outer core cannot currently be ruled out as the COs component.

5.3.2 BMS and mantle metasomatism

Alternatively, metasomatic enrichment of the source region, resulting in the movement of Pt-rich BMS, may also be capable of generating variations in $^{186}Os/^{188}Os$ ratios. This hypothesis is consistent with a recent study that suggested the Hawaiian source may form via a two-stage process that involves the formation of a hybrid pyroxenite-peridotite source (Sobolev et al., 2005, 2007). Luguet et al. (2008) purported that during these metasomatic processes, HSE abundances are largely controlled by the movement of BMS. BMS tend to be enriched in Pt relative to Os (Bockrath et al., 2004; Maier and Barnes, 2004; Ballhaus et al., 2006); therefore these sulfides may have sufficiently high Pt/Os to evolve to high $^{186}Os/^{188}Os$.

This hypothesis is consistent with the new data presented for the Hawaiian picrites, however, how the grain-scale variations in BMS translates to larger scales remains a problem. The COs and BMS hypotheses are not mutually exclusive, and both provide viable mechanisms to potentially generate the Os isotopic data.

5.4 Crystal-liquid fractionation processes

The recycling of oceanic crust or pyroxenitic material is likely not responsible for absolute and relative HSE variations observed at Hawaii, due to the typically lower concentrations of these elements in recycled materials (Tatsumi et al., 1998; Peucker-

Ehrenbrink et al., 2003; Luguet et al., 2008; van Acken et al., 2009). For example, Figure 2.8 shows that recycling of oceanic crust will have a small, mainly dilutional effect on the absolute abundances of the HSE, but virtually no effect on the relative abundances.

Instead, the abundances of the HSE in these picrites are likely predominantly controlled by crystal-liquid fractionation processes. These elements are evidently sited in phases that have a close association with olivine, which is shown by strong linear correlations with MgO (Figure 3.2). Small changes in the degree of partial melting, the presence of residual sulfides in the mantle source, or sulfide/chromite removal in magma chambers may serve to fractionate the HSE from each other and account for the variations in chondrite-normalized HSE-patterns (Figure 3.1). This interpretation is consistent with HSE data for Hawaiian samples from previous studies (Tatsumi et al., 1999; Bennett et al., 2000). The effects of crystal-liquid fractionation processes, however, can be compensated for by estimating a parental melt composition for each volcanic center.

The estimated parental melts for each volcanic center are similar to each other, indicating that each volcanic center experienced similar melting conditions and implying that the mantle source HSE abundances were comparable. Differences in HSE abundances between the parental melts can be attributed to recent melt percolation processes, or in the case of Loihi, to lower degrees of partial melting in the source region.

5.5 W abundances of the Hawaiian mantle source regions

The abundances of W in the Hawaiian mantle source regions may be expected to mirror the Kea- and Loa-trend distinctions because W is highly enriched in the subducted component and is highly incompatible during partial melting of the mantle. An enrichment of W in Loa-trend volcanoes, however, was not observed. In fact the estimated W source abundances are similar between Kea- and Loa-trend volcanoes.

When W source estimates were combined, the mean Hawaiian source had an average of 10 ± 3 ng/g W, which is three-times as enriched as the DMM; 3.0 ± 2.3 ng/g, but comparable to the primitive mantle (13 ± 10 ng/g). The relatively high abundances of W in the mantle sources that contribute to Hawaiian lavas may be explained as a consequence of the recycling of W-rich oceanic crust and sediment into a depleted mantle source, such as the depleted MORB mantle (DMM). However, this scenario requires varying proportions of recycled materials with different mean ages to account for the diversity of radiogenic isotope compositions observed between Kea- and Loa-trend volcanoes. Alternatively, the modeled W enrichments may also reflect a primary source component that is less depleted in incompatible trace elements than the DMM. If this interpretation is correct, small amounts (~10 to 15%) of a modeled subducted component can be added to Loa-trend volcanoes within the uncertainties of the source W estimates, which would be consistent with the Kea- and Loa-trend distinction based on [187]Os isotopes.

5.6 Future directions of research

The most crucial aspect of future research is the gathering of more comprehensive datasets for upper mantle materials, putative plume systems, and various other reservoirs. These datasets need to include a combination of HSE abundance measurements, with respect to whole-rock and mineral compositions, along with high-precision Os isotopic measurements. The characterization of pyroxenites, along with the associated base-metal sulfides, is a key parameter in the modeling of processes that may result in HSE variations and $^{186}Os/^{188}Os$ and $^{187}Os/^{188}Os$ anomalies.

A better understanding of the partitioning behaviour of the HSE during various mantle processes is also of great importance. This includes solid metal/liquid metal partitioning behaviour at the high pressure-temperature conditions in the core, as well as the melt/crystal partitioning in BMS-phases and pyroxenites. These problems may be best addressed through experimental petrology techniques, especially through the use of diamond-anvil cells that can create relatively high pressure-temperature conditions.

References

Abouchami W., Galer S. J. G., and Hofmann A. W. 2000. High precision lead isotope systematics of lavas from the Hawaiian Scientific Drilling Project. Chemical Geology 169(1-2), 187-209.

Alard, O., Luguet, A., Pearson, N.J., Griffin, W.L., Lorand, J.-P., Gannoun, A., Burton, K.W., O'Reilly, S.Y., 2005. In situ Os isotopes in abyssal peridotites bridge the isotopic gap between MORBs and their source mantle. Nature 436, 1005-1008.

Allègre, C.J., Moreira, M. 2004. Rare gas systematics and the origin of oceanic islands: the key role of entrainment at the 670 km boundary layer. Earth Planet. Sci. Lett. 228, 85-92.

Anderson, D.L., 1998. A model to explain the various paradoxes associated with mantle noble gas geochemistry. Proceedings of the National Academy of Sciences of the United States of America 95, 9087-9092.

Arnórsson, S., and Óskarsson, N. 2007. Molybdenum and tungsten in volcanic rocks and in surface and <100 degrees C ground waters in Iceland. Geochimica et Cosmochimica Acta 71, 284-304.

Arevalo Jr. R. and McDonough W. F. 2008. Tungsten geochemistry and implications for understanding the Earth's interior. Earth and Planetary Science Letters 272, 656-665.

Baker, J.A., Jensen, K.K., 2004. Coupled Os-186-Os-187 enrichments in the Earth's mantle - core-mantle interaction or recycling of ferromanganese crusts and nodules? Earth Planet. Sci. Lett. 220, 277-286.

Ballhaus, C., Bockrath, C., Wohlgemuth-Ueberwasser, C., Laurenz, V., Berndt, J., 2006. Fractionation of the noble metals by physical processes. Contrib. Mineral. Petrol. 152, 667-684.

Barnes, S.J., Naldrett, A.J., Gorton, M.P., 1985. The origin of the fractionation of platinum-group elements in terrestrial magmas. Chem. Geol. 53, 303-323.

Barnes, S.J., Picard, C.P., 1993. The behavior of platinum-group elements during partial melting, crystal fractionation, and sulfide segregation – an example from the Cape-Smith fold belt, northern Quebec. Geochim. Cosmochim. Acta. 57, 79-87.

Becker, H., Shirey, S.B., Carlson, R.W., 2001. Effects of melt percolation on the Re-Os systematics of peridotites from a Paleozoic convergent plate margin. Earth Planet. Sci. Lett. 188, 107-121.

Becker, H., Horan, M.F., Walker, R.J., Gao, S., Lorand, J.-P., Rudnick, R.L., 2006. Highly siderophile element composition of the Earth's primitive upper mantle: Constraints from new data on peridotite massifs and xenoliths. Geochim. Cosmochim. Acta. 70, 4528-4550.

Bennett V. C., Esat T. M., and Norman M. D. 1996. Two mantle-plume components in Hawaiian picrites inferred from correlated Os-Pb isotopes. Nature 381(6579), 221-224.

Bennett, V.C., Norman, M.D., Garcia, M.O., 2000. Rhenium and platinum group element abundances correlated with mantle source components in Hawaiian picrites: sulphides in the plume. Earth Planet. Sci. Lett. 183, 513-526.

Birck, J.-L., Roy-Barman, M., Capmas, F., 1997. Re-Os isotopic measurements at the femtomole level in natural samples. Geostand. Newsl. 21, 19-27.

Bird, J.M., Meibom, A., Frei, R., Nagler, T.F. 1999. Osmium and lead isotopes of rare OsIrRu minerals: derivation from the core-mantle boundary region? Earth Planet. Sci. Lett. 170, 83-92.

Bizimis, M., Griselin, M., Lassiter, J.C., Salters, V.J.M., Sen, G., 2007. Ancient recycled mantle lithosphere in the Hawaiian plume: Osmium-Hafnium isotopic evidence from peridotite mantle xenoliths. Earth Planet. Sci. Lett. 257, 259-273.

Blichert-Toft J. and Albarede F. 1999. Hf isotopic compositions of the Hawaii Scientific Drilling Project core and the source mineralogy of Hawaiian basalts. Geophysical Research Letters 26(7), 935-938.

Bockrath, C., Ballhaus, C. and Holzheid, A., 2004. Fractionation of the platinum-group elements during mantle melting. Science 3053, 1951-1953.

Boyd, F.R., and Mertzman, S.A., 1987. Composition of structure of the Kaapvaal
  lithosphere, southern Africa: In: Magmatic Processes - Physicochemical
  Principles, B.O. Mysen, Ed., The Geochemical Society, Special Publication #1,
  pp. 13-24.

Brandon, A.D., Walker, R.J., Morgan., J.W., Norman, M.D., Prichard, H.M. 1998.
  Coupled ^{186}Os and ^{187}Os evidence for core-mantle interaction. Science 280,
  1570-1573.

Brandon, A.D., Norman, M.D., Walker, R.J., Morgan, J.W., 1999. ^{186}Os-^{187}Os
  systematics of Hawaiian picrites. Earth Planet. Sci. Lett. 174, 25-42.

Brandon, A.D., Walker, R.J., Puchtel, I.S., Becker, H., Humayun, M., Revillon, S.,
  2003. ^{186}Os-^{187}Os systematics of Gorgona Island komatiites: implications for
  early growth of the inner core. Earth Planet. Sci. Lett. 206, 411-426.

Brandon, A.D. and Walker, R.J., 2005. The debate over core-mantle interaction. Earth
  Planet. Sci. Lett. 232, 211-225.

Brandon, A.D., Humayun, H., Puchtel, I.S., Leya, I., Zolensky, M. 2005. Osmium
  isotope evidence for an s-process carrier in primitive chondrites. Science 309,
  1233-1236.

Brandon, A.D., Walker, R.J., Puchtel, I.S. 2006. Platinum-osmium isotope evolution
  of the Earth's mantle: Constraints from chondrites and Os-rich alloys. Geochim.
  Cosmochim. Acta. 70, 2093-2103.

Brandon, A.D., Graham, D.W., Waight, T., Gautason, B. 2007. ^{186}Os and ^{187}Os enrichments and high-^{3}He/^{4}He sources in the Earth's mantle: Evidence from Icelandic picrites. Geochim. Cosmochim. Acta. 71, 4570-4591.

Brenan, J.M., McDonough, W.F., Dalpe, C. 2003. Experimental constraints on the partitioning of rhenium and some platinum-group elements between olivine and silicate melt. Earth Planet. Sci. Lett. 212, 135-150.

Brenan, J.M., McDonough, W.F., Ash, R. 2005. An experimental study of the solubility and partitioning of iridium, osmium and gold between olivine and silicate melt. Earth Planet. Sci. Lett., 237: 855-872.

Buffett B. A., Huppert H. E., Lister J. R., and Woods A. W. 1996. On the thermal evolution of the Earth's core. Journal of Geophysical Research-Solid Earth 101(B4), 7989-8006.

Brügmann, G.E., Arndt, N.T., Hofmann, A.W., Tobschall, H.J., 1987. Noble-metal abundances in komatiite suites from Alexo, Ontario, and Gorgona Island, Colombia. Geochim. Cosmochim. Acta. 51, 2159-2169.

Bryce, J.G., DePaolo, D.J. and Lassiter, J.C., 2005. Geochemical structure of the Hawaiian plume: Sr, Nd, and Os isotopes in the 2.8 km HSDP-2 section of Mauna Kea volcano. Geochem. Geophys. Geosys. 6, 1-36.

Büchl, A., Brügmann, G., Batanova, V.G., Münker, C., Hofmann, A.W. 2002. Melt percolation monitored by Os isotopes and HSE abundances: a case study from

the mantle section of the Troodos Ophiolite. Earth Planet. Sci. Lett. 204, 385-402.

Büchl, A., Brügmann, G., Batanova, V.G., 2004a. Formation of podiform chromitite deposits: implications from PGE abundances and Os isotopic compositions of chromites from the Troodos complex, Cyprus. Chem Geol. 208, 217-232.

Büchl, A., Brügmann, G., Batanova, V.G., Hofmann, A.W., 2004b. Os mobilization during melt percolation: The evolution of Os isotope heterogeneities in the mantle sequence of the Troodos Ophiolite, Cyprus. Geochim. Cosmochim. Acta. 68, 3397-3408.

Cabri, L.J., Harris, D.C., Weiser, T.W., 1996. Mineralogy and distribution of platinum-group mineral (PGM) placer deposits of the world. Explor. Min. Geol. 5, 73-167.

Campbell, I.H., Griffiths, R.W., 1990. Implications of mantle plume structure for the evolution of flood basalts. Earth Planet. Sci. Lett. 99, 79-93.

Chabot, N.L., Campbell, A.J., Jones, J.H., Humayun, M., Agee, C.B. 2003. An experimental test of Henry's law in solid metal-liquid metal systems with implications to iron meteorites. Meteorit. Planet. Sci. 38, 181-196.

Chauvel, C., Hofmann, A.W., Vidal, P. 1992, HIMU-EM: the French Polynesia connection. Earth Planet Sci. Lett. 110, 99-119.

Chauvel, C., Goldstein, S.L., Hofmann, A.W. 1995. Hydration and dehydration of oceanic crust controls Pb evolution in the mantle. Chemical Geology 126, 65-75.

Chen, C.Y., Frey, F.A., Garcia, M.O., Dalrymple, G.B., Hart, S.R., 1991. The tholeiite to alkalic basalt transition at Haleakala volcano, Maui, Hawaii. Contrib. Min. Petrol. 106, 183-200.

Cohen, A.S. and Waters, F.G., 1996. Separation of osmium from geological materials by solvent extraction for analysis by thermal ionization mass spectrometry. Anal. Chem. 332, 269-275.

Cook, D.L., Walker, R.J., Horan, M.F., Wasson, J.T., Morgan, J.W. 2004. Pt-Re-Os systematics of group IIAB and IIIAB iron meteorites. Geochim. Cosmochim. Acta. 68, 1413-1431.

Courtillot V., Davaille A., Besse J., and Stock J. 2003. Three distinct types of hotspots in the Earth's mantle. Earth and Planetary Science Letters 205(3-4), 295-308.

Crocket, J.H., Macrae, W.E., 1986. Platinum-group element distribution in komatiitic and tholeiitic volcanic-rocks from Munro township, Ontario. Econ. Geol. 81, 1242-1251.

Crocket, J.H., 2000. PGE in fresh basalt, hydrothermal alteration products, and volcanic incrustations of Kilauea volcano, Hawaii. Geochim. Cosmochim. Acta. 64, 1791-1807.

Dale, C.W., Burton, K.W., Pearson, D.G., Gannoun, A., Alard, O., Argle, T.W., Parkinson, I.J., 2009. Highly siderophile element behaviour accompanying subduction of oceanic crust: Whole rock and mineral-scale insights from a high-pressure terrain. Geochim. Cosmochim. Acta. 73, 1394-1416.

Danyushevsky, L.V., Della-Pasqua, F.N., Sokolov, S., 2000. Re-equilibration of melt inclusions trapped by magnesian olivine phenocrysts from subduction-related magmas: petrological implications. Contrib. Mineral. Petrol. 138, 68-83.

Eggins, S.M., Rudnick, R.L. and McDonough, W.F., 1998. The composition of peridotites and their minerals: A laser-ablation ICP-MS study. Earth Planet. Sci. Lett. 154, 53-71.

Eiler J. M., Farley K. A., Valley J. W., Stolper E. M., Hauri E. H., and Craig H. 1995. Oxygen isotope evidence against bulk recycled sediment in the mantle sources of Pitcairn island lavas. Nature 377(6545), 138-141.

Eiler, J.M., Farley, K.A., Valley, J.W., Hofmann, A.W. and Stolper, E.M., 1996. Oxygen isotope constraints on the sources of Hawaiian volcanism. Earth Planet. Sci. Lett. 144, 453-467.

Feigenson, M.D., Patino, L.C. and Carr, M.J. 1996. Constraints on partial melting imposed by rare earth element variations in Mauna Kea basalts. Journal of Geophysical Research 101, 11815-11829.

Feigenson M. D., Bolge L. L., Carr M. J., and Herzberg C. T. 2003. REE inverse modeling of HSDP2 basalts: Evidence for multiple sources in the Hawaiian plume. Geochemistry Geophysics Geosystems 4.

Fleet., M.E., Stone, W.E. 1991. Partitioning of platinum-group elements in the Fe-Ni-S system and their fractionation in nature. Geochim. Cosmochim. Acta. 55, 245-253.

Fleet, M.E., Liu, M., Crocket, J.H. 1999. Partitioning of trace amounts of highly siderophile elements in the Fe-Ni-S system and their fractionation in nature. Geochim. Cosmochim. Acta. 63, 2611-2622.

Frey F. A. and Rhodes J. M. 1993. Intershield geochemical differences among Hawaiian volcanoes - Implications for source compositions, melting process and magma ascent paths. Philosophical Transactions of the Royal Society of London Series a-Mathematical Physical and Engineering Sciences 342(1663), 121-136.

Gaffney, A.M., Nelson, B.K., Reisberg, L., Eiler, J., 2005. Oxygen-osmium isotope systematics of West Maui lavas: A record of shallow-level magmatic processes. Earth Planet. Sci. Lett. 239, 122-139.

Galer S. J. G. and O'Nions R. K. 1985. Residence time of thorium, uranium and lead in the mantle with implications for mantle convection. Nature 316, 778–782.

Garcia, M.O., Foss, D.J.P., West, H.B. and Mahoney, J.J., 1995. Geochemical and isotopic evolution of Loihi Volcano, Hawaii. J. Petrol. 36, 1647-1674.

Gurriet, P.C. 1988, Geochemistry of Hawaiian dredged lavas. MSc Thesis, Massachusetts Institute of Technology.

Hart, S.R., Hauri, E.H., Oschmann, L.A., and Whitehead, J.A. 1992. Mantle plumes and entrainment – isotopic evidence. Science 256, 517-520.

Hauri, E.H., 1996. Major-element variability in the Hawaiian mantle plume. Nature 382, 415-419.

Hauri, E.H., Lassiter, J.C., DePaolo, D.J., 1996. Osmium isotope systematics of drilled lavas from Mauna Loa, Hawaii. J. Geophys. Res. 101, 11793-11806.

Hauri, E.H., Kurz, M.D., 1997. Melt migration and mantle chromatography, 2: a time-series Os isotope study of Mauna Loa Volcano, Hawaii. Earth Planet. Sci. Lett. 153, 21-36.

Hawkesworth C. J., Mantovani M. S. M., Taylor P. N., and Palacz Z. 1986. Evidence from the Parana of South Brazil for a continental contribution to Dupal basalts. Nature 322, 356–359.

Hawkesworth, C. and Scherstén A 2007. Mantle plumes and geochemistry. Chemical Geology 241, 319-331.

Helz, R.T., 1987. Differentiation behavior of Kilauea Iki lava lake, Kilauea volcano, Hawaii: An overview of past and current work. In Mysen, B.O., ed., Magmatic Processes: Physicochemical Principles. The Geochemical Society Special Publication No. 1, 241-258.

Hoffman, E.L., Naldrett, A.J., Vanloon, J.C., Hancock, R.G.V., Manson, A. 1978. Determination of all platinum group elements and gold in rocks and ore by neutron-activation analysis after preconcentration by a nickel sulfide fire-assay technique on large samples. Analytica Chimica Acta. 102, 157-166.

Hofmann, A.W. and White, W.M., 1982. Mantle plumes from ancient oceanic crust. Earth Planet. Sci. Lett. 57, 421-436.

Hofmann, A.W., 1988. Chemical differentiation of the Earth: the relationship between mantle, continental crust, and oceanic crust. Earth Planet. Sci. Lett. 90. 297-314.

Hofmann A. W. and Jochum K. P. 1996. Source characteristics derived from very incompatible trace elements in Mauna Loa and Mauna Kea basalts, Hawaii Scientific Drilling Project. Journal of Geophysical Research-Solid Earth 101(B5), 11831-11839.

Hofmann A. W. 1997. Mantle geochemistry: The message from oceanic volcanism. Nature 385(6613), 219-229.

Hofmann A. W. 2003. Sampling mantle heterogeneity through oceanic basalts: Isotopes and trace elements. In The Mantle and Core (ed. R.W. Carlson) Vol. 2 Treatise on Geochemistry (eds. H.D. Holland and K.K Turekian), pp. 61-101. Elsevier-Pergamon.

Horan, M.F., Walker, R.J., Morgan, J.W., Grossman, J.N., Rubin, A.E., 2003. Highly siderophile elements in chondrites. Chem. Geol. 196, 5-20.

Hu Z. C. and Gao S. 2008. Upper crustal abundances of trace elements: A revision and update. Chemical Geology 253(3-4), 205-221.

Huang, S., Frey, F.A., 2003. Trace element abundances of Mauna Kea basalt from phase 2 of the Hawaii Scientific Drilling Project: Petrogenetic implications of correlations with major element content and isotopic ratios. Geochem. Geophys. Geosyst. 4: 43.

Huang S. C. and Frey F. A. 2005. Recycled oceanic crust in the Hawaiian Plume: evidence from temporal geochemical variations within the Koolau Shield. Contributions to Mineralogy and Petrology 149(5), 556-575.

Huang S. C., Frey F. A., Blichert-Toft J., Fodor R. V., Bauer G. R., and Xu G. P. 2005. Enriched components in the Hawaiian plume: Evidence from Kahoolawe volcano, Hawaii. Geochemistry Geophysics Geosystems 6.

Humayun, M., Qin, L.P. and Norman, M.D., 2004. Geochemical evidence for excess iron in the mantle beneath Hawaii. Science 306, 91-94.

Ireland, T.J., Walker, R.J., Garcia, M.O. 2009a. Highly siderophile element and 187Os isotope systematics of Hawaiian picrites: Implications for parental melt composition and source heterogeneity. Chem. Geol. 260, 112-128.

Ireland, T.J., Arevalo Jr., R.D., Walker, R.J., McDonough, W.F. 2009b. Tungsten in Hawaiian picrites: A compositional model for the sources of Hawaiian lavas. Geochim. Cosmochim. Acta. 73, 4517-4530.

Jagoutz E., Palme H., Baddenhausen H., Blum K., Cendales M., Dreibus G., Spettel
B., Lorenz V., and Wanke H. 1979. The abundances of major, minor and trace
elements in the earth's mantle as derived from primitive ultramafic nodules.
10th Proceedings of Lunar and Planetary Sciences, 2031-2050.

Jamais, M., Lassiter, J.C. and Brügmann, G., 2008. PGE and Os isotopic variations in
lavas from Kohala Volcano Hawaii: Constraints on PGE behavior and
melt/crust interaction. Chem. Geol. 250, 16-28.

Jochum, K.P., Stoll, B., Herwig, K. and Willbold, M., 2007. Validation of LA-
ICPMS trace element analysis of geological glasses using a new solid-state 193
nm Nd:YAG laser and matrix-matched calibration. J. Analyt. Atom. Spec. 22,
112-121.

Jochum, K.P., Stoll, B., Herwig, K., Willbold, M., Hofmann, A.W., Amini, M.,
Aarburg, S., Abouchami, W., Hellebrand, E., Mocek, B., Raczek, I., Stracke, A.,
Alard, O., Bouman, C., Becker, S., Ducking, M., Bratz, H., Klemd, R., de
Bruin, D., Canil, D., Cornell, D., de Hoog, C.J., Dalpe, C., Danyushevsky, L.,
Eisenhauer, A., Premo, W.R., Sun, W.D.D., Tiepolo, M., Vannucci, R.,
Vennemann, T., Wayne, D. and Woodhead, J.D., 2006. MPI-DING reference
glasses for in situ microanalysis: New reference values for element
concentrations and isotope ratios. Geochem. Geophys. Geosyst. 7, 1-44.

Jochum, K.P., Willbold, M., Raczek, I., Stoll, B. and Herwig, K. 2005. Chemical
characterization of the USGS reference glasses GSA-1G, GSC-1G, GSD- 1G,

GSE-1G, BCR-2G, BHVO-2G and BIR-1G using EPMA, ID-TIMS, IDICP-MS and LA-ICP-MS. Geostd. Geoanalyt. Res. 29, 285-302.

Kishida, K., Sohrin, Y., Okamura, C. and Ishibachi., J. 2004. Tungsten enriched in submarine hydrothermal fluids. Earth and Planetary Science Letters 222, 819-827.

Kleine, T., Munker, C., Mezger, K. and Palme, H. 2002. Rapid accretion and early core formation on asteroids and the terrestrial planets from Hf-W chronometry. Nature 418, 952-955.

König, S., Münker, C., Schuth, S. and Garbe-Schönberg, D. 2008. Mobility of tungsten in subduction zones. Earth and Planetary Science Letters 274, 82-92.

Kurz M. D., Jenkins W. J., Hart S. R., and Clague D. 1983. Helium isotopic variations in volcanic - Rocks from Loihi seamount and the island of Hawaii. Earth and Planetary Science Letters 66(1-3), 388-406.

Kurz M. D., Kenna T. C., Lassiter J. C., and DePaolo D. J. 1996. Helium isotopic evolution of Mauna Kea Volcano: First results from the 1-km drill core. Journal of Geophysical Research-Solid Earth 101(B5), 11781-11791.

Labrosse S., Poirier J. P., and Le Mouel J. L. 2001. The age of the inner core. Earth and Planetary Science Letters 190(3-4), 111-123.

Labrosse, S. 2003. Thermal and magnetic evolution of the Earth's core. Physics of the Earth and Planetary Interiors 140, 127-143.

Lassiter J. C., DePaolo D. J., and Tatsumoto M. 1996. Isotopic evolution of Mauna Kea volcano: Results from the initial phase of the Hawaii Scientific Drilling Project. Journal of Geophysical Research-Solid Earth 101(B5), 11769-11780.

Lassiter, J.C. and Hauri, E.H., 1998. Osmium-isotope variations in Hawaiian lavas: evidence for recycled oceanic lithosphere in the Hawaiian plume. Earth Planet. Sci. Lett. 164, 483-496.

Lassiter, J.C., 2003. Rhenium volatility in subaerial lavas: constraints from subaerial and submarine portions of the HSDP-2 Mauna Kea drillcore. Earth Planet. Sci. Lett. 214, 311-325.

Lassiter, J.C. 2006. Constraints on the coupled thermal evolution of the Earth's core and mantle, the age of the inner core, and the origin of the 186Os/188Os "core signal" in plume-derived lavas. Earth. Planet. Sci. Lett. 250, 306-317.

Lauer, H.V., Jones, J.H., 1998. Partitioning of Pt and Os between solid and liquid metal in the iron-nickel-sulfur system. Proc. Lunar Planet. Sci. Conf. XXIX, 1796.

Liu, Y., Huang, M., Masuda, A., Inoue, M., 1998. High-precision determination of osmium and rhenium isotope ratios by in-situ oxygen isotope correction using negative thermal ionization mass spectrometry. Int. J. Mass Spectrom. Ion Process 173, 163-175.

Luguet, A., Alard, O., Lorand, J.-P., Pearson, N.J., Ryan, C., O'Reilly, S.Y., 2001. Laser-ablation microprobe (LAM)-ICPMS unravels the highly siderophile

element geochemistry of the oceanic mantle. Earth Planet. Sci. Lett. 189, 285-294.

Luguet, A., Lorand, J.-P., Alard, O., Cottin, J.-Y., 2004. A multi-technique study of platinum group element systematics in some Ligurian ophiolitic peridotites, Italy. Chem. Geol. 208, 175-194.

Luguet, A., Shirey, S.B., Lorand, J.P., Horan, M.F., Carlson, R.W., 2007. Residual platinum-group minerals from highly depleted harzburgites of the Lherz massif (France) and their role in HSE fractionation of the mantle. Geochim. Cosmochim. Acta. 71, 3082-3097.

Luguet, A., Pearson, D.G., Nowell, G.M., Dreher, S.T., Coggon, J.A., Spetsius, Z.V., Parman, S.W., 2008. Enriched Pt-Re-Os isotope systematics in plume lavas explained by metasomatic sulfides. Science, 319, 453-456.

Luguet, A., Nowell, G.M., Pearson, D.G., 2008. $^{184}Os/^{188}Os$ and $^{186}Os/^{188}Os$ measurements by negative thermal ionization mass spectrometry (N-TIMS): Effects of interfering element and mass fractionation corrections on data accuracy and precision. Chem. Geol. 248, 342-362.

Maier, W.D., Roelofse, F., Barnes, S.J., 2003. The concentration of the platinum-group elements in south African komatiites: Implications for mantle sources, melting regime and PGE Fractionation during crystallization. J. Petrol. 44, 1787-1804.

Maier, W.D., Barnes, J., 2004. Pt/Pd and Pd/Ir ratios in mantle-derived magmas: A possible role for mantle metasomatism. South African Journal of Geology, 107, 333-340.

Malvin, D.J., Jones, J.H., Drake, M.J., 1986. Experimental investigations of trace-element fractionation in iron-meteorites. 3. Elements partitioning in the system Fe-Ni-S-P. Geochim. Cosmochim. Acta. 50, 1221-1231.

Marcantonio, F., Zindler, A., Elliott, T., Staudigel, H., 1995. Os isotope systematics of La Palma, Canary Islands – evidence for recycled crust in the mantle source of HIMU ocean islands. Earth Planet. Sci. Lett. 133, 397-410.

Martin, C.E., Carlson, R.W., Shirey, S.B., Frey, F.A., Chen, C.Y., 1994. Os isotopic variation in basalts from Haleakala volcano, Maui, Hawaii – a record of magmatic processes in oceanic mantle and crust. Earth Planet. Sci. Lett. 128, 287-301.

McDaniel, D.K., Walker, R.J., Heming, S.R., Horan, M.F., Becker, H., Grauch, R.L., 2004. Source of osmium in the modern oceans: new evidence from the 190Pt-186Os system. Geochim. Cosmochim. Acta. 68, 1243-1252.

McDonough W. F. and Sun S. S. 1995. The composition of the Earth. Chemical Geology 120(3-4), 223-253.

McDonough, W.F., 2003. Compositional model for the Earth's core, The Mantle and Core (ed. R.W. Carlson) Vol. 2 Treatise on Geochemistry (eds. H.D. Holland and K.K Turekian). Elsevier-Pergamon, Oxford, pp. 547-568.

McKenzie, D, and O'Nions, R.K. 1995. The source regions of ocean island basalts. Journal of Petrology 36, 133-159.

Meibom., A., Anderson, D.L., Sleep, N.H., Frei, R., Chamberlain, C.P., Hren, M.T. Wooden, J.L. 2003. Are high He-3/He-4 ratios in oceanic basalts an indicator of deep-mantle plume components? Earth and Planetary Science Letters 208, 197-204.

Meibom, A., Frei, R., Sleep, N.H., 2004. Osmium isotopic compositions of Os-rich platinum group element alloys from the Klamath and Siskiyou Mountains. Journal of Geophysical Research – Solid Earth. 109, B2.

Meisel, T., Walker, R.J., Irving, A.J., Lorand, J.-P. 2001. Osmium isotopic compositions of mantle xenoliths: a global perspective. Geochim. Cosmochim. Acta. 65, 1311-1323.

Momme, P., Oskarsson, N. and Keays, R.R., 2003. Platinum-group elements in the Icelandic rift system: melting processes and mantle sources beneath Iceland. Chem. Geol. 196, 209-234.

Montelli, R., Nolet, G., Dahlen, F.A., Masters, G., Engdahl, E.R. and Hung, S.H., 2004. Finite-frequency tomography reveals a variety of plumes in the mantle. Science 303, 338-343.

Morgan, W.J., 1971. Convection plumes in the lower mantle. Nature 230, 42-43.

Mukhopadhyay S., Lassiter J. C., Farley K. A., and Bogue S. W. 2003. Geochemistry of Kauai shield-stage lavas: Implications for the chemical evolution of the Hawaiian plume. Geochemistry Geophysics Geosystems 4.

Newsom H. E. and Palme H. 1984. The depletion of siderophile elements in the Earth's mantle - New evidence from molybdenum and tungsten. Earth and Planetary Science Letters 69(2), 354-364.

Newsom, H.E., White, W.M., Jochum, J.P., and Hofmann, A.W. 1986. Siderophile and chalcophile element abundances in oceanic basalts, Pb-isotope evolution and growth of the Earth's core. Earth and Planetary Science Letters 80, 299-313.

Newsom, H.E., White, Sims, K.W.W., Noll, P.D., Jaeger, W.L., Maehr, S.A., and Beserra, T.B. 1996. The depletion of tungsten in the bulk silicate Earth: Constraints on core formation. Geochimica et Cosmochimica Acta 60, 1155-1169.

Nielsen, S.G., Rehkamper, M., Norman, M.D., Halliday, A.N. and Harrison, D., 2006. Thallium isotopic evidence for ferromanganese sediments in the mantle source of Hawaiian basalts. Nature 439, 314-317.

Niu, Y.L., Langmuir, C.H., Kinzler, R.J. 1997. The origin of abyssal peridotites: a new perspective. Earth Planet. Sci. Lett. 152, 251-265.

Niu, Y.L., O'Hara, M.J., 2003. Origin of ocean island basalts: A new perspective
from petrology, geochemistry, and mineral physics considerations. Journal of
Geophysical Research-Solid Earth. 108 B4.

Noll, P.D. 1994. Siderophile and chalcophile trace element concentrations in young
subduction-related volcanics: Implications for continental crust formation and
crust-mantle evolution. Ph.D. dissertation, Univ. New Mexico.

Noll, P.D, Newsom, H.E., Leeman, W.P., and Ryan, J.G. 1996. The role of
hydrothermal fluids in the production of subduction zone magmas: evidence
from siderophile and chalcophile trace elements and boron. Geochimica et
Cosmochimica Acta. 60, 587-611.

Norman, M.D., Griffin, W.L., Pearson, N.J., Garcia, M.O. and O'Reilly, S.Y., 1998.
Quantitative analysis of trace element abundances in glasses and minerals: a
comparison of laser ablation inductively coupled plasma mass spectrometry,
solution inductively coupled plasma mass spectrometry, proton microprobe and
electron microprobe data. J. Analyt. Atom. Spec. 13, 477-482.

Norman, M.D. and Garcia, M.O., 1999. Primitive magmas and source characteristics
of the Hawaiian plume: petrology and geochemistry of shield picrites. Earth and
Planet. Sci. Lett. 168, 27-44.

Norman, M.D, Garcia, M.O., Bennett, V.C., 2004. Rhenium and chalcophile elements
in basaltic glasses from Ko'olau and Moloka'i volcanoes: magmatic outgassing

and composition of the Hawaiian plume. Geochim. Cosmochim. Acta. 68, 3761-3777.

Pearce, N.J.G., Perkins, W.T., Westgate, J.A., Gorton, M.P., Jackson, S.E., Neal, C.R. and Chenery, S.P. 1997. Compilation of new and published major and trace element data for NIST SRM 610 and NIST SRM 612 glass reference materials. Geostd. News. 21, 115-144.

Pearson, D.G., Irvine, G.J., Ionov, D.A., Boyd, F.R., Dreibus, G.E., 2004. Re-Os isotope systematics and platinum group element fractionation during mantle melt extraction: a study of massif and xenolith peridotite suites. Chem. Geol. 208, 29-59.

Peuker-Ehrenbrink. B., Bach, W., Hart., S.R., Blusztajn, J.S., Abbruzzese, T., 2003. Rhenium-osmium isotope systematics and platinum group element concentrations in oceanic crust from DSDP/ODP Sites 504 and 417/418. Geochem. Geophys. Geosyst. 4, 1-28.

Pietruszka, A.J., Hauri, E.H., Carlson, R.W. and Garcia, M.O. 2006. Remelting of recently depleted mantle within the Hawaiian plume inferred from the ^{226}Ra-^{230}Th-^{238}U disequilibria of Pu'U 'O'O eruption lavas. Earth and Planetary Science Letters 244, 155-169.

Pitcher, L., Helz, R.T., Walker, R.J., Piccoli, P. 2009. Fractionation of the platinum-group elements and Re during crystallization of basalt in Kilauea Iki lava lake, Hawaii. Chem. Geol. 260: 196-210.

Plank, T. Langmuir, C.H., 1998. The chemical composition of subducting sediment
and its consequences for the crust and mantle. Chemical Geology 145, 325-394.

Puchtel, I., Humayun, M., 2000. Platinum group elements in Kostomuksha komatiites
and basalts: Implications for oceanic crust recycling and core-mantle
interaction. Geochim. Cosmochim. Acta. 64, 4227-4242.

Puchtel, I.S., Humayun, M., 2001. Platinum group element fractionation in a
komatiitic basalt lava lake. Geochim. Cosmochim. Acta. 65, 2979-2993.

Puchtel, I.S., Humayun, M., Campbell, A.J., Sproule, R.A., Lesher, C.M., 2004.
Platinum group element geochemistry of komatiites from the Alexo and Pyke
Hill areas, Ontario, Canada. Geochim. Cosmochim. Acta. 68, 1361-1383.

Puchtel, I.S., Humayun, M., 2005. Highly siderophile element geochemistry of Os-
187-enriched 2.8 Ga Kostomuksha komatiites, Baltic shield. Geochim.
Cosmochim. Acta. 69, 1607-1618.

Putirka, K.D., 2005. Mantle potential temperatures at Hawaii, Iceland, and the mid-
ocean ridge system, as inferred from olivine phenocrysts: Evidence for
thermally driven plumes. Geochem. Geophys. Geosys. 6, 1-14.

Putirka, K.D., Perfit, M., Ryerson, F.J., Jackson, M.G., 2007. Ambient and excess
mantle temperatures, olivine thermometry, and active vs. passive upwelling.
Chem Geol. 241, 177-206.

Ravizza, G., Blusztajn, J., Prichard, H.M., 2001. Re-Os systematics and platinum-group element distribution in metalliferous sediment from the Troodos ophiolite. Earth. Planet. Sci. Lett. 188, 369-381.

Rehkamper, M., Halliday, A.N., Barfod, D., Fitton, J.G., 1997. Platinum-group element abundance patterns in different mantle environments. Science 278, 1595-1598.

Rehkamper, M., Halliday, A.N., Fitton, J.G., Lee, D.-C., Wieneke, M., Arndt, N.T. 1999. Ir, Ru, Pt and Pd in basalts and komatiites: New constraints for the geochemical behavior of the platinum group elements in the mantle. Geochim. Cosmochim. Acta. 63, 3915-3934.

Ren Z. Y., Ingle S., Takahashi E., Hirano N., and Hirata T. 2005. The chemical structure of the Hawaiian mantle plume. Nature 436(7052), 837-840.

Rhodes, J.M., 1996. Geochemical stratigraphy of lava flows sampled by the Hawaii Scientific Drilling Project. J. Geophys. Res. 101, 11729-11746.

Rhodes, J.M., Vollinger, M.J., 2004. Composition of basaltic lavas sampled by phase-2 of the Hawaii Scientific Drilling Project: Geochemical stratigraphy and magma types. Geochem. Geophys. Geosys. 5, 1-38.

Ribe, N.M., Christensen, U.R., 1999. The dynamical origin of Hawaiian volcanism. Earth Planet. Sci. Lett. 171, 517-531.

Roden M. F., Trull T., Hart S. R., and Frey F. A. 1994. New He, Nd, Pb, and Sr isotopic constraints on the constitution of the Hawaiian plume - Results from Koolau volcano, Oahu, Hawaii, USA. Geochimica Et Cosmochimica Acta 58(5), 1431-1440.

Roeder, P.L., Emslie, R.F., 1970. Olivine-liquid equilibrium. Contrib. Mineral. Petrol. 29, 275-289.

Roy-Barman, M., Allégre, C.J., 1995. $^{187}Os/^{186}Os$ in oceanic island basalts – tracing oceanic crust recycling in the mantle. Earth Planet. Sci. Lett. 129, 145-161.

Rudnick R. L. and Gao S. 2003. Composition of the continental crust. In The Crust (ed. R.L. Rudnick) Vol. 3 Treatise on Geochemistry (eds. H.D. Holland and K.K Turekian), pp. 1-64. Elsevier-Pergamon.

Russell S. A., Lay T., and Garnero E. J. 1998. Seismic evidence for small-scale dynamics in the lowermost mantle at the root of the Hawaiian hotspot. Nature 396(6708), 255-258.

Salters V. J. M. and Stracke A. 2004. Composition of the depleted mantle. Geochemistry Geophysics Geosystems 5(5), 1-27.

Schersten, A., Elliott, T., Hawkesworth, C. and Norman, M., 2004. Tungsten isotope evidence that mantle plumes contain no contribution from the Earth's core. Nature 427, 234-237.

Schulte, R.F., Schilling, M., Anma, R., Farquhar, J., Horan, M.F., Komiya, T., Piccoli, P.M., Pitcher, L., Walker, R.J., 2009. Chemical and chronologic complexity in the convecting upper mantle: Evidence from the Taitao ophiolite, southern Chile. Geochim. Cosmochim. Acta. In press.

Shaw, D.M. 1970. Trace element fractionation during anatexis. Geochimica et Cosmochimica Acta 34, 237-243.

Shirey, S.B., Walker, R.J., 1995, Carius tube digestion for low-blank rhenium-osmium analysis: Anal. Chem. 67, 2136-2141.

Shirey, S.B., Walker, R.J., 1998. The Re-Os isotope system in cosmochemistry and high-temperature geochemistry. Annual Review of Earth and Planetary Sciences, 26: 423-500.

Sims, K.W., Newsom, H.E. and Gladney, E.S. 1990. Chemical fractionation during formation of the Earth's core and continental crust: Clues from As, Sb, W and Mo. In: H.E. Newsome and J.H. Jones (Editors), Origin of Earth. Oxford Press, pp. 291-317.

Sims K. W. W., DePaolo D. J., Murrrell M. T., Baldridge W. S., Goldstein S. J., and Clague D. 1995. Mechanisms of magma generation beneath Hawaii and Mid-Ocean ridges: U-Th and Sm-Nd isotopic evidence. Science 267, 508-5 12.

Sims, K.W.W., DePaolo, D.J., Murrell, M.T., Baldridge, W.S., Goldstein, D., Clague, D. and Jull, M. 1999. Porosity of the melting zone and variations in the solid

mantle upwelling rate beneath Hawaii: Inferences from ^{238}U-^{230}Th-^{226}Ra and ^{235}U-^{231}Pa disequilibria. Geochimica et Cosmochimica Acta 63, 4119-4138.

Sleep, N.H., 1990. Hotspots and mantle plumes – some phenomenology. Journal of Geophysical Research-Solid Earth and Planets 95, 6715-6736.

Sleep, N.H., 1992. Hotspot volcanism and mantle plumes. Annual Review of Earth and Planetary Sciences 20, 19-43.

Smith, A.D., Lewis, C. 1999. The planet beyond the plume hypothesis. Earth-Science Reviews 48, 135-182.

Smith, A.D., 2003. Critical evaluation of Re-Os and Pt-Os isotopic evidence on the origin of intraplate volcanism. J. Geodyn. 36, 469-484.

Smoliar, M.I., Walker, R.J., Morgan, J.W. 1996. Re-Os ages of group IIA, IIIA, IVA and IVB iron meteorites. Science. 271, 1099-1102.

Snow, J.E., Hart, S.R., Dick, H.J.B., 1994. Nd and Sr isotope evidence linking mid-ocean ridge basalts and abyssal peridotites. Nature 371, 57-60.

Snow, J.E. and Schmidt, G., 1998. Constraints on Earth accretion deduced from noble metals in the oceanic mantle. Nature 391, 166-169.

Sobolev, A.V., Hofmann, A.W., Sobolev, S.V. and Nikogosian, I.K., 2005. An olivine-free mantle source of Hawaiian shield basalts. Nature 434, 590-597.

Sobolev, A.V., Hofmann, A.W., Kuzmin, D.V., Yaxley, G.M., Arndt, N.T., Chung, S.L., Danyushevsky, L.V., Elliott, T., Frey, F.A., Garcia, M.O., Gurenko, A.A.,

Kamenetsky, V.S., Kerr, A.C., Krivolutskaya, N.A., Matvienkov, V.V., Nikogosian, I.K., Rocholl, A., Sigurdsson, I.A., Sushchevskaya, N.M., Teklay, M., 2007. The amount of recycled crust in sources of mantle derived melts. Science 316, 412-417.

Staudigel H., Zindler A., Hart S. R., Leslie T., Chen C. Y., and Clague D. 1984. The isotope systematics of a juvenile intraplate volcano - Pb, Nd, and Sr isotope ratios of basalts from Loihi seamount, Hawaii. Earth and Planetary Science Letters 69(1), 13-29.

Strekopytov, S.V. 1998. Molybdenum and tungsten in oceanic sediments and nodules. Geochemistry International 36, 838-845.

Sun S. S. 1982. Chemical composition and origin of the earth's primitive mantle. Geochimica et Cosmochimica Acta 46(2), 179-192.

Sun. S.-S., McDonough, W.F. 1989. Chemical and isotopic systematics of oceanic basalts: implications of mantle composition and processes. In *Magmatism in the Ocean Basins*, Geological Society Spec. Publ. 42 (eds. A.D Saunders and M.J. Norry). Oxford, 313-345.

Sun, W., Bennett, V.C., Eggins, S.M., Kamenetsky, V.S., Arculus, R.J. 2003. Enhanced mantle-to-crust rhenium transfer in undegassed arc magmas. Nature 422, 294-297.

Takamasa, A., Nakai, S., Sahoo, Y., Hanyu, T. and Tatsumi, Y. 2009. W isotope compositions of oceanic island basalts from French Polynesia and their meaning for core-mantle interaction. Chemical Geology 260, 37-46.

Tanaka, R., Nakamura, E., Takahashi, E., 2002. Geochemical evolution of Koolau volcano, Hawaii, in: E. Takahashi, P.W. Lipman, M.O. Garcia, J. Naka, S. Aramaki (Eds.), Hawaiian Volcanoes; Deep Underwater Perspectives, American Geophysical Union, Washington, DC, United States, 311-332.

Tatsumi, Y., Oguri, K. and Shimoda, G., 1999. The behaviour of platinum-group elements during magmatic differentiation in Hawaiian tholeiites. Geochemical Journal 33, 237-247.

van Acken, D., Becker, H., Walker, R.J., McDonough, W.F., Wombacher, F., Ash, R.D., Piccoli, P.M., 2009. Formation of pyroxenite layers in the Totalp ultramafic massif (Swiss Alps) – insights from highly siderophile elements and Os isotopes.

van der Hilst, R.D., Widiyantoro, S. Engdahl, E.R. 1997. Evidence for deep mantle circulation from global tomography. Nature 386, 578-584.

van Orman, J.A., Keshav, S., Fei, Y. 2008. High-pressure solid/liquid partitioning of Os, Re and Pt in the Fe-S system. Earth Planet. Sci. Lett. 274, 250-257.

van der Plas, L. and Tobi, A.C. 1965. A chart for judging the reliability of point counting results. American Journal of Science 263, 37-90.

Walker, D., 2000. Core participation in mantle geochemistry: Geochemical Society Ingerson Lecture, GSA Denver, October 1999. Geochim. Cosmochim. Acta. 64, 2897-2911.

Walker, R.J., Morgan, J.W. and Horan, M.F., 1995. Os-187 enrichment in some plumes – evidence for core-mantle interaction. Science, 269, 819-822.

Walker, R.J., Morgan, J.W., Beary, E., Smoliar, M.I., Czamanske, G.K, Horan, M.F., 1997. Applications of the ^{190}Pt-^{186}Os isotope system to geochemistry and cosmochemistry. Geochim. Cosmochim. Acta. 61, 4799-4808.

Walker, R.J., Brandon, A.D., Bird, J.M., Piccoli, P.M., McDonough, W.F., Ash, R.D. 2005. ^{187}Os-^{186}Os systematics of Os-Ir-Ru alloy grains from southwestern Oregon. Earth Planet Sci. Lett. 230, 211-226.

West H. B., Gerlach D. C., Leeman W. P., and Garcia M. O. 1987. Isotopic constraints on the origin of Hawaiian lavas from the Maui volcanic complex, Hawaii. Nature 330(6145), 216-220.

West, H.B., Garcia, M.O., Gerlach, D.C., Romano, J., 1992. Geochemistry of tholeiites from Lanai, Hawaii. Contrib. Min. Petrol. 112, 520-542.

White, W.M., Schilling, J.-G., 1978. The nature and origin of geochemical variation in Mid-Atlantic Ridge basalts from the central North Atlantic. Geochim. Cosmochim. Acta. 42, 1501-1516.

Widom, E., Shirey, S.B., 1996. Os isotope systematics in the Azores: implications for mantle plume sources. Earth Planet. Sci. Lett. 142, 279-296.

Wilson, J.T. 1963. A possible origin of the Hawaiian islands. Canadian Journal of Physics. 41: 863-870.

Workman, R.K., Hart, S.R., Blusztajn, J., Jackson, M., Kurz, M. Staudigel, H. 2003. Enriched mantle: II. A new view from the Samoan hotspot. Geochem. Geophys. Geosys.

Workman, R.K., Hart, S.R., 2005. Major and trace element composition of the depleted MORB mantle (DMM). Earth. Planet Sci. Lett. 231, 53-72.

Wright, T.L., 1973. Magma mixing as illustrated by the 1959 eruption, Kilauea Volcano, Hawaii. Geol. Soc. Am. Bulletin. 84, 849-858.

Yi, W., Halliday, A.N., Alt, J.C., Lee, D.C., Rehkamper, M., Garcia, M.O., Su, Y., 2000. Cadmium, indium, tin, tellurium and sulfur in oceanic basalts: Implications for chalcophile element fractionation in the Earth. J. Geophys. Res. 105, 18927-18948.

Yokoyama, T., Rai., V.K., Alexander, C.M.O'D., Lewis, R.S., Carlson, R.W., Shirey, S.B., Thiemens, M.H., Walker, R.J. 2007. Osmium isotope evidence for uniform distribution of s- and r-process components in the early solar system. Earth Planet. Sci. Lett. 259, 567-580.

Zhao D. 2001. Seismic structure and origin of hotspots and mantle plumes. Earth and Planetary Science Letters 192(3), 251-265.

Zindler, A. Hart, S., 1986. Chemical Geodynamics. Ann. Rev. Earth Planet. Sci. 14, 493-571.

Zoller, W. H., Parrington, J. R., Kotra, J. M. P., 1983. Iridium enrichment in airborne particles from Kilauea Volcano. Science 222, 1118-1121.